EFFECTS OF ACETYL COA SYNTHETASE AND CITRATE SYNTHASE ON PYRUVATE PRODUCING STRAINS OF *ESCHERICHIA COLI*.

by

GEOFFREY M. SMITH

(Under the Direction of Mark A. Eiteman)

ABSTRACT

Escherichia coli ALS 929 (YYC 202 (Hfr *zbi*::Tn*10 poxB1* Δ(*aceEF*) *rpsL pps-4 pfl-1*) *ldhA*) requires acetate to sustain cell growth due to the deletion in several biochemical pathways associated with pyruvate. The accumulation of pyruvate and the consumption of acetate of this strain were examined in a series of batch and continuous fermentations. Acetyl Coenzyme A Synthetase (ACS) from *E. coli,* which catalyzes the conversion of acetate to acetyl CoA, was overexpressed in ALS 929 to examine the effect of increased acetate utilization on cell growth and pyruvate production. The overexpression of ACS in ALS 929 was also investigated in both batch and continuous culture fermentations. Results have shown that the presence of overexpressed ACS resulted in a higher acetate consumption rate, and a reduced maximum cell concentration. Citrate Synthase (CS) from *Bacillus subtilis*, which catalyzes the condensation of acetyl CoA and oxaloacetate to citrate, was also investigated.

INDEX WORDS: pyruvate, acetate, acetyl CoA synthetase, citrate synthase, batch fermentation, continuous (chemostat) fermentation

EFFECTS OF ACETYL COA SYNTHETASE AND CITRATE SYNTHASE ON PYRUVATE PRODUCING STRAINS OF *ESCHERICHIA COLI*.

by

GEOFFREY M. SMITH

B.S.B.E., The University of Georgia, 2001

A Thesis Submitted to the Graduate Faculty of The University of Georgia in Partial Fulfillment of the Requirements for the Degree

MASTER OF SCIENCE

ATHENS, GEORGIA

2005

EFFECTS OF ACETYL COA SYNTHETASE AND CITRATE SYNTHASE ON PYRUVATE PRODUCING STRAINS OF *ESCHERICHIA COLI*.

by

GEOFFREY M. SMITH

Major Professor: Mark A. Eiteman

Committee: Brahm Verma
Joy Peterson

Electronic Version Approved:

Maureen Grasso
Dean of the Graduate School
The University of Georgia
August 2005

ACKNOWLEDGEMENTS

I would like thank my major professor Dr. Mark A. Eiteman for his guidance and support throughout the thesis process. I would also like to thank my committee members Dr. Joy Peterson and Dr. Brahm Verma for their insights and comments on my research. Dr. Elliot Altman, Kris DeWitt and Jim Warren have been invaluable in there help and guidance in strain development and molecular biology. I also owe a debt of gratitude to the Center of Molecular BioEngineering, especially Sarah Lee who has been there to help with any technical issues and conversation

Special thanks to Chester Brewer, who helped keep me sane throughout my research and writing. I would finally like to thank all my friends and family, including Emily DeCrescenzo, Sean Ireland and Javier Sayago who have been there to listen to me complain, and allow me to subject them to my presentations and editing questions.

TABLE OF CONTENTS

Page

LIST OF TABLES

Page

LIST OF FIGURES

Page

CHAPTER 1

INTRODUCTION

The α-oxocarboxylic acid pyruvic acid plays a pivotal role in both metabolic as well as industrial processes. In the cell it plays a key role in central metabolism as an intermediate compound between the glycolytic pathway and those pathways relating to energy and biomass production. Industrially, pyruvate has been used as a starting material for several compounds. Pyruvate has been used in the manufacturing a variety pharmaceuticals, which include L-tryptophan (Nakazawa et al. 1972), L-tyrosine, and 3,4-dihydroxyphenyl-L-alanine (Yamada et al. 1972), as well as L-alanine (Lee et al. 2004). Pyruvic acid has also been used as precursor for the synthesis of agricultural compounds used for crop protection, polymers, cosmetics, and food additives (Li et al. 2001).

Clinical studies have shown that pyruvate salts, when taken as a dietary supplement, may promote weight loss due to accelerated metabolism of fatty acids in the body (Stanko et al. 1992a, 1992b; Ivy et al. 1994) and enhance endurance during strenuous exercise (Stanko et al. 1990). When pyruvate was used in conjunction with a low-cholesterol and low-fat diet, subjects displayed lower blood concentrations of lipids than did those given a glucose placebo (Stanko et al. 1994). In medical studies pyruvate had been shown to be a potent antioxidant (DeBoer et al. 1993) capable of reducing anoxic injury and free radical formation (Borle and Stanko 1996). Pyruvate salts have been also used in treatment of ischemia, hypoxia, or hypoglycemia as it prevented neuronal damage associated with these diseases (Izumi and Olney 1995). Because of

these many applications of pyruvic acid, including use as a media component in cell cultures (Miyata and Yonehara 1999), there is an increasing commercial demand for its production.

Pyruvate Production

Pyruvate has been produced at an industrial scale predominantly by a chemical process by which tartaric acid was dehydrated and decarboxylated in the presence of saturating concentrations of potassium hydrogen sulfates at 220° C (Howard and Fraser 1932). The final product was distilled under vacuum. Although this technique was useful, it was not cost effective and was unable to meet the current demands: the method had cost $8 000 to $9 000/ton based on the market price of the materials used, which prevented the extensive use of pyruvate for many applications (Li et al. 2001). Other means of producing this three-carbon sugar were via biotechnological methods; including enzymatic, resting cell or fermentative processes.

Enzymatic processes involve raw or purified enzyme preparations to mediate a single enzymatic step. *Acetobacter sp.* ATCC 21490 has been used in a reaction mixture with D-lactic acid to produce almost 20 g/L pyruvate (Cooper 1990). However, this process was not readily commercialized due to the higher cost of D-lactate compared with L-lactate. Glycolate oxidase ((S)-2-hydroxy-acid oxidase, EC 1.1.3.15), an enzyme ubiquitous in leafy green plants and mammalian cells and catalyzing the reaction of glycolate to glyoxylate, is capable of converting L-lactate to pyruvate and hydrogen peroxide. In order to eliminate the subsequent oxidation of pyruvate to alanine by the hydrogen peroxide generated, the enzyme catalase must also be included. Two yeasts, *Hansenula polymorpha* and *Pichia pastoris,* carrying glycolate oxidase, have been used in permeabilized cell reactors to produce pyruvic acid from L-lactic acid. Both yeasts produced catalase endogenously and thus effectively removed the hydrogen peroxide

produced from the reaction catalyzed by glycolate oxidase (Anton et al. 1996; Eisenberg et al. 1997).

Pyruvate produced via a resting cell method involves microbial cells accumulating pyruvate from a substrate via several cellular mechanisms. This method differs from the enzymatic processes mentioned above where the microorganisms are used for only one reaction (Li et al. 2001). An example resting cell process utilized *Acinetobacter sp.* 80-M to produce pyruvate grown on 1,2-propanediol as the sole carbon source (Izumi et al. 1982). Resting cell reactions using either *Proteus vulgaris* or *Proteus mirabilis* grown on (R)-lactate produced pyruvic acid with over 95% conversion (Schinschel and Simon 1993). A *Pseudomonas* sp. accumulated pyruvate using a cyclic-imide-transforming pathway - 94 mM pyruvate from 100 mM fumarate in 24 h (Ogawa et al. 2001).

Direct fermentative processes have also been utilized in the manufacturing of pyruvic acid and numerous microorganisms are able to grow on a carbon source while accumulating pyruvate (Table 1). For example, several fungal reactors were utilized for the production of pyruvic acid. The basidiomycete *Schizophyllum commune* accumulated 19 g/L of pyruvate in five days when cultured in a glucose medium (Takao and Tanida 1982). Uchio et al. (1976) used *Candida lipolytica,* which normally requires methionine and thiamine for growth, to generate 43.6 g/L in 72 hours. Thiamine is a cofactor for both the pyruvate dehydrogenase (PDH) complex and pyruvate decarboxylase. This vitamin deficiency results in a reduced activity of these pyruvate metabolizing enzymes and thus an accumulation of pyruvate (Li et al. 2001). Another thiamine auxotroph yeast, *Saccharomyces cerevisiae,* generated pyruvic acid during thiamine limitation (Li et al. 2001). Dried cells of *Debaryomyces coudertii* converted saccharified citrus peel, of which galacturonic acid is the major constituent, to about 7 - 9 g/L

Table 1: A summary of pyruvate production using microbial fermentation processes.

Organism	Pyruvate	% $Y_{P/S}$	Time	Reference
	g/L	g/g	h	
S. commune	19	38 (glucose)	120	Takao et al. 1982
C. lipolytica	43.6	43.6 (glucose)	72	Uchio et al. 1976
D. coudertii	8	26.6 (galacturonic acid)	10	Moriguchi et al.1984
T. glabrata	68	49 (glucose)	63	Miyata et al. 1996
E. casseliflavus	16	32 (gluconate)	72	Yanase et al. 1992
E. aerogenes	4.7	23.5 (glucose)	72	Yokota et al. 1989
E. coli W1485*lip*2 *atpA*	31	64 (glucose)	48	Yokota et al. 1994
E. coli 6162	40	72 (glucose)	36	Tomar et al. 2003
E. coli YYC202 *ldhA*	62	54.2 (glucose)	30	Zelic et al. 2003
E. coli TC44	66	75 (glucose)	20	Causey et al. 2004

pyruvate in 10 hours (Moriguchi et al. 1984). *Torulopsis glabrata* has been the most commonly used microorganism for the production of pyruvic acid generating about 68 g/L in 63 h from glucose with a 49.4 % yield. This yeast required nicotinic acid, thiamine, pyridoxine and biotin in the growth media (Miyata and Yonehara 1996). Nicotinic acid is another cofactor for the PDH complex, while biotin is a cofactor for pyruvate carboxylase and pyridoxine is the cofactor of transaminase. A deficiency of these vitamins and thiamine resulted in an accumulation of pyruvate due to the lower activities of the enzymes for which they are required (Li et al. 2001). In order to increase the yield, a pyruvate decarboxylase mutant was developed from which 60 g/L was produced in 47 h with a 67.3 % yield (Miyata and Yonehara 1999).

While yeasts have been the common microbes used in pyruvate fermentations, bacteria have displayed a greater range of substrates from which the cells can generate pyruvic acid (Li et al. 2001). An *Enterococcus casseliflavus* strain, grown on gluconate in alkaline conditions, accumulated 16 g/L pyruvate in 72 h (Yanase et al. 1992). Lipoic acid, like thiamine and nicotinic acid, is a required cofactor of the PDH complex; however, thiamine is also a cofactor for an enzyme of the pentose phosphate pathway. Thus, a thiamine deficiency might negatively impact cell growth (Li et al. 2001). On a similar note, due to the importance of nicotinic acid as a precursor of $NAD(P)^-$, which are both involved in the oxidative-reductive reactions in cell metabolism, a deficiency for this cofactor would negatively impact cell growth. A lipoic acid auxotroph of *Enterobacter aerogenes* accumulated pyruvate and α-ketoglutarate due to decreased activity of the PDH complex under lipoic acid deficiency (Yokota and Takao 1989).

Using such a strategy *Escherichia coli* strain W1485*lip*2 *atpA*, auxotrophic for lipoic acid, grew on glucose to generate 31 g/L of pyruvate in 48 h (64 % yield) (Yokota et al. 1994). A direct mutation of one or more components of the PDH complex in *Escherichia coli* also

resulted in an accumulation of pyruvate from glucose when acetate was provided for growth. *E. coli* CGSC 6162 carries an *aceF* mutation, which encodes dihydrolipoamide S-acetyltransferase, a component of the PDH complex. This mutation prevented the oxidative decarboxylation of pyruvate to acetyl coenzyme A and resulted in 40 g/L pyruvic acid in 36 h with a 72 % yield (Tomar et al. 2003). Another *E. coli* strain called YYC202 *ldhA*, which has the *aceF* mutation and several other mutations, similarly generated about 62 g/L in 30 h with a 54.2 % yield (Zelic et al. 2003). Causey et al. (2004) developed *E. coli* TC44, which carried mutations to minimize ATP yield, cell growth, CO_2 production, and eliminated the production of acetate and other fermentation products. This strain when grown with 5 % oxygen and excess glucose accumulated around 66 g/L pyruvate in 20 h with a yield of 75 %.

Objectives

The overall objective of this research is to increase the yield and productivity of pyruvate by optimizing acetate utilization in a pyruvate accumulating *E. coli* strain containing deletions in key central metabolic pathways. The specific objectives are to overexpress *E. coli* acetyl CoA synthetase and *Bacillus subtilis* citrate synthase in order to increase acetate utilization.

***Escherichia coli* and its Metabolism**

Escherichia coli is a Gram-negative bacterium that is used frequently as a host for biological production processes. This organism has several advantages that make it well suited for use in many biotechnological techniques. *E. coli* is a physiologically well-characterized bacterium with known genome (Blattner et al. 1997), and is relatively simple to alter genetically via standard molecular biology techniques. These characteristics along with rapid growth and inexpensive maintenance requirements ensure that this microbe is one of the foremost hosts for

many biological production methods. Like many organisms, *E. coli* uses glycolysis and the tricarboxylic acid (TCA) cycle in the metabolism of the carbohydrate glucose (Figure 1).

Glycolysis

E. coli is a facultative anaerobe, capable of growth either in the presence or absence of oxygen and utilizes a wide array of carbon sources. Several transport systems exist, and each provides a means for a carbon substrate to enter the cell through the cell membrane. For glucose the transport system is termed the phosphoenolpyruvate: glucose phosphotransferase system, or PTS (A, Figure 1)(Gottschalk 1986). This system is a cascade mechanism in which the phosphate group from phosphoenolpyruvate, PEP, is first transferred to a small soluble protein HPr by Enzyme I (EI) producing pyruvate. These proteins are utilized in the transfer of other carbon sources such as mannose and fructose as well as that of glucose. The phosphorylated HPr protein then transfers the phosphate group to the glucose-specific Enzyme III^{Glc} (EIII), which is then able to enter the cell membrane due to an increased solubility. The phosphorylated EIII is used to convert glucose to glucose-6-phosphate by the activity of Enzyme II (EII), a membrane bound protein specific for glucose, transferring the product into the cells cytoplasm (Gottschalk 1986). Once the activated glucose enters the cell as glucose 6-phosphate, it is further degraded to pyruvate via the glycolytic, Embden-Meyerhof-Parnas (EMP) pathway. This pathway produces two moles each of pyruvate, adenosine triphosphate (ATP), and reduced nicotinamide adenine dinucleotide ($NADH_2^+$, but abbreviated NADH) (Gottschalk 1986). The fate of pyruvate differs in aerobically and anaerobically grown cells.

Figure 1. Metabolic pathways of *E. coli* under aerobic conditions when grown on glucose.

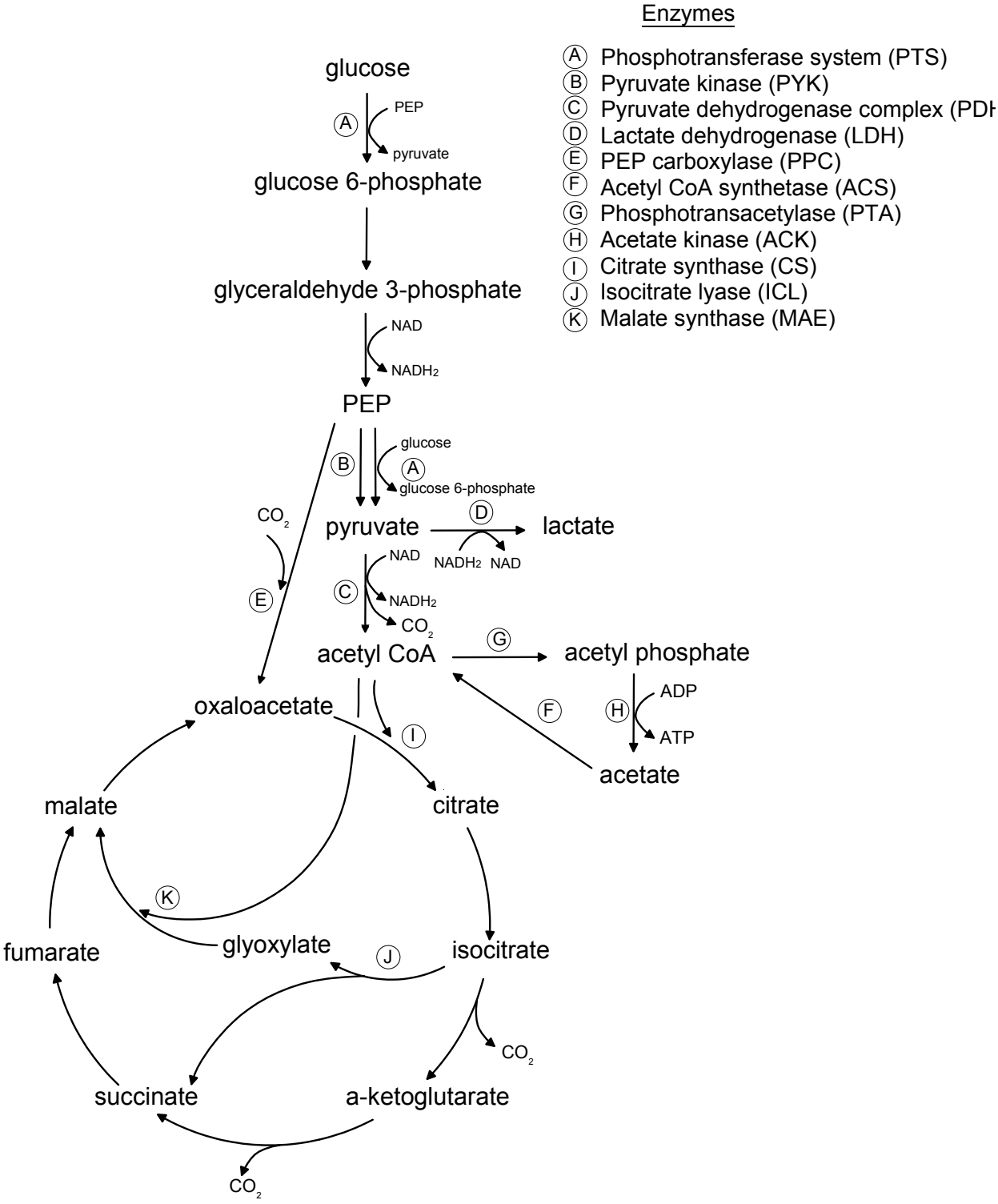
Enzymes
A Phosphotransferase system (PTS)
B Pyruvate kinase (PYK)
C Pyruvate dehydrogenase complex (PDH
D Lactate dehydrogenase (LDH)
E PEP carboxylase (PPC)
F Acetyl CoA synthetase (ACS)
G Phosphotransacetylase (PTA)
H Acetate kinase (ACK)
I Citrate synthase (CS)
J Isocitrate lyase (ICL)
K Malate synthase (MAE)
glucose
PEP
pyruvate
glucose 6-phosphate
glyceraldehyde 3-phosphate
NAD
NADH2
PEP
glucose
glucose 6-phosphate
CO2
pyruvate
lactate
NADH2 NAD
NAD
NADH2
CO2
acetyl CoA
acetyl phosphate
ADP
ATP
oxaloacetate
acetate
malate
citrate
glyoxylate
fumarate
isocitrate
CO2
succinate
a-ketoglutarate
CO2

Aerobic Growth

Under aerobic conditions pyruvate is oxidized to acetyl Coenzyme A (CoA) by a complex of enzymes collectively referred to as the PDH complex (B, Figure 1). This complex is composed of three specific enzymes: pyruvate dehydrogenase, dihydrolipoate transacetylase, and dihydrolipoate dehydrogenase (Gottschalk 1986). Through a series of steps the PDH complex removes an acetyl group from pyruvate and transfers it to a CoA while generating carbon dioxide and one mole of NADH per mole of pyruvate. The enzyme citrate synthase (I, Figure 1) subsequently condenses the acetyl group of acetyl CoA with oxaloacetate releasing CoA and citrate. Through several steps forming the TCA cycle, oxaloacetate is regenerated from citrate forming two CO_2, two moles of NADH, and one mole each of oxidized nicotinamide adenine dinucleotide phosphate (NADPH), oxidized flavin adenine dinucleotide ($FADH_2$) and ATP (Gottschalk 1986). In aerobic cultures the majority of these coenzymes are regenerated by the oxidative phosphorylation respiratory chain, which uses energy stored in NADH and $FADH_2$ to create an electron cascade. This cascade in turn creates a pH gradient across the plasma membrane that is used to create cellular energy as ATP via a membrane bound ATP synthase (Gottschalk 1986). The cell also has many pathways, which regenerate the oxidized forms of these coenzymes. The majority of these pathways are anabolic processes involved in biomass synthesis.

Anaplerotic Pathways

During cellular growth and maintenance *E. coli* utilizes several intermediates from primary metabolism (the EMP pathway, the TCA cycle, and pentose phosphate pathway) for the production of amino acids, nucleotides, cofactors, and/or other compounds required for the synthesis of biomass. These anabolic pathways effectively remove intermediates from primary

metabolism and thus reduce metabolites available for subsequent reactions. The cells have several pathways that replenish such withdrawn compounds, and these pathways are called anaplerotic pathways (Gottschalk 1986). One such reaction in *E. coli* is catalyzed by PEP carboxylase, an enzyme that generates oxaloacetate and phosphate from PEP and CO_2 (Gottschalk 1986). When grown on acetate as the sole carbon source *E. coli* makes use of a pathway known as the glyoxylate shunt, which uses two acetyl CoA molecules to produce one mole of oxaloacetate (Holms 1986). The enzymes that comprise this shunt are isocitrate lyase and malate synthase. Anaplerotic pathways such as these two examples are required for growth on a single carbon substrate. A strain that lacks activity in these anaplerotic pathways can only grow in the presence of at least two or more carbon sources. For example, a strain lacking PEP carboxylase activity cannot grow on glucose, but can grow on glucose and succinate (McAlister et al. 1981).

Anaerobic Growth

Under anaerobic growth conditions pyruvate is not oxidized significantly by PDH. Because of the absence of oxygen as an electron acceptor, oxidized cofactors must be generated by reduction of pyruvate. Thus, fermentative products of *E. coli* are generated from glucose: lactate, acetate, ethanol, formate and succinate. A mixture of these compounds is generated in order to maintain redox and energy balance. During conditions of pyruvate accumulation, and more acidic conditions, the cell can direct more pyruvate through lactate dehydrogenase (LDH) to generate lactate and oxidize NADH to NAD (Clark 1989). Present aerobically to a lower activity, one function of LDH is to decrease the rate at which the culture pH is lowered (Clark 1989). In the absence of oxygen, PDH is repressed (Clark 1989). Instead, pyruvate is partially converted via pyruvate formate lyase (PFL) to acetyl CoA and formate. This reaction releases no

CO_2 nor does it produce NADH, eliminating the necessity of its reoxidation (Clark 1989). Some formic acid can be degraded to H_2 and CO_2 by formate hydrogen lyase. These two products are available to increase the yield of ethanol (H_2) or used in the formation of other compounds such as oxaloacetate and malate (CO_2), precursors to succinate (Clark 1989). The acetyl CoA generated by PFL is itself primarily converted to acetate and ethanol. The synthesis of ethanol from acetyl CoA is catalyzed by acetaldehyde CoA dehydrogenase (ACDH) and alcohol dehydrogenase (ADH), each step regenerating one mole of NAD from NADH (Clark 1989). The synthesis of acetate from acetyl CoA is catalyzed by phosphotransacetylase (PTA) and acetate kinase (ACK). The first step generates the high-energy intermediate acetyl phosphate, which transfers the high-energy phosphate subsequently to ADP to yield ATP and acetate (Clark 1989). Another enzyme, acetyl CoA synthetase (ACS) (H, Figure 1), is involved in the formation of acetyl CoA from acetate. This reaction is typically encountered when the primary carbon source such as glucose has been exhausted. ACS adenylates acetate at the expense of an ATP releasing AMP, and then transfers the acetyl group to CoA to produce acetyl CoA (Clark 1989). All three enzymes are active in aerobic and anaerobic cultures (Clark 1989).

Pyruvate Metabolism

Pyruvate occupies an important position in the central pathways from cellular growth and maintenance in both aerobic and anaerobic cultures. The biochemical steps to and from pyruvate are shown in Figure 2. Pyruvate is generated principally from PEP via pyruvate kinase or PTS. Pyruvate can also be generated from malate by either a NADP- or NAD-linked malic enzyme. Pyruvate may be directly metabolized by the PDH complex to acetyl CoA, by LDH to lactate, by pyruvate oxidase (POX) to acetate, or by PEP synthase (PPS) to PEP. Other enzymes play a more indirect role in metabolizing pyruvate. The enzymes PTA/ACK, ACS and citrate synthase

Figure 2: Immediate metabolic network around the pyruvate node with aerobic and anaerobic pathways shown.

Enzymes

1. PEP synthase (PPS)
2. Phosphotransferase system (PTS)
3. Pyruvate kinase (PYK)
4. Lactate dehydrogenase (LDH)
5. Pyruvate formate lyase (PFL)
6. Pyruvate dehydrogenase complex (PDH)
7. Pyruvate oxidase (POX)
8. Phosphotransacetylase (PTA)
9. Acetate kinase (ACK)
10. Acetyl CoA synthetase (ACS)
11. Citrate synthase (CS)
12. PEP carboxylase (PPC)
13. Malic enzyme (MAE)
14. Malate dehydrogenase (MDH)

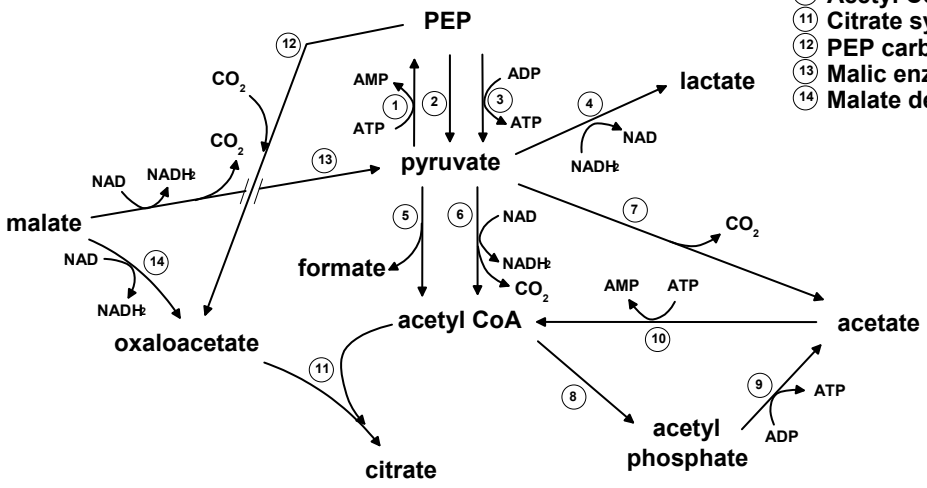

affect acetyl CoA, while PEP carboxylase (PPC) affects PEP, the principal precursor to pyruvate. Each of these enzymes, as well as unknown regulatory proteins, is likely to impact the accumulation of pyruvate in *E. coli*. A more detailed description will now be provided for these enzymes.

PEP: Phosphotransferase System (PTS)

The PTS (2, Figure 2) is the major pathway in which glucose is activated to glucose-6-phosphate and transported into the cell with the concomitant generation of pyruvate from PEP. The first reaction involves the phosphorylation of the HPr protein by PEP via a phosphorylated E1, with E1 K_m values of 200 to 400 μM for HPr and 5 μM for PEP (Postma et al. 1993). The phosphorylated HPr in turn phosphorylates the glucose specific IIA^{Glc} (EIII), which has a K_m of 0.3 μM for the HPr-P protein (Postma et al. 1993). IIA^{Glc}-P then transfers the phosphoryl group to IIBC (EII), with a K_m of 2 – 5 μM, which in turn binds to glucose, with a K_m of 3 – 10 μM (Postma et al. 1993). The activated IIBC-P facilitates the diffusion of glucose through the membrane where it is then phosphorylated (Postma et al. 1993). There are several proposed feedback associated regulation mechanisms for PTS, which include the membrane potential, energy-dependent efflux of substrates, competition for HPr-P, and regulation by intracellular phospho-compounds (Postma et al. 1993).

Pyruvate Kinase (PYK)

Pyruvate kinase (PYK) EC 2.7.1.40 (3, Figure 2) catalyzes the transphosphorylation of PEP to ADP generating pyruvate and ATP in the EMP pathway (Boiteux et al. 1983). *E. coli* expresses the two isozymes of PYK, PYK I and PYK II, which are encoded by *pykF* and *pykA*, respectively. PYK I is activated by fructose 1,6-bisphosphate (FBP) and inhibited by ATP, and succinyl CoA (Malcovati and Valentini 1982). The PYK II isozyme is activated by AMP and

several carbohydrate phosphates such as ribose 6-phosphate and glucose 6-phosphate (Malcovati and Valentini 1982). PYK I, the primary PYK (Emmerling et al. 1999), has K_m values of 3.63 mM for pyruvate and 0.3 mM for ADP. When activated by FBP, PYK I has a K_m value of 0.08 mM (Valentini et al. 2000).

Pyruvate Dehydrogenase (PDH)

The pyruvate dehydrogenase complex in *E. coli* (6, Figure 2) is composed of three enzyme subunits: pyruvate dehydrogenase (E1, EC 1.2.4.1), dihydrolipoyl transacetlyase (E2, EC 2.3.1.12) and dihydrolipoyl dehydrogenase (E3, EC 1.8.1.4). The complex is composed of 24 molecules of the E1 subunit, 24 molecules of E2, and 12 molecules of E3 (CaJacob et al. 1985). The core of the complex is the 24 dihydrolipoyl transacetylase subunits arranged in octahedral symmetry to which bind the pyruvate dehydrogenase and dihydrolipoyl dehydrogenase subunits (Reed et al. 1975). The E1 subunits, encoded by the gene *aceE*, catalyze the reaction in which pyruvate is bound to thiamine pyrophosphate, releasing CO_2. The lipoyl group of the E2 subunits, product of the *aceF* gene, subsequently binds the remaining acetyl group where it is transferred to CoASH. The inactive reduced lipoyl group is then oxidized by flavoprotein subunits, E3, reducing NAD to NADH. The E3 subunit is a product of the gene *lpd* (Perham et al. 1987). As noted previously, several studies have exploited the dependency of the PDH complex for thiamine, lipoic acid or nicotinic acid to reduce its activity and thus accumulate pyruvate. Generally, this approach was accomplished by subjecting corresponding auxotrophs to vitamin deficiencies in the media (Uchio et al.1976; Yokota and Takao 1989; Yokota et al. 1994; Miyata and Yonehara 1996). While E1 and E2 of the PDH complex are specific for pyruvate, the third subunit E3 is also a component of the α-ketoglutarate dehydrogenase complex, and therefore a mutation of the *lpd* gene would affect the activity of

that complex (Perham et al. 1987). For strains lacking PDH activity, acetate is a required component for cell growth since acetyl compounds required for biomass synthesis cannot be synthesized from common carbohydrate substrates (e.g. glucose, fructose) (Chang and Cronan 1982). The PDH complex has an apparent K_m value of 0.48 mM for pyruvate (Danson et al. 1978) and an apparent K_m value of 0.176 mM for NAD^+ (Akiyama and Hammes 1980). It was also demonstrated that a concentration of NAD^+ greater than 3.2 mM was inhibitory, possibly attributed to NADH, which is a strong inhibitor of the complex (Akiyama and Hammes 1980).

Lactate Dehydrogenase (LDH)

E. coli has three lactate dehydrogenase enzymes, two of which are membrane bound flavoproteins (one specific for L-lactate and the other for D-lactate) used in the respiratory chain and are necessary for aerobic growth on lactic acid as a sole carbon source (Mat-Jan et al. 1989). During conditions of pyruvate accumulation and low pH, lactic acid is generated by the third soluble NAD-linked lactate dehydrogenase (LDH, EC 1.1.1.28) (4, Figure 2) expressed by the *ldhA* gene (Clark 1989; Mat-Jan et al. 1989). At a pH of 7.5 LDH has a K_m value of 7 mM for pyruvate once the enzyme has been activated (Tarmy and Kaplan 1968). The reaction catalyzed by the soluble LDH consumes one mole of reduced NADH per mole of lactate produced, and thus this reaction has the affect of modulating the NAD/NADH concentrations in the cell quickly based on pyruvate concentration (Mat-Jan et al. 1989). LDH is allosterically activated by pyruvate and α-ketobutyrate, and is competitively inhibited by oxamate (Tarmy et al. 1968). At the genomic level *ldhA* is induced by anaerobic and acidic conditions with a 10-fold increase over native aerobic expression (Bunch et al. 1997). Although *E. coli ldhA* mutants can grow anaerobically and redistribute the products acetate, formate, ethanol and succinate to meet a redox requirement, an *ldhA pflB* double mutant is no longer able to grow anaerobically on any

fermentable sugar even in the presence of acetate (Bunch et al. 1997; Mat-Jan et al. 1989). However, this *ldhA pflB* double mutant is able to grow with nitrate or fumarate as an electron acceptor during anaerobic respiration (Mat-Jan et al. 1989)

Pyruvate-formate Lyase (PFL)

As noted previously PFL (EC 2.3.1.54) (5, Figure 2) encoded by the gene *pflB* is responsible for the conversion of pyruvate to acetyl CoA and formate during anaerobic conditions. A mutation in *pflB* prevents cell growth on glucose minimal media due to the inability of the cells to generate acetyl units, and as such requires the supplementation of acetate to the media (Mat-Jan et al. 1989). PFL is present in its inactive form in aerobic cultures, but in anaerobic conditions is activated by an iron-dependent flavoprotein that requires pyruvate and S-adenosylmethionine for activity (Knappe et al. 1974). In the forward reaction of PFL, pyruvate to acetyl CoA and formate, the enzyme has K_m values of 2.05 mM for pyruvate and 0.0068 mM for CoA. For the reverse reaction, which catalyzes the condensation of acetyl CoA and formate, PFL has K_m values of 24.5 mM and 0.051 mM for formate and acetyl CoA, respectively (Knappe et al. 1974).

Pyruvate Oxidase (POX)

Pyruvate oxidase (EC 1.2.2.2) (7, Figure 2), also referred to as pyruvate dehydrogenase (cytochrome), is a membrane bound enzyme that catalyzes the oxidative decarboxylation of pyruvate to acetate and CO_2 (Mather and Gennis 1985). The enzyme is composed of four identical subunits, products of the *poxB* gene. Each subunit is tightly bound with FAD and loosely bound by TPP with Mg^{2+} (Chang et al. 1994). The K_m value of POX for pyruvate is 10 mM, while the K_m value for TPP is about 1 μM (Williams and Hager 1966). During the oxidation of pyruvate the enzyme reduces the FAD component, which then is believed to reduce

ubiquinone *in vivo* (Mather and Gennis 1985). POX is strongly activated by lipids, which has shown a 20-fold increase in maximum velocity and reduced the concentration of pyruvate required for enzyme saturation by 10-fold (Abdel-Hamid et al. 2001). As previously noted, the PDH complex and PFL also convert pyruvate to acetyl groups (Chang et al. 1994). The PDH complex is active in strictly aerobic cultures while PFL is active in strictly anaerobic cultures. During the transition between aerobic and anaerobic phases, or between the exponential and stationary growth phases, neither the PDH complex nor PFL are very active. It has been proposed that POX plays a role in producing the acetyl units during this transition (Chang et al. 1994). Further evidence of this function is that the expression of *poxB* is increased by the σ^s factor, a sigma factor that is a stationary growth phase global regulation protein (Abdel-Hamid et al. 2001). POX activity is similar to that of PDH, and it was originally hypothesized that a PDH mutant would not require acetate for growth due to the activity of POX (Chang and Cronan 1982). Despite the significant activity of POX, PDH mutants are not able to sustain growth without acetate, either as a result of limited flux via POX or a limited rate of acetate utilization (Chang and Cronan 1982). Studies of *poxB* under an alternate promoter such as one that is constitutive or IPTG inducible demonstrated that POX could sustain growth in PDH mutants (Abdel-Hamid et al. 2001). These strains had a 33 % decrease in maximum growth rates in batch fermentations, 9-25 % lower maximum growth yields on glucose and 29-39 % lower carbon (glucose) conversion efficiencies to biomass in continuous cultures. Although POX was able to support aerobic growth of a PDH mutant, the result suggests that it was less energetically efficient due to the requirement of ATP in activating acetate to acetyl CoA by ACS (Abdel-Hamid et al. 2001). Mutants of *poxB* grew to lower cell densities compared to wild type and are unable to utilize the acetate produced during exponential growth (Contiero et al. 2000).

PEP Synthase (PPS)

Another enzyme involved in the direct conversion of pyruvic acid and PEP is PEP synthetase (PPS) (1, Figure 2). This gluconeogenic enzyme catalyzes the phosphorylation of pyruvate with ATP to produce one molecule each of PEP, AMP and inorganic phosphate (Narindrasorasak and Bridger 1977). This reaction is believed to follow a ping-pong kinetic pattern during which the enzyme is first phosphorylated by ATP, and then this enzyme intermediate transfers the phosphoryl group to pyruvate (Narindrasorasak and Bridger 1977). The over-expression of PPS in *E. coli* grown on glucose appeared to create a futile cycle (Patnaik et al. 1992). The PEP generated from PPS will primarily be used by both PTS and pyruvate kinase (PYK) in the regeneration of pyruvate and ATP from ADP (Patnaik et al. 1992). When overexpressed 15- fold above native activity, an increase in oxygen consumption was observed (Patnaik et al. 1992). A 30-fold increase of PPS expression resulted in a two-fold increase in glucose consumption presumably due to an increased PEP/pyruvate ratio; this increase led to an accumulation of pyruvate and acetate (Patnaik et al. 1992). The formation of acetate associated with the over-expression of PPS generates one mole of ATP via the action of ACK and PTA and is thought to alleviate partially the ATP debt produced by PPS (Patnaik et al. 1992).

Malic Enzyme (MAE)

Malic enzyme (13, Figure 2)catalyzes the reversible $NAD(P)^-$ mediated oxidation of malate to pyruvate and CO_2 with the concomitant reduction of the coenzyme (Yamaguchi et al. 1973). *E. coli* contains two malic enzymes: one specific for $NADP^+$ (EC 1.1.1.40) encoded by *maeB* and the other specific for NAD^+ (EC 1.1.1.38) encoded by *sfcA*. Both enzymes are involved in oxidation of malate, decarboxylation of OAA and the reduction of an α-keto acid (Iwakura et al. 1979). The NAD^+ linked malic enzyme is associated with the catabolism of malic

acid (Iwakura et al. 1979) and has K_m values of 0.4 mM for malate, 55 μM for NAD^+, and 5 mM for OAA. The enzyme requires a divalent metal ion for activity with a K_m value for Mn^{2+} of 0.32 mM (Yamaguchi et al. 1973). This enzyme is inhibited by CoA and ATP, and is activated by aspartate (Sanwal 1970). The $NADP^-$ specific malic enzyme supplies the cell with pyruvate and acetyl CoA with a K_m value of 2.3 mM for malate and requires K^+ for activity with a K_m value of 5.9 mM (Iwakura et al. 1979). This enzyme is inhibited by malonate, tartronate glutarate, and DL-tartrate (Iwakura et al. 1979) as well as by acetyl CoA, NADPH and cyclic AMP (Sanwal 1970). While the reaction between malate and pyruvate is reversible, the kinetics and thermodynamics of the reaction mediated by the malic enzymes strongly favors the oxidative decarboxylation of malate to pyruvate with a final malic acid concentration at only 3.5 % of the pyruvate concentration at equilibrium under normal physiological conditions (Harary et al. 1953).

Acetyl CoA Synthetase (ACS), Acetate Kinase (ACK), Phosphotransacetylase (PTA)

When grown under aerobic conditions in the presence of excess glucose, *E. coli* excretes acetate due to an imbalance between the glycolytic pathway and the TCA cycle. The accumulation of acetate is attributed to an "overflow metabolism" which permits the cell to generate ATP when the TCA cycle and respiratory chain are saturated (Chang et al. 1999). This accumulation of acetate limits cell growth and can decrease the production of recombinant proteins (Kleman and Strohl 1994). The concentration of acetate accumulated is strongly dependent on the strain with up to a 3-fold difference in acetate between strains grown under the same conditions (Kleman and Strohl 1994; van de Walle and Shiloach 1996). Growth rate and media composition also influence the generation of acetate (Kleman and Strohl 1994). There are three major enzymes involved in the interconversion of acetate and acetyl CoA in *E. coli*:

phosphotransacetylase (PTA) EC 2.3.1.8, which is coupled with acetate kinase (ACK) EC 2.7.2.1, and acetyl CoA synthetase (ACS) EC 6.2.1.1.

ACS (10, Figure 2) is repressed by glucose, and this enzyme is induced by acetate as the stationary phase is approached and glucose becomes limiting. This high affinity enzyme catalyzes the irreversible activation of acetate to acetyl CoA through an enzyme bound intermediate acetyl AMP releasing pyrophosphate (Kumari et al. 2000). This enzyme has a K_m value for acetate of 200 μM and scavenges low concentrations of acetate once the primary carbon source (glucose) is consumed (Kumari et al. 1995; Contiero et al. 2000). ACS plays a key role in the switch from exponential growth to stationary growth, and it is regulated at the transcription level by cyclic AMP receptor protein (CRP), the oxygen regulator FNR, the glyoxylate shunt repressor IclR and activator FadR, the stationary phase sigma factor σ^s, as well as ACK, PTA and isocitrate lyase (Shin et al. 1997; Kumari et al. 2000). An ACS mutant initially grew similar to the wild type in a glucose controlled high cell density fermentation, but eventually growth rate decreased because cells were unable to utilize the low concentrations of acetate accumulated during exponential growth (Contiero et al. 2000). Another strain of ACS mutant grew comparable to wild type cells at high acetate concentrations, but did not grow as well when grown on low acetate concentrations (Kumari et al. 1995).

PTA (8, Figure 2) and ACK (9, Figure 2) are constitutively expressed and reversibly catalyze the reaction of the excess acetyl CoA produced by the PDH complex during exponential growth to acetate and ATP (Chang et al. 1999). ACK and PTA are also utilized in the consumption of excreted acetate. However, since these enzymes have a low affinity for acetate and acetyl phosphate (K_m values between 7-10 mM), they seem to function for acetyl CoA generation principally during high concentrations of acetate (Contiero et al. 2000). Strains with a

mutation in ACK accumulated some acetate due to the spontaneous hydrolysis of acetyl phosphate produced by PTA and decreased assimilation of acetate (Luli and Strohl 1990; Contiero et al. 2000). Furthermore, these strains did not reach as high a cell density as the wild type although their growth rate was only slightly reduced (Contiero et al. 2000). PTA mutants could not divert excess acetyl CoA from aerobic growth on glucose, and accumulated pyruvate, D-lactate and L-glutamate (Diaz-Ricci et al. 1991; Chang et al. 1999). These mutants displayed a long lag phase and slower growth with a lower final cell density compared to wild type, characteristics which result from a retardation of the glucose uptake rate caused by a lower PEP/pyruvate ratio (Chang et al. 1999; Contiero et al. 2000).

Citrate Synthase

Acetate accumulates in *E. coli* due to an imbalance between the rates of the glycolytic pathway and the subsequent utilization of the carbon for biomass and energy production. Citrate synthase (CS, EC 2.3.3.1) (11, Figure 2) catalyzes what is believed to be the rate limiting reaction for the incorporation of carbon into the cycle (Krebs and Lowenstein 1960). *E. coli* citrate synthase, like those found in other Gram-negative bacteria, is a homo-hexameric enzyme. In *E. coli* CS is a product of the *gltA* gene and is allosterically inhibited by NADH (Nguyen et al. 2001). *E. coli* CS has a K_m value of 200 μM for acetyl CoA and 100 μM for OAA with sigmoidal substrate dependence (Patton et al. 1993). Expression of the *E. coli* CS during both aerobic and anaerobic growth is controlled by ArcA, which responds to the availability of nutrients and carbon source in the media (Park et al. 1994). The CS of Gram-positive bacteria, archaea and eukaryotes are homo-dimers and are not inhibited by NADH, but instead are isosterically inhibited by ATP (Robinson et al. 1983). A dimeric CS-like enzyme, similar to those found in Gram-positive bacteria, archaea and eukaryotes, is also found in some Gram-

negative bacteria including *E. coli* (Patton et al. 1993) and *Pseudomonas aeroginosa* (Solomon and Weitzman 1983). This second CS-like enzyme displayed a K_m of around 11 μM for acetyl CoA and 7 μM for OAA (Patton et al. 1993). This enzyme was later found to be methylcitrate synthase (*prpC*, EC 4.1.3.31), which catalyzes the condensation of propionyl CoA and OAA to form methylcitrate and is induced during growth on propionate (Gerike et al. 1998). Gram-positive *Bacillus subtilis* possesses two dimeric citrate synthases that are not affected by NADH (Jin and Sonenshein 1994). These two enzymes are encoded by the genes *citA* and *citZ*. A *citA* mutation did not affect cell growth and sporulation, while a *citZ* mutation reduced CS activity significantly and caused sporulation defectives, results that suggested that the *citZ* product is the primary CS of *B. subtilis* (Jin and Sonenshein 1994). This major CS of *B. subtilis* is hyperbolically dependent on acetyl CoA and OAA with K_m values of 7-15 μM and 6.5-22 μM, respectively. The enzyme displayed competitive inhibition by ATP for acetyl CoA (Jin and Sonenshein 1996). A study in which the primary CS from *B. subtilis* was expressed in *E. coli* KO11 increased cell growth and ethanol production, a result which demonstrates that the native *E. coli* CS limited the carbon flux into the TCA cycle (Underwood et al. 2002).

PEP Carboxylase

As noted previously PPC (EC 4.1.1.31) (12, Figure 2) carboxylates PEP to replenish the OAA depleted by various biosynthetic pathways. While this reaction does not directly affect the pyruvate pool within the cell, a reduction of the PEP concentration has a twofold impact upon the pyruvate concentration: 1) PEP is directly converted to pyruvate via the glycolytic enzyme PYK, and 2) the reduction of PEP decreases the glucose consumption rate due to the requirement of PTS for PEP (Gokarn et al. 2001). PPC is activated by acetyl CoA, fructose 1,6-bisphosphate, and cytidine 5'-diphosphate (CDP) with some synergism occurring between acetyl CoA and

fructose 1,6-bisphosphate or CDP, and is competitively inhibited by aspartate (McAlister et al. 1981) and malate (Yoshinaga 1977). In its active form PPC has a K_m value for PEP of 1.77 mM, while the K_m value for the inactive form is 23.5 mM (McAlister et al. 1981). The over-expression of PPC in *E. coli* in conjunction with the derepression of the glyoxylate shunt decreased the accumulation of acetate with little change in cell growth due to the diversion of carbon, in the form of PEP, to biomass (Farmer and Liao 1997).

Synopsis

The numerous enzyme reactions described above, which involve pyruvate, demonstrate this biochemical's importance in central metabolism. To achieve the ultimate goal of accumulating pyruvate, mutations in the genes that metabolize pyruvate are required. The greatest accumulation of pyrvate in *E. coli* in which these deletions were introduced was observed in a *aceE, aceF, ldhA, poxB, pps, pflB* strain (Zelic et al. 2003). A high concentration of pyruvate has also been achieved in an *aceF* strain (Tomar et al. 2003). Both of these strains require acetate for growth, and thus it is necessary for acetate to be consumed in the presence of glucose. Unfortunately, previous research has shown that *acs* is repressed by glucose. Ideally, in order to consume acetate in the presence of glucose, ACS activity would need to be high in the presence of glucose. As a rate-limiting step in the TCA cycle, CS might also prevent the complete utilization of acetyl CoA. As such, both ACS and CS may be implicated in the limited consumption of acetate. The rate of acetate uptake and growth were observed to slow in both pyruvate-accumulating strains (Tomar et al. 2003; Zelic et al. 2003). These results suggest that the uptake of acetate may be limiting higher cell growth, and increasing the rate of acetate utilization might increase cell growth and the subsequent production of pyruvate.

CHAPTER 2

HYPOTHESES

The analysis of previous work leads to the following hypotheses:

1. The overexpression of the *acs* gene coding for acetyl CoA synthetase will increase cell growth rate and acetate utilization, and thus increase the rate of pyruvate accumulation in a pyruvate-generating strain.
2. The overexpression of the *citZ* gene from *B. subtilis* coding for CS will increase cell growth rate and acetate utilization, and thus increase the rate of pyruvate accumulation in a pyruvate-generating strain.

CHAPTER 3

MATERIALS AND METHODS

The following experiments were conducted to test the above hypotheses.

Strain Selection:

E. coli YYC202 (Hfr *zbi*::Tn*10 poxB1* Δ(*aceEF*) *rpsL pps-4 pfl-1*) (kindly provided by Professor John E. Cronan, Jr. of the Department of Microbiology, University of Illinois) was used in this study. An additional deletion of *ldhA:*Kan was introduced into this strain and the resulting strain, ALS 929, was used in subsequent studies. The deletion of the lactate dehydrogenase gene was verified by an enzyme assay developed by Bunch et al. (1997), the protocol of which is located in Appendix B.1. The biochemical steps from pyruvate that have been deleted in *E. coli* ALS 929 are shown in Figure 3. The *E. coli* MG1655 *acs* gene and the *B. subtilis citZ* gene were independently isolated and expressed on the plasmid pTrc99A. These two strains (i.e., ALS 929 (pTrc99A-*acs*) and ALS 929 (pTrc99A-*citZ*)) in addition to the "control" ALS 929 were compared for acetate consumption, cell growth and pyruvate accumulation. The construction of pTrc99A-*acs* and pTrc99A-*citZ* are detailed below.

Citrate synthase:

Bacillus subtilis genomic DNA was purified using a Gentra Puregene DNA purification kit (DNA Purification from from 5 mL Gram-Positive Bacterial Culture) using 5 mL of a 50 mL culture grown to mid exponential phase (5 mL overnight culture used to inoculate 50 mL Nutrient broth at 100X dilution grown to an OD of approx. 0.5). The citrate synthase gene (*citZ*) was isolated from genomic DNA using PCR (*Pfu*) with primers developed to introduce four

Figure 3. Aerobic and anaerobic metabolic pathways immediately surrounding the pyruvate node, with the deletions present in ALS 929 (YYC 202 *ldhA*) depicted by double lines through the pathway.

Enzymes

1. PEP synthase (PPS)
2. Phosphotransferase system (PTS)
3. Pyruvate kinase (PYK)
4. Lactate dehydrogenase (LDH)
5. Pyruvate formate lyase (PFL)
6. Pyruvate dehydrogenase complex (PDH)
7. Pyruvate oxidase (POX)
8. Phosphotransacetylase (PTA)
9. Acetate kinase (ACK)
10. Acetyl CoA synthetase (ACS)
11. Citrate synthase (CS)
12. PEP carboxylase (PPC)
13. Malic enzyme (MAE)
14. Malate dehydrogenase (MDH)

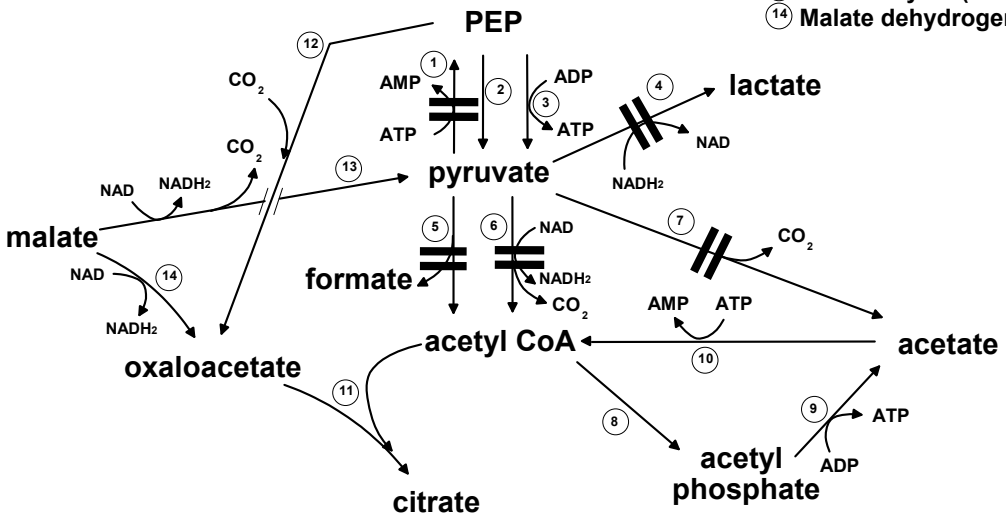

Shine-Dalgarno sequences of different distances from the ribosomal binding site (notated SD4, SD5, SD6, and SD7). The resulting PCR products were gel isolated (Qiagen QIAquick Gel Extraction Kit) to separate the amplified genes from the genomic DNA and primers. The isolated PCR product and a pTrc99a plasmid were then digested using the *HndIII* and *KpnI* restriction enzymes. The resulting digests were subsequently ligated into the prepared plasmid and used to transform electrocompetently prepared *E. coli* ALS 225 (BTX Electroporation System Electrocell Manipulator 600). The resulting transformants were plated on Luria-Bertani plates supplemented with glucose and ampicillin at varying dilutions for isolation. Individual colonies were selected and grown in an overnight 5 mL tube for miniprep (Qiagen QIAprep Spin MiniprepKit). The isolated plasmids were then digested with the *KpnI* and *HindIII* restriction enzymes and analyzed on a gel to verify the insertion of *citZ* (1143 bp). Four isolates from each Shine-Dalgarno length product were selected upon positive DNA gel results, which displayed bands for both the plasmid and insert, and were frozen. These isolates were then used to conduct enzyme assays in order to select the best clone for use in research. In order to measure enzyme activity the plasmids from the *E. coli* ALS 225 clones were used to transform *E. coli* W620, a strain that has a deletion in the native citrate synthase gene (*gltA*$^{-}$). The ALS 225 (pTrc99a-*citZ*) strains were also analyzed on SDS-Page gels to verify the presence of a protein correlating with the size of *B. subtilis* citrate synthase monomer (41-42 kDa). The codons of *citZ* from *B. subtilis* were also compared to the preferred codon usage of *E. coli* as further analysis of the compatibility of gene in the expression host. The samples used for enzyme assay were dialyzed in a solution of 20 mM Tris-HCl (pH 8.0) and 20% glycerin after preparation using a French Pressure Cell. A strain of *E. coli* W620 was also transformed with the plasmid pLOI2514 (kindly provided by Dr. Lonnie Ingram at the University of Florida), which contains a *Taq*-

prepared *citZ* from *B. subtilis*. Enzyme activity was measured using an assay adapted from the protocol developed by Srere et al. (1963). The complete details of the enzyme assay are described in Appendix B.2.

Acetyl CoA synthetase:

E. coli MG1655 genomic DNA using a Gentra Puregene DNA purification kit (DNA Purification from from 5 mL Gram-Negative Bacterial Culture) using 5 mL of a 50 mL culture grown to mid exponential phase (5 mL overnight culture used to inoculate 50 mL Nutrient broth at 200X dilution grown to an OD of approx. 0.5). The acetyl CoA synthetase gene (*acs*) was isolated from genomic DNA using PCR (*Pfu*) with primers developed to introduce four Shine-Dalgarno sequences of different distances from the ribosomal binding site (notated SD4, SD5, SD6, and SD7). Of the four primers used, only three amplified the *acs* gene (SD4, SD5, and SD6). The resulting PCR products were gel isolated (Qiagen QIAquick Gel Extraction Kit) to separate the amplified genes from the genomic DNA and primers. These genes and a pTrc99a plasmid were then digested using the *HndIII* and *KpnI* restriction enzymes. The resulting digested genes were subsequently ligated into the prepared plasmid and used to transform electrocompetently prepared *E. coli*, ALS 225 (BTX Electroporation System Electrocell Manipulator 600). The resulting transformants were plated on Luria-Bertani plates supplemented with glucose and ampicillin at varying dilutions for isolation. Individual colonies were selected and grown in an overnight 5 mL tube for miniprep (Qiagen QIAprep Spin MiniprepKit). The isolated plasmids were then digested with the *KpnI* and *HindIII* restriction enzymes and analyzed on a gel to verify the insertion of *acs* (2148 bp). Four isolates from each Shine-Dalgarno length product were selected upon positive DNA gel results, which displayed bands for both the plasmid and insert, and were frozen. These isolates were then used to conduct enzyme assays in

order to select the best clone for use in research. The activity of the enzyme was measured using a combination of the protocols of Jones and Lipmann (1955) and Brown, Jones-Mortimer and Kornberg (1977). The enzyme assay protocol can be found listed in Appendix B.3.

Batch Fermentations:

Batch fermentations of ALS 929 were conducted using a New Brunswick BioFlo 2000 2L vessel with a 1.5 L working volume. The media used was adapted from the media developed by Zelic et al. (2003) and contained per liter: 10 g glucose, 6.42 g ammonium acetate, 1.5 g $NaH_2PO_4 \cdot H_2O$, 3.25 g KH_2PO_4, 3.27 g $K_2HPO_4 \cdot 3H_2O$, 0.2 g NH_4Cl, 2.0 g $(NH_4)_2SO_4$, 1.0 g $MgSO_4 \cdot 7H_2O$, 10.0 mg $CaCl_2 \cdot 2H_2O$, 20.0 mg thiamine·HCl, 0.5 g L-isoleucine, 18.3 mg $FeSO_4 \cdot 7H_2O$, 50 mL of a trace element solution, and 100 mg kanamycin. The trace element solution contained per liter: 15.0 mg $ZnSO_4 \cdot 7H_2O$, 7.6 mg $CuCl_2 \cdot H_2O$, 75.0 mg $MnSO_4 \cdot H_2O$, 52.6 mg $CoCl_2 \cdot 6H_2O$, 3.6 mg H_3BO_3, 53.2 mg $AlCl_3 \cdot xH_2O$, and 15.0 mg $Na_2MoO_4 \cdot 2H_2O$. The pre-inoculum was developed by Chang and Cronan (1982) and contained per liter: 10.00 g tryptone, 1.00 g yeast extract, 5.00 g NaCl, 1.33 g $Na(CH_3COO) \cdot 3H_2O$, and 40 mg kanamycin. A 30 mL pre-inoculum was grown in a 250 mL shake flask for 8 - 10 hours at 37°C and 250 rpm, 5 mL of which were used to inoculate a 50 mL inoculum culture. The inoculum, also developed by Zelic et al. (2003), contained per liter: 10.0 g glucose, 2.3 g sodium acetate, 5.66 g $Na_2HPO_4 \cdot 7H_2O$, 1.5 g KH_2PO_4, 0.25 g NaCl, 0.5 g NH_4Cl, 0.1 g $MgSO_4 \cdot 7H_2O$, 13.0 mg $CaCl_2 \cdot 2H_2O$, 20 mg thiamine·HCl, 0.5 g L-isoleucine, and 100 mg kanamycin. The 50 mL inoculum was grown in a 250 mL shake flask for 8 - 10 hours at 37°C and 250 rpm, and the entire volume was used to inoculate the fermenter. The fermenter was operated at 37° C with pH control at 7.0 using 20% NH_4OH and 20% H_2SO_4. The agitation at inoculation was 500 rpm, but was increased to 750 rpm and 1000 rpm as the fermentation progressed in order to maintain the

DO at or above 30% to 40%. Foaming was controlled using a 5% Antifoam C solution. During the fermentation 30 g of glucose and 9.63 g of ammonium acetate (in a total volume of 70 mL) were added to prolong the growth and pyruvate production phase of the organism.

Batch fermentations of ALS 929 (pTrc99a-*acs*) were conducted with the same conditions and media except for the addition of ampicillin at 50 mg/L (fermenter and inoculum) or 100 mg/L in the pre-inoculum. When the OD reached between 1.5 and 2.5 the fermentation was induced with isopropyl-β-D-thiogalactoside (IPTG) at a concentration of 20 μM.

Continuous Fermentation:

Glucose Limiting Conditions:

Glucose limiting continuous culture fermentations of ALS 929 were conducted in New Brunswick BioFlo III in a 2.5 L vessel and 1.5 L working volume. The media used was adapted from the media developed by Zelic et al. (2003) and contained per liter: 5.0 g glucose, 6.42 g ammonium acetate, 3.4 g $Na_2HPO_4 \cdot 7H_2O$, 1.5 g KH_2PO_4, 0.2 g NH_4Cl, 2.0 g $(NH_4)_2SO_4$, 0.2 g $MgSO_4 \cdot 7H_2O$, 10.0 mg $CaCl_2 \cdot 2H_2O$, 20.0 mg thiamine·HCl, 0.5 g L-isoleucine, 11.0 mg $FeSO_4 \cdot 7H_2O$, 50 mg $Na_2EDTA \cdot 2H_2O$, 50 mL of a trace element solution, 100 mg kanamycin, and 0.2 ml (dilution rates < 0.18 h^{-1}), or 0.6 ml (dilution rate > 0.18 h^{-1}) of Antifoam C. The trace element solution was the same as described in the batch experiments. The pre-inoculum was identical to that used with the batch fermentations, while the inoculum differed in containing $Na_2HPO_4 \cdot 7H_2O$ at 3.4 g/L instead of 5.66 g/L. The fermenter was operated at 37° C with pH control at 7.0 using 20% NH_4OH and 20% H_2SO_4. An initial batch phase was conducted until the OD reached approximately 2.0 (about 16 hours after inoculation). At this time the feed pump from the reservoir commensed at 0.39 L/hr to initiate a fed-batch phase transition period before the continuous phase. This fed-batch phase continued until approximately 200 mL was added to

the vessel, at which time the effluent pump was turned on and the fermentation entered a continuous operation. The target dilution rates for the continuous fermentations were 0.15 h^{-1}, 0.18 h^{-1}, 0.26 h^{-1}, 0.33 h^{-1}, and 0.4 h^{-1}. Steady state samples were collected after 3 - 5 volume changes. The agitation was maintained at 500 rpm.

Glucose limiting continuous fermentations of ALS 929 (pTrc99a-*acs*) were conducted as above with 50 mg/L ampicillin and 11.3 g/L sodium acetate included in the media. The culture was induced by introducing IPTG into the reservoir to achieve a final concentration of 20 μM. The target dilution rates for the continuous fermentations were 0.14 h^{-1}, 0.18 h^{-1}, 0.26 h^{-1}, 0.3 h^{-1}, 0.33 h^{-1}, and 0.40 h^{-1}.

Nitrogen Limiting Conditions:

One nitrogen limiting continuous fermentation of ALS 929 was also completed. The medium was adapted from the glucose limiting conditions (Zelic et al. 2003), and contained per liter: 5.0 g glucose, 11.3 g sodium acetate, 3.4 g $Na_2HPO_4 \cdot 7H_2O$, 1.5 g KH_2PO_4, 0.2 g NH_4Cl, 0.853 g $(NH_4)_2SO_4$, 1.183 g $KHSO_4$, 0.2 g $MgSO_4 \cdot 7H_2O$, 10.0 mg $CaCl_2 \cdot 2H_2O$, 20.0 mg thiamine·HCl, 0.5 g L-isoleucine, 11.0 mg $FeSO_4 \cdot 7H_2O$, 50 mg $Na_2EDTA \cdot 2H_2O$, 50 mL of a trace element solution, and 100 mg kanamycin. The pH was adjusted to 6.8 by adding 2.7 ml/L 20% KOH. The nitrogen limiting culture was operated under the same conditions as the glucose limiting culture. The target dilution rate studied for nitrogen limitation was 0.26 h^{-1}, and the pH was controlled with 20% KOH instead of 20% NH_4OH.

Analyses

Cell growth was monitored via optical density measurements at a wavelength of 550 nm. During the batch fermentation approximately 10 mL of sample were collected for each data point, with an additional 10 mL sample taken for enzyme analysis of acetyl CoA synthetase

(Jones and Lipmann, 1955; Brown et al. 1977). A separate batch fermentation was conducted to correlate the dry cell weight (DCW) for a given OD.

For the continuous fermentation two 10 mL samples were withdrawn directly from the vessel into two vials containing 20 mL -80 ºC methanol to measure the intracellular concentrations of NADH and NAD^+ using a cycled assay developed by Bernofsky and Swan (1973) and Leonardo et al. (1996) described in Appendix B.4. Three 20 mL samples were also taken to calculate the DCW, for acetyl CoA synthetase analysis and for HPLC analysis. Off gas analyses were utilized to calculate the O_2 and CO_2 consumption (or production) rates at each dilution rate volume. The flow rate of the continuous culture was measured by timed collection of an effluent.

For HPLC analysis, samples were centrifuged at 5468 x *g* for 20 minutes and the supernatant solution used for subsequent analyses. The supernatant was measured for several products, including glucose, lactate, pyruvate, acetate, succinate, formate and ethanol. The method used a Shimadzu HPLC (LC-6A pump, SCL-6B systems controller and auto-injector) with a refractive index detector (Waters Model 2410) using a Coregel 64-H ion-exclusion column (Transgenic) and a mobile phase of 4 mN H_2SO_4 (Eiteman and Chastain, 1997).

CHAPTER 4

RESULTS

Citrate Synthase:

SDS-Page results of *E. coli* ALS 225 (pTrc99a-*citZ*) (Figure 4) illustrated that there was a protein band present in the area of 41-42 kDa in the lanes of the transformed strains, while being absent in the lane of the control wild type strain (ALS 225). However, there appeared to be an additional band in the 35 kDa area in the lanes of the transformed strains. Two of the isolates (ALS 225 (pTrc99a-*citZ* SD5B and SD4A)) appeared to have the thickest band of citrate synthase and were selected for further analysis in *E. coli* W620. The enzyme activity of the two new isolates W620 (pTrc99a-*citZ* 5B and 4A) were measured alongside MG1655 and W620 as a positive and negative control strain, respectively. These strains were grown and concentrated to 100X prior to cell lysis via a French Pressure cell and enzyme activity was measured both initially and after dialysis. However, the two isolates showed negligible enzyme activity when compared to the positive wild type control, and the activity of all the samples was lower after dialysis. *E. coli* codon usage comparison with the *citZ* codons showed a 51.9% preference of *E. coli* for the codons used in *citZ*.

Acetyl CoA Synthetase:

Shake flask studies were conducted using the four isolates of the three clones of *E. coli* ALS 225 (pTrc99a-*acs*) and *E. coli* ALS 225 as negative control for selection of the strain with the highest enzyme activity. The isolate SD4.2 was chosen as the transformant with the highest

Figure 4: SDS-PAGE gel of ALS 225 pTrc99a-*citZ* and ALS 225 as control. The citrate synthase monomer can be seen at 41 kDa while being absent in the control. An additional band around 35 kDa can also be found in the plasmid containing isolates.

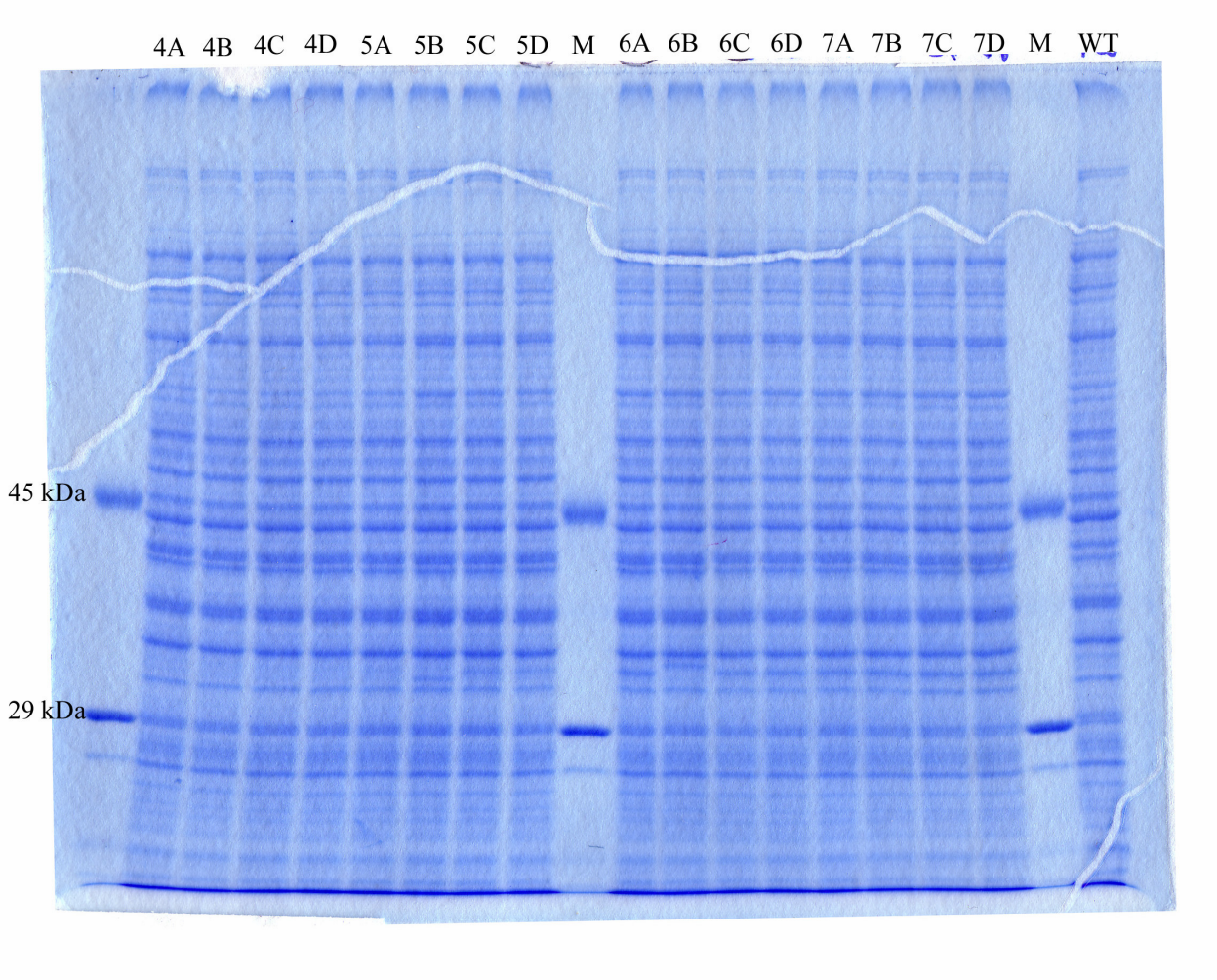
4A
4B
4C
4D
5A
5B
5C
5D
M
6A
6B
6C
6D
7A
7B
7C
7D
M
WT
45 kDa
29 kDa

enzyme activity, and the plasmid was isolated and transformed into ALS 929. The resulting strain ALS 929 (pTr99a-*acs*) SD4.2 (named KD423) was studied under varying degree of induction using IPTG concentrations of 10, 20, 50, 100, and 250 μM to optimize protein (Table 2).

Control Strain Batch Fermentations:

The batch fermentation of ALS 929 was replicated three times to establish the performance of this control strain used in these experiments. Figure 5 illustrates the behavior of the strain in these batch fermentations (complete results of experiments found in Appendix C.1). The protocol was to add a single dose of glucose and acetate when the OD reached about 7.0. When the OD of the cultures approached 25, the acetate concentration reached zero and the OD began to decrease. At this point, some glucose remained (e.g., about 4 g/L), and there was an increase in pyruvate production. The pyruvate concentration ultimately produced was around 12 g/L when the glucose was exhausted.

Two intervals of time during the fermentation were selected to calculate the rates of cell growth, substrate consumption and product formation. The two intervals selected were centered at an OD of 5 and an OD of 10, or times immediately preceding and following the addition of glucose and acetate. A summary of these results for the batch runs can be found in Table 3. The maximum growth rate observed for ALS 929 was 0.47 h^{-1}, which occurred centered at an OD of 5. By an OD of 10, the growth rate had fallen by about 33% to 0.31 h^{-1}. At an OD of 5 the mean mass ratio of the glucose to acetate uptake was about 1.68 g/g, the mean specific pyruvate production rate was 0.42 g/gh, and the mean mass ratio of pyruvate production to glucose consumption was 0.31 g/g. This glucose to acetate rate indicates that the cells require

Table 2: Summary of specific enzyme activity for KD 423 grown in shake flasks, and induced with varying amounts of IPTG. ALS 929 was used as the control strain.

Sample	Average Specific Activity	Standard Deviation
mM IPTG	mU/mg	
10	2.7	1.2
20	12.5	0.5
50	8.9	5.1
100	7.5	7.4
250	16.7	4.0
control	7.9	

Figure 5: Cell growth and substrate and product concentrations during the course of a fermentation of ALS 929 (conducted 6/22/04). Fermentation conducted in BioFlo 2000 at 37º C and pH 7.0. The dissolved oxygen was maintained at above 40% using 1.5 L/min air and by increasing the agitation from 500 rpm. Cell concentration (○) was monitored by optical density, while glucose (□), acetate (■) and pyruvate (▲) were measured via HPLC analysis.

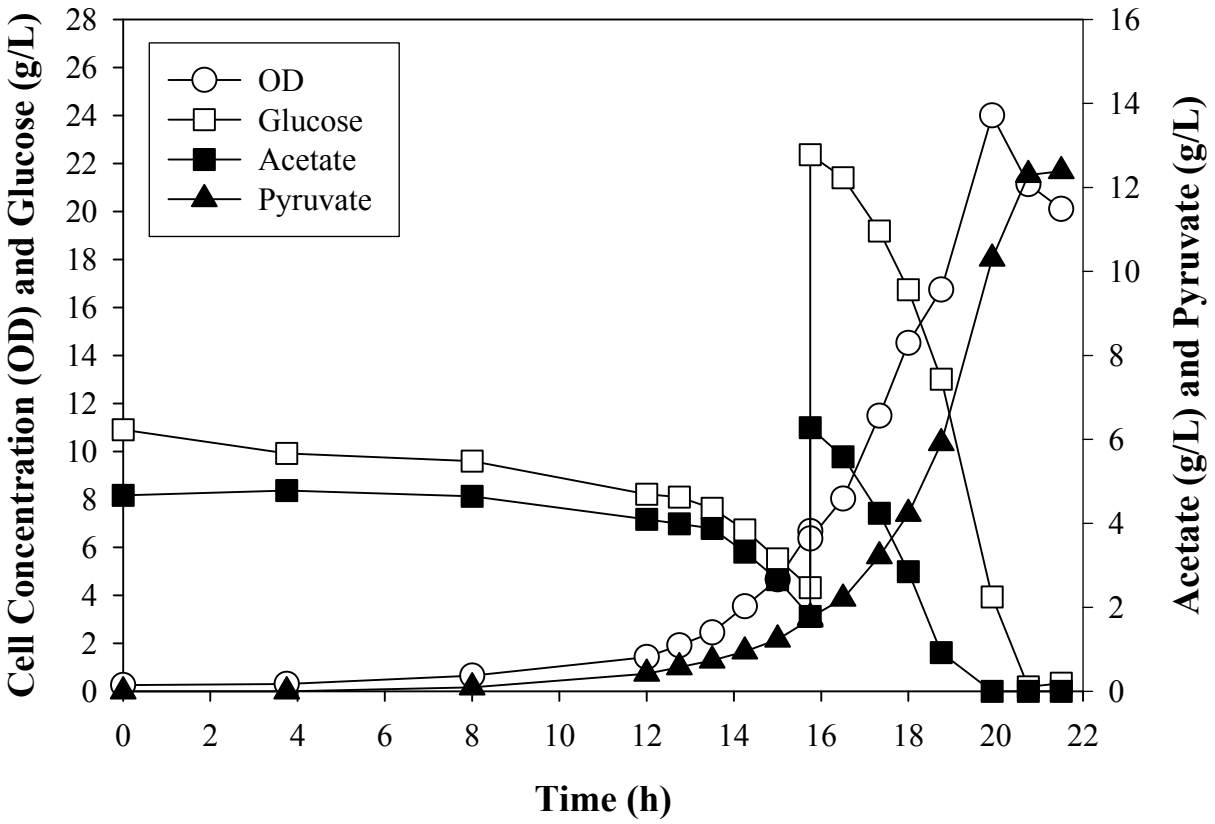
OD
Glucose
Acetate
Pyruvate
Cell Concentration (OD) and Glucose (g/L)
Acetate (g/L) and Pyruvate (g/L)
Time (h)
0
2
4
6
8
10
12
14
16
18
20
22
24
26
28

Table 3: Batch fermentations of ALS 929. Summary of growth rate μ, volumetric rates of glucose and acetate consumption (Q_G and Q_A) and pyruvate production (Q_P), the specific rates of glucose and acetate consumption (q_G and q_A) and pyruvate production (q_P), and the mass ratios of glucose to acetate consumption (G/A) and pyruvate production to glucose consumption (P/G).

	OD = 5									OD = 10								
	μ	Q_G	q_G	Q_A	q_A	Q_P	q_P	G/A	P/G	μ	Q_G	q_G	Q_A	q_A	Q_P	q_P	G/A	P/G
	h^{-1}	g/Lh	g/gh	g/Lh	g/gh	g/lh	g/gh	g/g	g/g	h^{-1}	g/Lh	g/gh	g/Lh	g/gh	g/lh	g/gh	g/g	g/g
6/8/04	0.48	1.93	1.40	1.05	0.76	0.65	0.48	1.84	0.34	0.28	3.44	1.25	1.85	0.67	1.20	0.44	1.86	0.35
6/14/04	0.47	2.00	1.46	1.17	0.85	0.55	0.40	1.71	0.27	0.26	3.17	1.15	1.69	0.61	0.68	0.25	1.87	0.21
6/22/04	0.46	1.71	1.25	1.14	0.83	0.54	0.39	1.50	0.31	0.37	2.59	0.94	1.56	0.57	1.15	0.42	1.66	0.44
mean	0.47	1.88	1.37	1.12	0.81	0.58	0.42	1.68	0.31	0.31	3.06	1.11	1.70	0.62	1.01	0.37	1.80	0.34
s.d.	0.01	0.15	0.11	0.06	0.05	0.06	0.05	0.17	0.03	0.06	0.44	0.16	0.15	0.05	0.29	0.11	0.12	0.12

1.68 g of glucose for every 1.0 g of acetate consumed for growth. Similarly, the organisms produce 0.31 g of pyruvate for every 1.0 g of glucose consumed at this growth rate. Although the growth was lower at an OD of 10 the glucose to acetate uptake ratio, the specific pyruvate production rate, and pyruvate yield remained statistically same as at the lower cell density (Student *t*-test, $p < 0.05$). In other words, the quantity of glucose required for growth relative to the amount of acetate required was not affected by cell growth. There was a 20% decrease in the rates of both acetate and glucose consumption. The volumetric rate of pyruvate production obviously was greater at the higher cell density. The maximum growth rate of 0.47 h^{-1} was used as the maximum dilution rate for the continuous fermentations.

Acetyl CoA Synthetase-Containing Strain Batch Fermentations:

The batch fermentations of the strain KD423 (ALS 929 (pTrc99a-*acs*)) were conducted both without induction and with induction using IPTG. Previous results from the shake flask experiment (Table 2) suggested that the range of 20 – 250 μM might permit sufficient protein formation, and therefore in these batch fermentations we examined cultures induced with IPTG initially at a concentration of 250 μM when the OD was between 1.5 and 2.0. IPTG concentrations of 100 μM and 20 μM were also explored in an attempt to improve cell growth while still allowing for sufficient protein production. Figure 6 illustrates the growth of a culture induced with 20 μM IPTG (replicate data found in Appendix C.2). Regardless of the IPTG concentration used the cultures consistently reached a maximum OD only of about 5.0. The ACS activity for the cells using 20 μM – 250 μM IPTG ranged from 60 to 90 mU/mg. An example of a batch fermentation of KD423 without induction is shown in Figure 7 (replicate data found in Appendix C.2). In this case, the culture attained an OD of about 20, and the ACS

Figure 6: Cell growth and substrate and product concentrations during the course of a fermentation of KD423 in the presence of 20 μM IPTG (conducted on 12/09/04). Fermentation conducted in BioFlo 2000 at 37º C and pH 7.0. The dissolved oxygen was maintained at above 40% using 1.5 L/min air and by increasing the agitation from 500 rpm. Cell concentration (○) was monitored by optical density, while glucose (□), acetate (■) and pyruvate (▲) were measured via HPLC analysis.

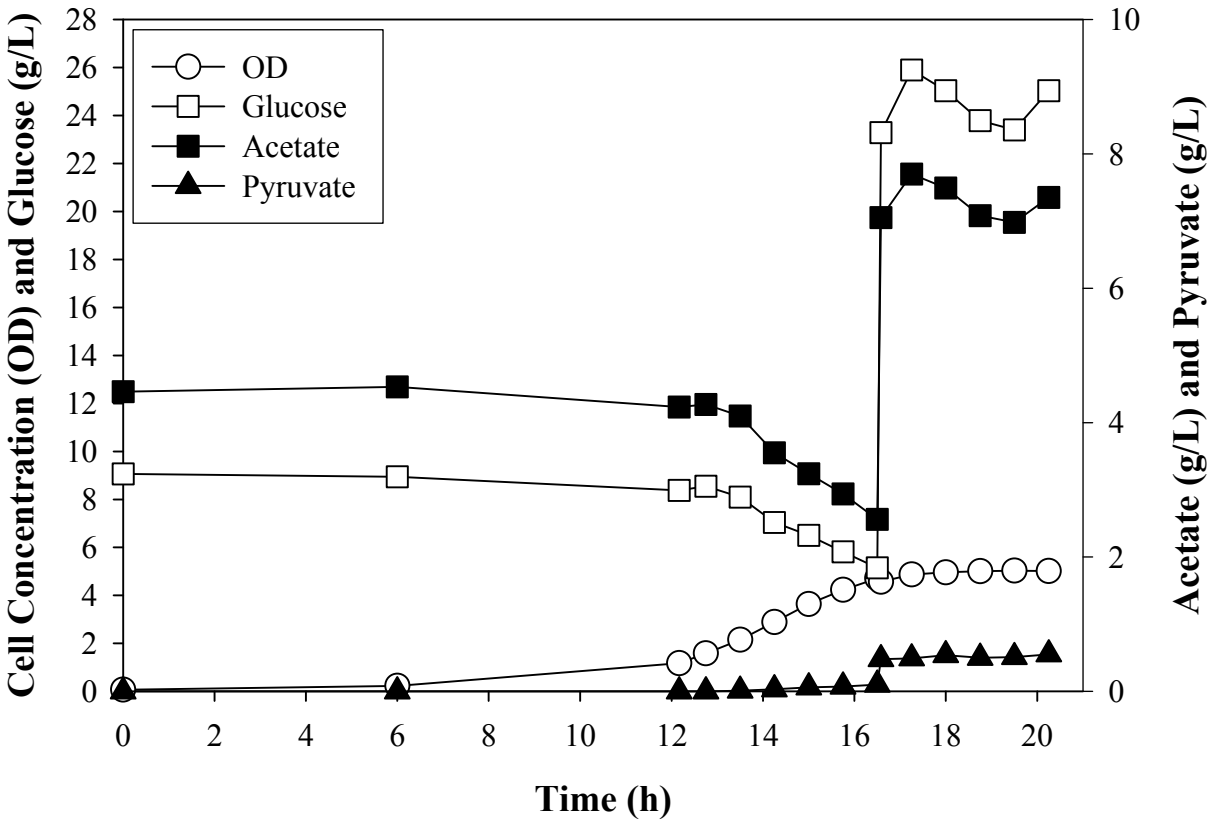
OD
Glucose
Acetate
Pyruvate
Cell Concentration (OD) and Glucose (g/L)
Acetate (g/L) and Pyruvate (g/L)
Time (h)
0
2
4
6
8
10
12
14
16
18
20
22
24
26
28

Figure 7: Cell growth and substrate and product concentrations during the course of an uninduced KD423 fermentation (conducted on 11/30/04). Fermentation conducted in BioFlo 2000 at 37º C and pH 7.0. The dissolved oxygen was maintained at above 40% using 1.5 L/min air and by increasing the agitation. Cell concentration (○) was monitored by optical density, while glucose (□), acetate (■) and pyruvate (▲) were measured via HPLC analysis.

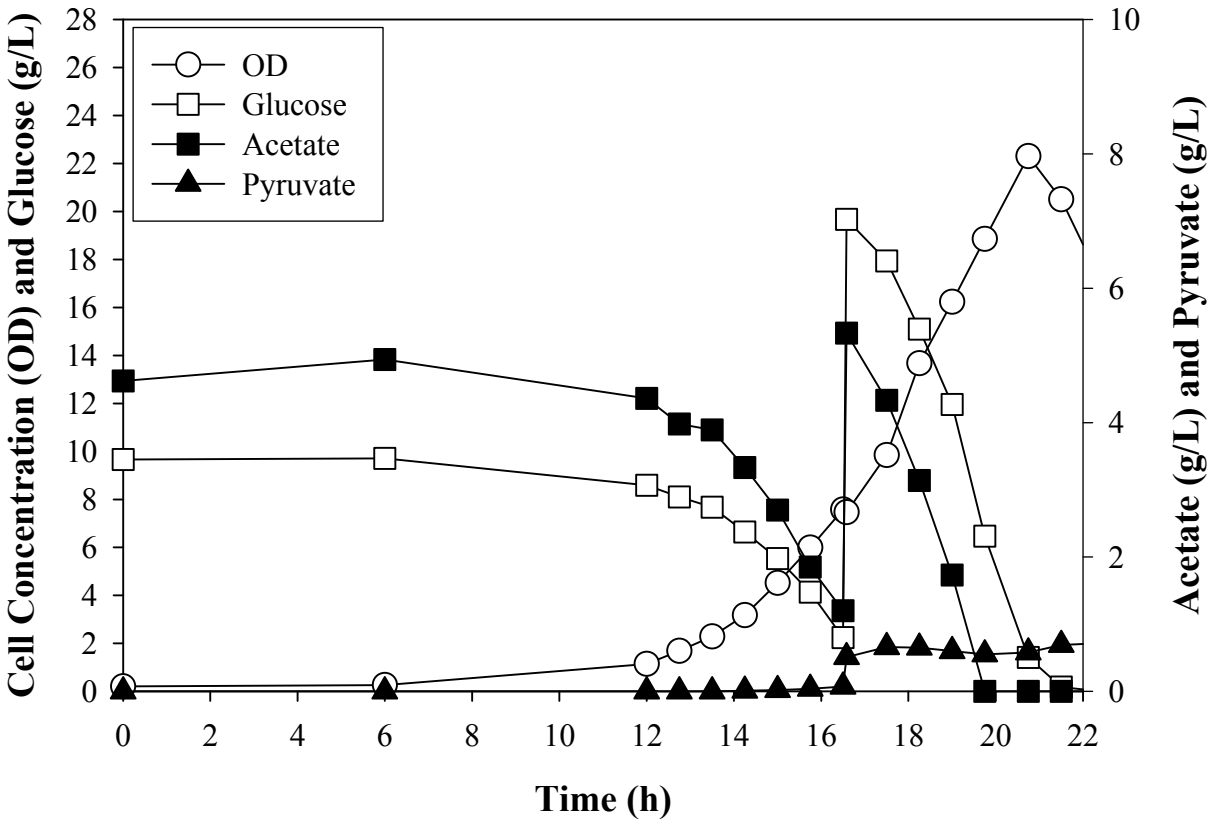
OD
Glucose
Acetate
Pyruvate
Cell Concentration (OD) and Glucose (g/L)
Acetate (g/L) and Pyruvate (g/L)
Time (h)
0
2
4
6
8
10
12
14
16
18
20
22
24
26
28

activity ranged from 2 to 5.5 mU/mg. In all KD423 fermentations (with and without IPTG) the pyruvate concentration never exceeded 1.0 g/L.

Table 4 is a summary of the consumption and production rates immediately before and immediately after the addition of glucose and acetate. A comparison of these rates from the batch cultures of KD 423 and ALS 929 was done using the Student *t*-test with a 95% confidence interval. For the uninduced cultures these calculations were made at an OD of 5 and an OD of 10, while for the induced culture the calculations were accomplished only at an OD of 2.5 since growth stopped an OD of about 5. For the uninduced fermentations the maximum growth rate was 0.4 h^{-1}, only slightly lower than was observed for ALS 929, but still comparable. At an OD of 5, the glucose to acetate ratio was about 1.9 g/g, while at an OD of 10 this ratio was not significantly different. Moreover, this ratio was the same as the values obtained for ALS 929 (Table 3). At both cell densities, the pyruvate production rates were very low (0.02 - 0.04 g/g), and hence so were the pyruvate yields (0.01 - 0.05 g/g). The specific rates of acetate consumption were not different in the fermentations of uninduced KD423 than in the fermentations of ALS 929.

In the fermentations induced with 20 μM IPTG, the growth rate, the ratio of acetate and glucose consumption rates, and pyruvate specific production rate, were similar ($p < 0.05$) to values observed for uninduced KD423 at the higher cell density. It is particularly noteworthy that the specific acetate consumption rate did not change despite expression of the *acs* gene, which serves to metabolize acetate.

Continuous Fermentations:

The media used for the batch fermentation had to be adapted for use in a continuous fermentation due to a small quantity of precipitate, which settled out and collected within the

Table 4: Batch fermentation of KD423 [ALS 929 (pTrc99a-*acs*)]. Summary of growth rate μ, volumetric rates of glucose and acetate consumption (Q_G and Q_A) and pyruvate production (Q_P), the specific rates of glucose and acetate consumption (q_G and q_A) and pyruvate production (q_P), and the mass ratios of glucose to acetate (G/A) and pyruvate production to glucose consumption (P/G).

No IPTG added

	OD = 5									OD = 10								
	μ h^{-1}	Q_G g/Lh	q_G g/gh	Q_A g/Lh	q_A g/gh	Q_P g/Lh	q_P g/gh	G/A g/g	P/G g/g	μ h^{-1}	Q_G g/Lh	q_G g/gh	Q_A g/Lh	q_A g/gh	Q_P g/Lh	q_P g/gh	G/A g/g	P/G g/g
11/30/04	0.39	1.87	1.42	0.93	0.71	0.02	0.02	2.00	0.01	0.35	2.58	0.96	1.27	0.47	0.12	0.04	2.04	0.04
12/16/04	0.41	1.89	1.45	1.04	0.80	0.03	0.02	1.80	0.02	0.36	2.23	0.81	1.61	0.58	0.12	0.04	1.40	0.05
mean	0.40	1.88	1.44	0.99	0.76	0.03	0.02	1.90	0.01	0.36	2.41	0.89	1.44	0.53	0.12	0.04	1.72	0.05
s.d.	0.01	0.01	0.02	0.08	0.06	0.00	0.00	0.14	0.00	0.01	0.25	0.11	0.24	0.08	0.00	0.00	0.45	0.01

20 μM IPTG added.

	OD = 2.5								
	μ h^{-1}	Q_G g/Lh	q_G g/gh	Q_A g/Lh	q_A g/gh	Q_P g/Lh	q_P g/gh	G/A g/g	P/G g/g
12/9/04	0.36	0.95	1.38	0.47	0.68	0.02	0.04	2.00	0.03
12/16/04	0.34	0.52	0.76	0.28	0.41	0.02	0.03	1.85	0.04
mean	0.35	0.73	1.07	0.37	0.54	0.02	0.03	1.93	0.03
s.d.	0.02	0.31	0.44	0.14	0.19	0.00	0.00	0.11	0.01

feed tube and reservoir. This precipitate was unnoticed in the batch culture, and might not have developed at all due to cell growth, which would have reduced the concentration of nutrients. Under the assumption that the precipitate involved a metal cation, EDTA was added as a chelating agent to a 50 mL culture of Zelic et al. (2003) media in 250 mL shake flasks. The growth of ALS 929 was measured over the course of approximately 24 hours with the goal of finding a concentration of EDTA that would eliminate the precipitate, but not affect cell growth. Figure 8 shows the growth curves from this shake flask study. The concentrations of EDTA that permitted maximum cell growth were 22 mg/L and 4.4 mg/L. Cell growth was improved by about 63% from the culture without EDTA for both of these concentrations. However, these concentrations still allowed for the formation of a precipitate. The precipitate was absent when the EDTA concentration was 176 mg/L. However, cell growth was reduced by 50% at this EDTA concentration when compared to the 22 mg/L and 4.4 mg/L concentrations. It is interesting to note that, while cell growth did not appear to be affected by the precipitate in the batch fermentations, the same media showed a depression in growth when used in a shake flask.

Since EDTA was not going to be a suitable chelator, other components of the media were examined individually in the absence of EDTA, and $FeSO_4$ was determined to cause the precipitate. As a result, a shake flask study in which the $FeSO_4$ concentration was varied was conducted (Figure 9). In addition to studying $FeSO_4$, the media was prepared using tap water instead of deinionized water, and in a separate experiment ferric citrate was also substituted for $FeSO_4$. Ferric citrate was selected as an alternative iron source because citrate is an excellent chelator. The concentration of $FeSO_4$ that allowed for maximum growth was at 80% the initial concentration of 18.3 mg/L, or 14.6 mg/L, and actually grew nearly 20% faster than the original

Figure 8: Cell growth of ALS 929 in Modified Zelic media with varying EDTA concentrations when grown in shake flasks at 37º C.

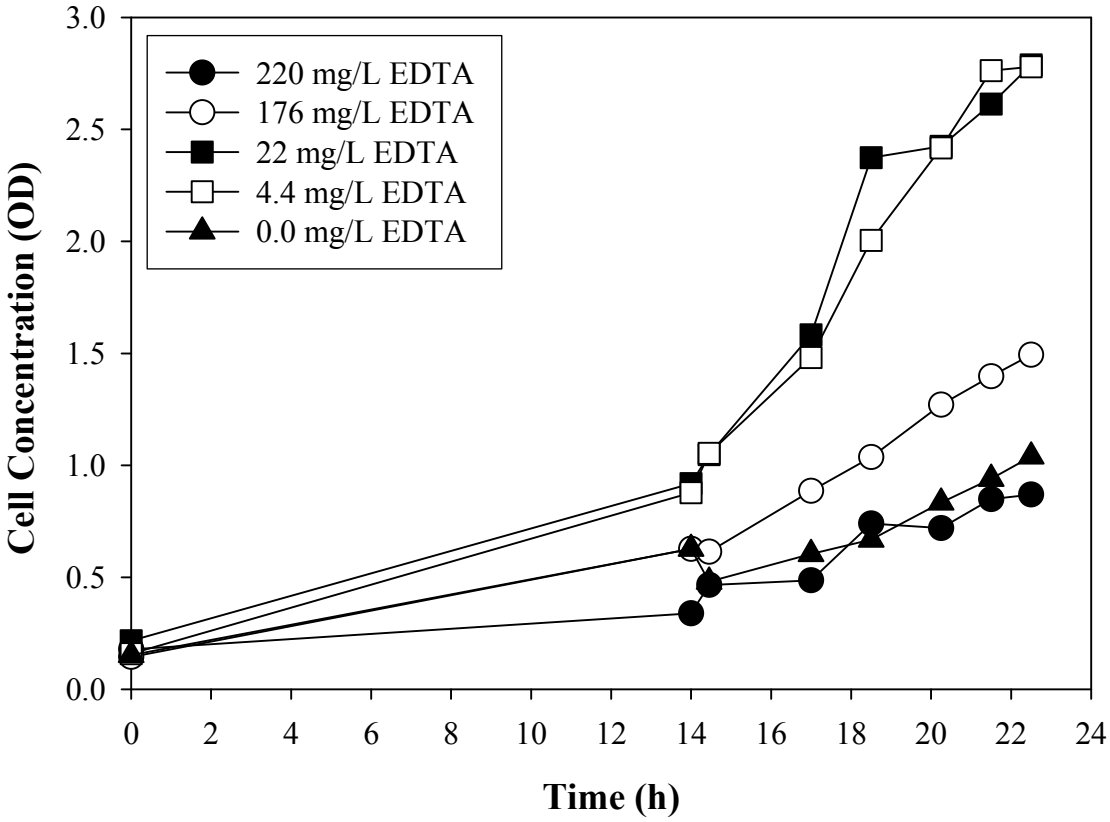
220 mg/L EDTA
176 mg/L EDTA
22 mg/L EDTA
4.4 mg/L EDTA
0.0 mg/L EDTA
Cell Concentration (OD)
Time (h)
0.0
0.5
1.0
1.5
2.0
2.5
3.0
0
2
4
6
8
10
12
14
16
18
20
22
24

Figure 9: Cell growth of ALS 929 in Modified Zelic media with varying $FeSO_4 \cdot 7H_2O$ concentrations grown in shake flasks at 37º C

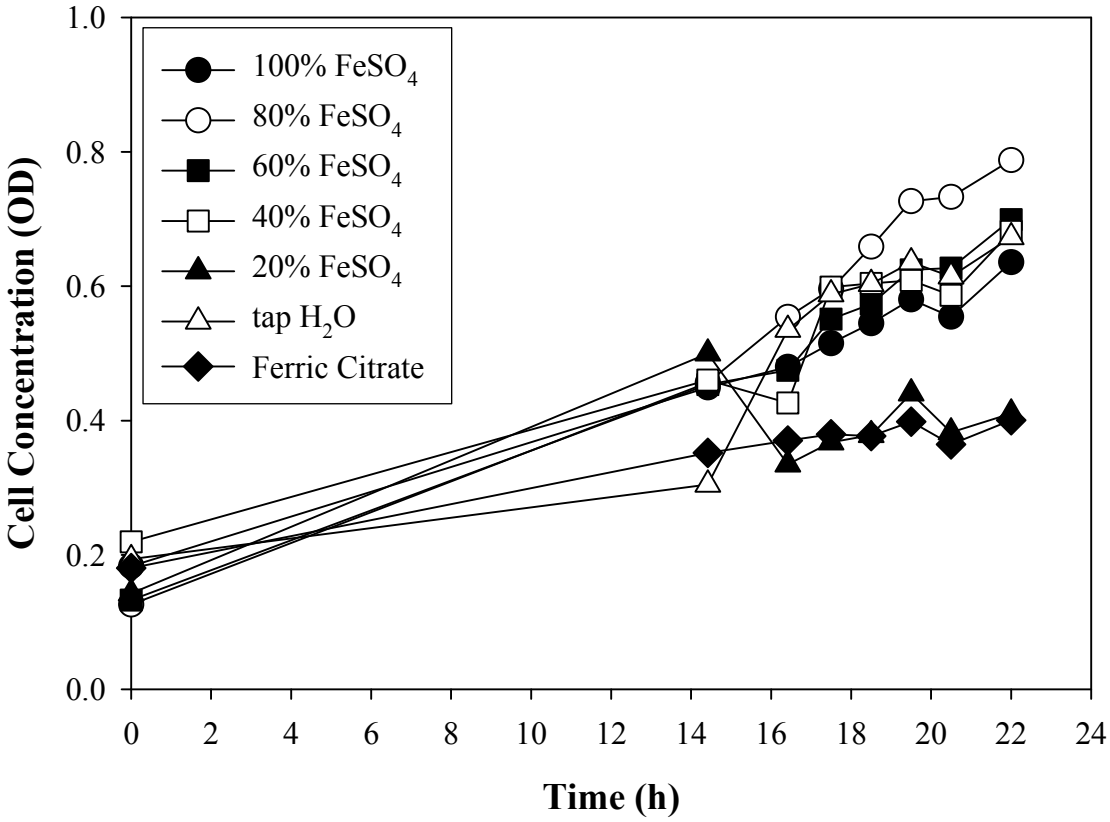
1.0
0.8
0.6
0.4
0.2
0.0
Cell Concentration (OD)
0
2
4
6
8
10
12
14
16
18
20
22
24
Time (h)
100% FeSO4
80% FeSO4
60% FeSO4
40% FeSO4
20% FeSO4
tap H2O
Ferric Citrate

18.3 mg/L $FeSO_4$. However, at this concentration the precipitate was still formed. Although the media with tap water or ferric citrate did not cause a precipitate, cell growth was respectively 15% and 49% less than in the media which contained 14.6 mg/L $FeSO_4$. To reduce the formation of the precipitate while still allowing for cell growth, a combination of 50 mg/L EDTA and 11 mg/L $FeSO_4$ was selected in addition to altering the phosphates in the media to 3.4 g/L $Na_2HPO_4 \cdot 7H_2O$ and 1.5 g/L KH_2PO_4, and the reducing $MgSO_4 \cdot 7H_2O$ to 0.2 g/L.

Continuous fermentations were first completed with ALS 929 and uninduced KD423 at several dilution rates (Appendix D), and the consumption and production rates were calculated. The linear regressions of these rates were fit into four statistical models, and then subjected to selection criteria using the SAS program to determine if the regression lines of the two strains were different or if they could be reduced to simpler models of parallel, concurrent, or coincidental lines. The selection criteria used to test for model reduction were hypothesis testing and Akaike's Information Criterion (AIC). The dilution rate of 0.4 h^{-1} for KD 423 was considered an outlier because of the possibility of being at non-steady state and was not included in the comparisons of the chemostat data of ALS 929 and KD 423.

The glucose uptake rate (q_S) increased with increasing dilution rates for both strains (Figure 10). Moreover, the glucose uptake rate was coincidental for the two strains for any given growth rate based upon the reduction of the regression models. For both strains the specific acetate consumption rate (q_A) also increased with increasing q_S (Figure 11). In this case, the acetate consumption rate of uninduced KD423 displayed a greater slope than the q_A of ALS929 while sharing an intercept. Interestingly, the q_A of KD423 at 0.4 h^{-1} (q_S equal to 7 mmol/gh) was lower in respect to q_S than the trend for the other dilution rates would have suggested. For both strains the pyruvate production rate (q_P) was not a function of q_S (Figure 12), except for

Figure 10: Specific glucose consumption rate as a function of growth rate for ALS 929 (●) and KD423 (▲) during glucose-limited chemostat fermentations. Also shown are the specific glucose consumption rate of ALS 929 under one nitrogen-limited condition (○) and the possible unsteady-state measurement for the KD 423 (△).

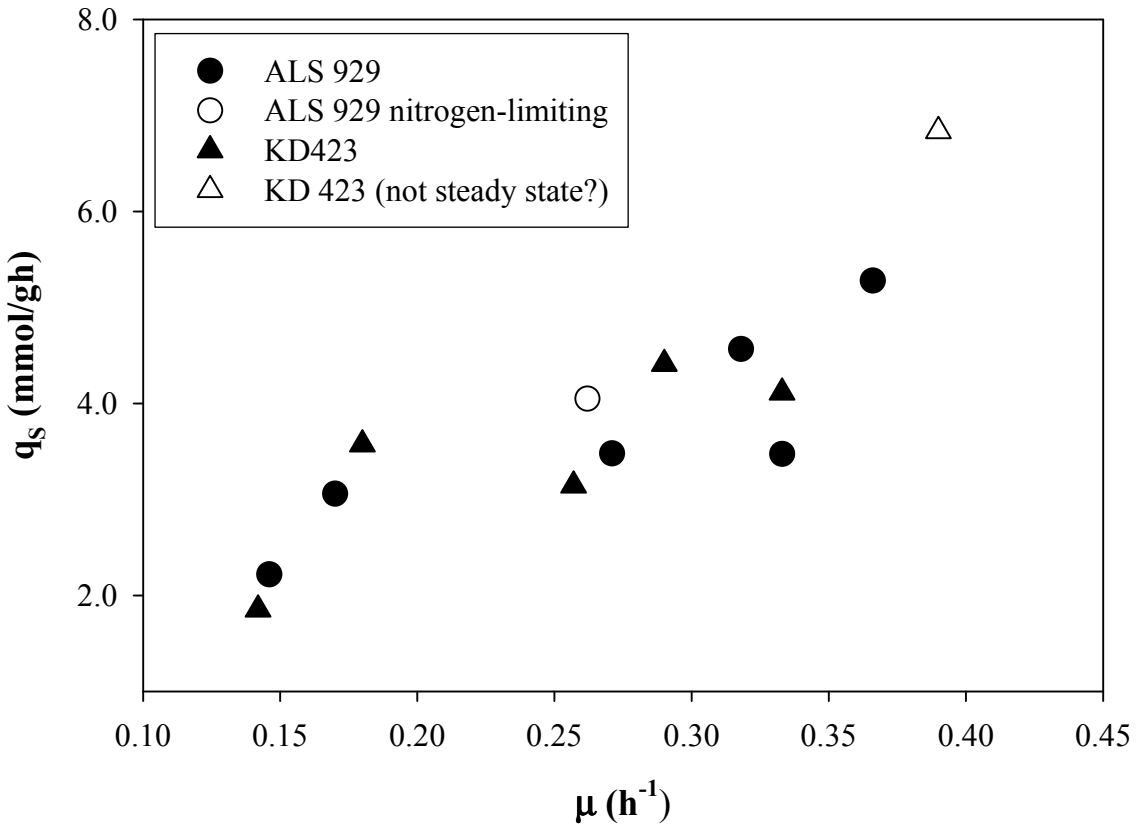
8.0
6.0
4.0
2.0
ALS 929
ALS 929 nitrogen-limiting
KD423
KD 423 (not steady state?)
q_S (mmol/gh)
0.10
0.15
0.20
0.25
0.30
0.35
0.40
0.45
μ (h^{-1})

Figure 11: Specific acetate consumption rate as a function of the specific glucose consumption rate for ALS 929 (●) and KD423 (▲) in glucose-limited chemostat fermentations. Also shown are the specific acetate consumption rate of ALS 929 under one nitrogen-limited condition (○) and the possible unsteady-state measurement for the KD 423 (△).

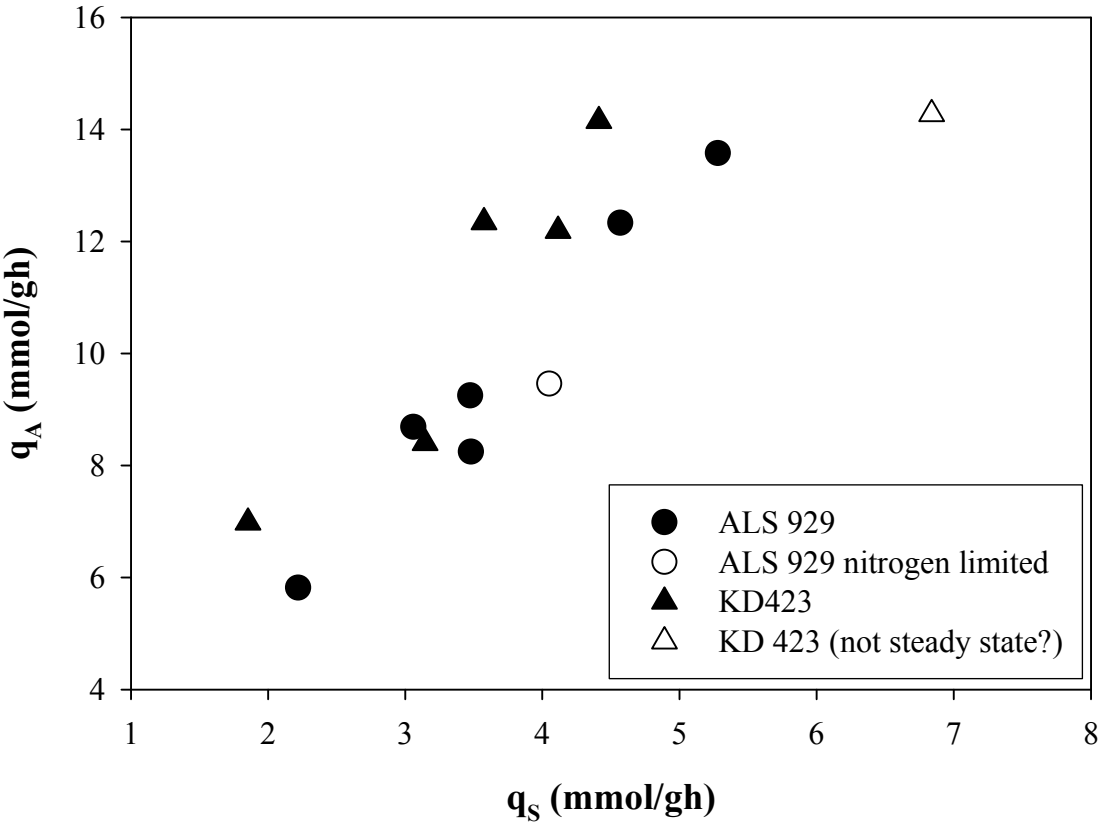
16
14
12
10
8
6
4
1
2
3
4
5
6
7
8
q_A (mmol/gh)
q_S (mmol/gh)
ALS 929
ALS 929 nitrogen limited
KD423
KD 423 (not steady state?)

Figure 12: Specific pyruvate production rate as a function of specific glucose consumption for ALS 929 (●) and KD423 (▲) in glucose-limited chemostat fermentations. Also shown are the specific pyruvate production rate of ALS 929 under one nitrogen-limited condition (○) and the possible unsteady-state measurement for the KD 423 (△).

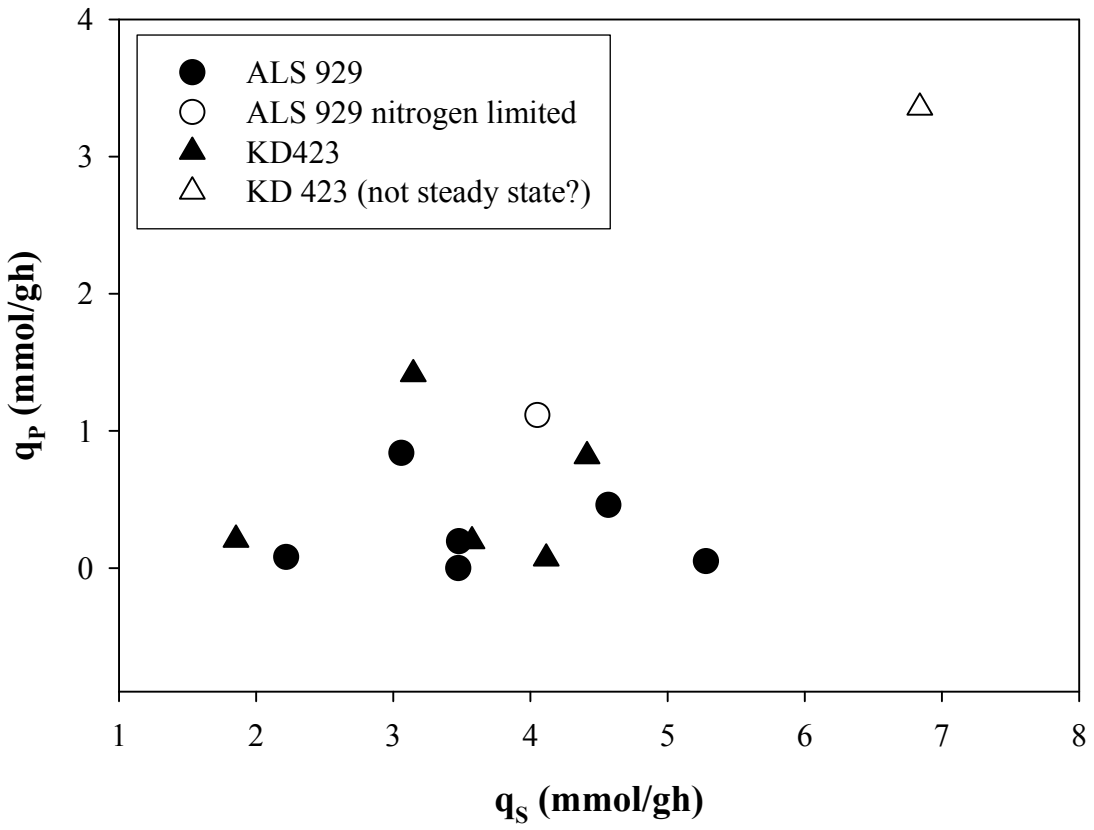
ALS 929
ALS 929 nitrogen limited
KD423
KD 423 (not steady state?)
q_P (mmol/gh)
q_S (mmol/gh)
0
1
2
3
4
1
2
3
4
5
6
7
8

KD423 at the dilution rate of 0.4 h^{-1}, at which condition about 3.5 mmol/gh pyruvate was generated. The specific oxygen consumption rate (q_{O2}) is directly a measure of the cell's conversion of NADH to NAD using oxygen as the terminal electron acceptor which ultimately results in the production of ATP. Figure 13 shows the relationship q_{O2} and q_S for both ALS 929 and KD423, demonstrating that no significant difference occurs between the two strains. The intracellular NADH/NAD ratio was also calculated for each growth rate of the continuous cultures for both strains. While q_{O2} for both strains were similar for a given q_S, there was an increase of the ratio in the KD423 than was seen in ALS 929, which had intracellular NADH/NAD ratios of 0.065 and 0.038, respectively. This suggests that the oxygen consumption rate for both strains was at its maximum, and the increase in the NADH/NAD ratio seen in KD423 was due the cell's inability to match an increase in NADH production.

The specific carbon dioxide generation rate (q_{CO2}) is a reflection of the pathways used to metabolize the carbon sources of glucose and acetate. For both strains q_{CO2} increased with q_S (Figure 14), and regression lines for the two strains were coincidental. The biomass yield for both strains did not significantly change with increasing glucose consumption rate (Figure 15). The enzyme activities of acetyl CoA synthetase in all the continuous fermentations are summarized in Table 5. While the plasmid containing the *acs* gene is not induced in KD423, there is a five to ten-fold increase in specific enzyme activity compared to that of the ALS 929. For all consumption and production rates described above the nitrogen-limited chemostat fermentation behaved similarly to the glucose-limited chemostat fermentations of ALS 929.

Figure 13: Specific oxygen consumption rate as a function of specific glucose consumption rate for ALS 929 (●) and KD423 (▲) in glucose-limited chemostat fermentations. Also shown are the specific oxygen consumption rate of ALS 929 under one nitrogen-limited condition (○) and the possible unsteady-state measurement for the KD 423 (△).

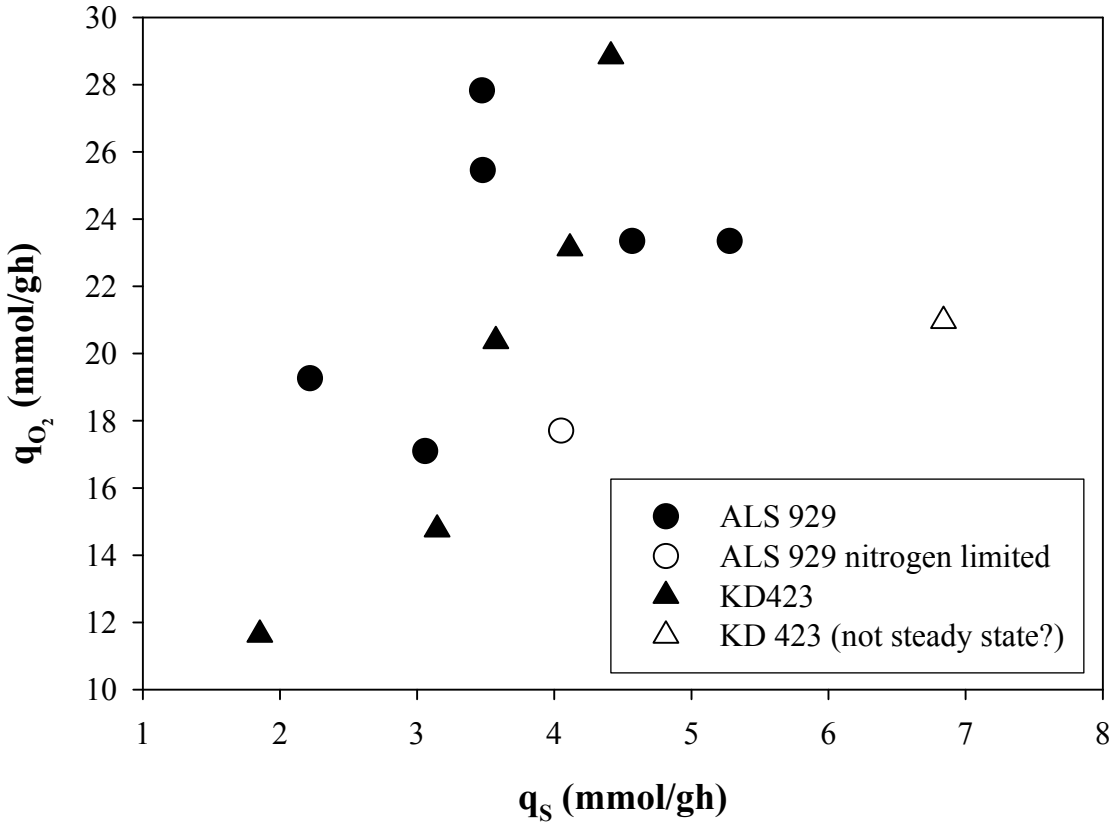
30
28
26
24
22
20
18
16
14
12
10
1
2
3
4
5
6
7
8
q_{O_2} (mmol/gh)
q_S (mmol/gh)
ALS 929
ALS 929 nitrogen limited
KD423
KD 423 (not steady state?)

Figure 14: Specific carbon dioxide generation rate as a function of the specific glucose consumption rate for ALS 929 (●) and KD423 (▲) during glucose-limited chemostat fermentations. Also shown are the specific carbon dioxide generation rate of ALS 929 under one nitrogen-limited condition (○) and the possible unsteady-state measurement for the KD 423 (△).

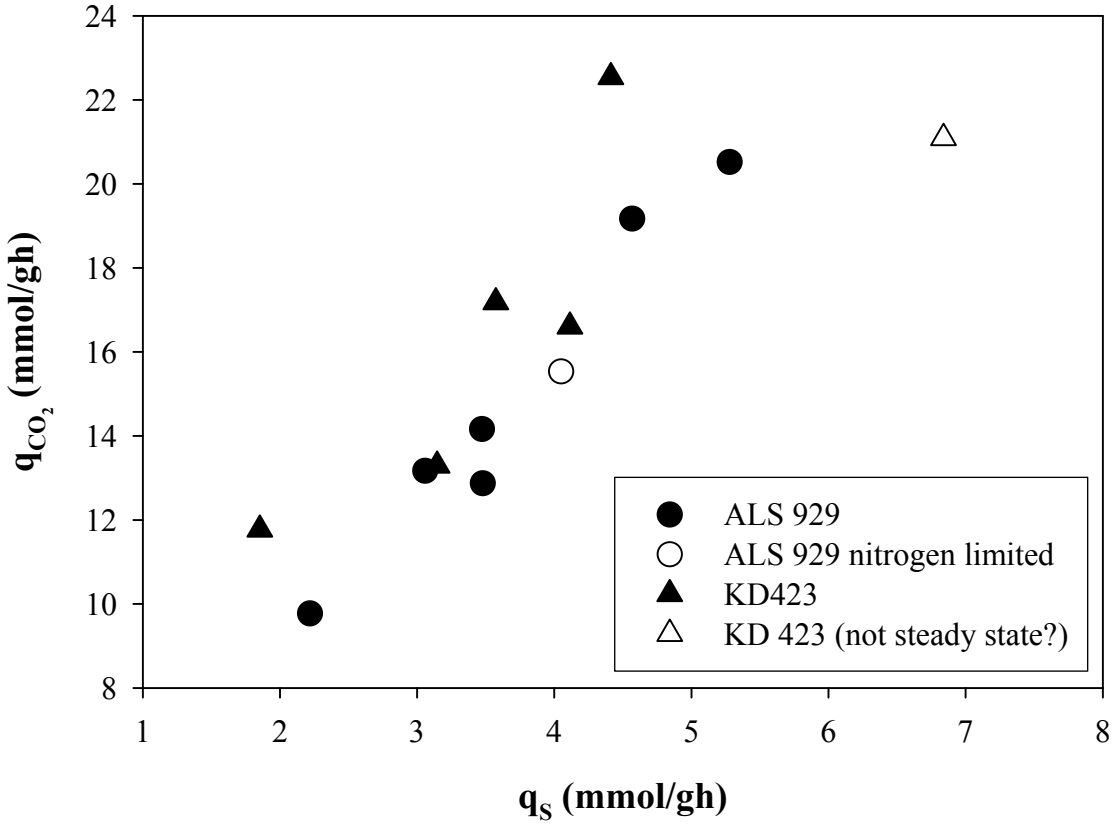
24
22
20
18
16
14
12
10
8
1
2
3
4
5
6
7
8
q_{CO_2} (mmol/gh)
q_S (mmol/gh)
ALS 929
ALS 929 nitrogen limited
KD423
KD 423 (not steady state?)

Figure 15: Biomass yield from glucose as a function of the specific glucose consumption rate for ALS 929 (●) and KD423 (▲) in the glucose-limited chemostat fermentations. Also shown are the biomass yield from glucose of ALS 929 under one nitrogen-limited condition (○) and the possible unsteady-state measurement for the KD 423 (△).

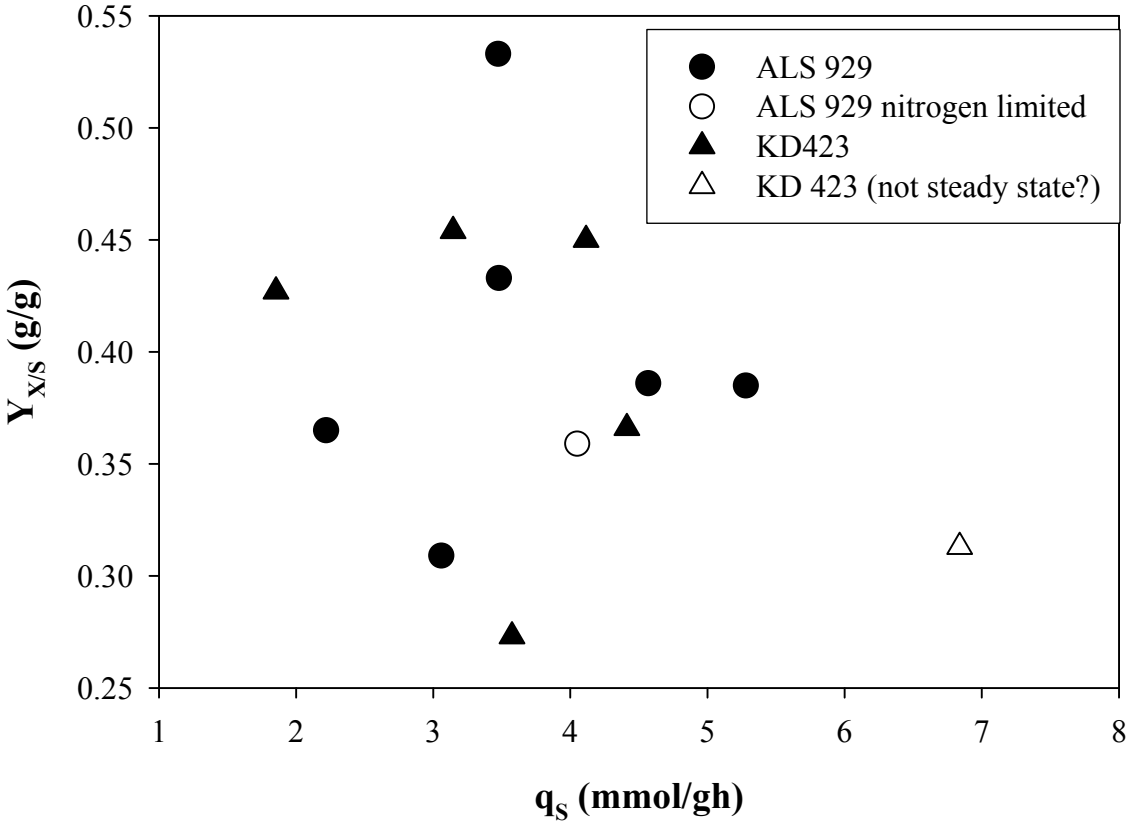
0.55
0.50
0.45
0.40
0.35
0.30
0.25
1
2
3
4
5
6
7
8
$Y_{X/S}$ (g/g)
q_S (mmol/gh)
ALS 929
ALS 929 nitrogen limited
KD423
KD 423 (not steady state?)

Table 5: A summary of acetyl CoA synthetase activities in both ALS 929 and KD423 glucose-limited chemostat fermentations. Also shown is the enzyme activity of ALS 929 when grown under one nitrogen-limited condition (*).

ALS 929				KD423			
D (h^{-1})	Enzyme Activity (U/L)	Protein Concentration (mg/L)	Spec. Enzyme (mU/mg)	D (h^{-1})	Enzyme Activity (U/L)	Protein Concentration (mg/L)	Spec. Enzyme (mU/mg)
0.18	1.20	306.2	3.9	0.14	10.34	453.7	22.8
0.33	0.45	357.3	1.3	0.18	10.45	299.0	35.0
0.40	2.77	370.9	7.5	0.26	6.43	376.3	17.1
0.26*	2.65	324.3	8.2	0.30	5.39	411.7	13.1
				0.34	5.68	406.3	14.0
				0.40	7.17	382.2	18.8

* nitrogen limited culture

CHAPTER 5

DISCUSSION

Initial analysis of the expression of *citZ* in *E. coli* ALS 225 with the enzyme assay resulted with the background citrate synthase activity in the control strain being higher than the ALS 225 (pTrc99a-*citZ*). It was later learned that the measurement of overexpressed citrate synthase is not possible in a host strain in which a native citrate synthase is expressed, thus *E. coli* W620 was subsequently used for the enzyme assay analyses (correspondence with Stuart Underwood). This strain has a deletion in *gltA,* which encodes for the native citrate synthase of *E. coli*, thus allowing for the measurement of citrate synthase activity due to the expression of *citZ.* However, in this strain the measured enzyme activity was negligible.

To try to understand why this poor activity was obtained, the codon usage in *citZ* were compared with the codon preference in *E. coli.* Of the 372 codons in the *citZ* gene, 164 were preferred and 51 were strongly preferred, but 73 were unfavorable for expression in *E. coli* resulting in an overall gene codon preference of 51.9%. As a point of comparison, strongly expressed genes in *E. coli* have a score of around 114%, while those of weakly expressed *E. coli* genes have a score of 40% - 50%. However, the protein gel analysis suggests that the organism is producing some citrate synthase where the band for monomer can be seen at 41 kDa in all of the *citZ* containing strains (Figure 4). This suggests that despite the low preference for the B. *subtilis citZ* gene there is still adequate expression for the cells to generate the protein. Thus, the absence of any measureable activity could be due to post translational problems such as the formation of inclusion bodies of the protein produced.

Initial results of the acetyl CoA synthetase assay demonstrated the need for a more efficient cell extract preparation method due to irreproducibility between different reactions of the same sample. The cell rupture process using the French Pressure Cell was at first believed to be the cause of the inconsistent results perhaps because this pressurized system was denaturing the enzyme. Varying pressures were applied to the cell solution at either one pass or two passes through the pressure cell without much improvement in consistency of enzyme activity measurements. Sonication was also examined as a means to prepare the cell free extract, but the resulting enzyme activity and protein concentration were too low, indicating this process was not efficient in disrupting the cells. Ultimately, the cells were ruptured using the French Pressure Cell with a cellular concentration factor of 100X for which more reproducible results were obtained. This investigation suggested that the inability to generate reproducible enzyme activity in shake flask studies was a result of a low concentration of the enzyme.

When grown in batch cultures ALS 929 generated pyruvate to a concentration of approximately 12 g/L, and presumably more if additional glucose were added. Interestingly, pyruvate continued to be generated after acetate was depleted and cell density declined (20 – 21h in Figure 4). From the slopes of the pyruvate and glucose concentration profiles, the pyruvate production rate declined slightly, and the ratio or pyruvate produced to glucose consumed remained about the same. Thus, cell growth is not necessary for pyruvate production. However, it is not clear whether pyruvate production can be sustained without cell growth.

Batch cultures of KD423 were initially studied using 250 μM IPTG for induction. However, these cultures did not grow to a significant cell density (OD of 1.5). The cells probably attained only such a low final density due to metabolic demands for which the media was insufficient. Thus, 2.0 g/L succinic acid was added as a supplement to the initial media in a

subsequent fermentation, and 2.0 g/L succinic acid was also included in the feed solution. This KD423 fermentation without induction resulted in growth to a final OD of about 20 and a pyruvate concentration of 6.0 g/L. When this KD423 fermentation was induced with 250 μM IPTG, cell growth stopped at an OD of 5. A possible explanation for the inability of cells to achieve a higher cell density may have been that IPTG was added too early. A set of experiments was therefore conducted (in the absence of succinic acid), one fermentation induced with 100 μM IPTG when the OD reached 1.5 to 2.0 (Figure 7) and a second fermentation that was not induced with IPTG. This uninduced fermentation behaved similarly to the uninduced batch containing succinic acid except for the amount of pyruvate produced. While the pyruvate concentration reached 6.0 g/L in the succinate supplemented fermentation, the batch in which succinate was absent only generated about 0.5 g/L pyruvic acid. The experiment with 100 μM IPTG but without succinate grew to a maximum OD of 5.0, and pyruvate to about 0.5 g/L. In order to determine if ACS expression placed a deleterious metabolic demand on the cells, the amount of IPTG added to the fermentation of KD423 was reduced to 20 μM. However, the culture behaved the same regardless of the amount of IPTG for plasmid induction (Figure 6). When the cells reached an OD of about 5, cell growth and glucose and acetate consumption stopped.

Any induction of ACS seems to have a detrimental effect on cell growth and the production of pyruvic acid. The plasmid utilized for these experiments (pTrc99a) is known to have a leaky promoter, and so even chemostat fermentations of uninduced KD423 did show around a two-fold increase in enzyme activity. Although this slight increase in expression did not inhibit cell growth, it is enough to affect metabolism and result in reduced pyruvate accumulation in batch fermentations. This reduced pyruvate accumulation was partially

overcome by the addition of succinic acid to the media. One can speculate why these results were obtained: An elevated level of acetyl CoA synthetase would presumably have the affect of increasing the intracellular pool of the product of this enzyme, acetyl CoA. In order for the cell to avoid accumulation of acetyl CoA, which would potentially reduce the availability of CoA for other cellular reactions, it must have the capacity to consume that acetyl CoA. A significant means to incorporate acetyl CoA is through its reaction with oxaloacetate via citrate synthase to form citrate. The primary means for *E. coli* to generate oxaloacetate is from PEP via the enzyme PEP carboxylase. Indeed, acetyl CoA is an activator for PEP carboxylase (McAlister et al. 1981). If *E. coli* responds to elevated acetyl CoA concentration by upregulating, or activating PEP carboxylase, that increase in activity could have two significant consequences. First, PEP is essentially the only precursor for pyruvate. Therefore, a redirection of PEP to oxaloacetate would tend to reduce the production of pyruvate. Second, PEP is a cosubstrate for the PTS, which ultimately transports glucose into the cell. A reduction in the PEP pool would tend to reduce glucose uptake. One might imagine the extreme scenario of PEP depleted so much as to deleteriously curtail glucose consumption by the cell, effectively ending cell growth. If the cell is able to transport succinate effectively, the addition of succinate to the external media has the affect of increasing the availability of oxaloacetate. In fact, the decrease in pyruvate accumulation in the uninduced batch fermentations of KD423 may reflect the activation of PEP carboxylase, and subsequent siphoning of PEP to oxaloacetate in lieu of pyruvate due to a larger acetyl CoA pool attributed to the expression of ACS. Also, once induced, KD423 stopped growing and consuming glucose at an OD of 5, suggesting the reduction of the PEP pool was preventing glucose uptake via the PTS. Malic enzyme is also a possible route that the cell could use for fulfilling the requirement of oxaloacetate. In this case the effect of pyruvate would be the

same since pyruvate is a substrate in malic enzyme. However, this route is less likely due to the inhibition of the enzyme by acetyl CoA (Sanwal 1970), and the slight thermodynamic favorability of the reverse reaction (Harary et al. 1953).

The cessation of growth at a low cell density (i.e., OD = 5.0) for the induced KD423 strain is puzzling considering growth up to that density was "normal." Certainly, high ACS higher activity may affect cell metabolism in a variety of ways. For example, the cells may be unable to regenerate CoASH from acetyl CoA at a high enough rate, and thus a limited CoASH pool prevents cells from growing further. Another possibility was the maintenance requirements of the plasmid imposed a substantial burden on the metabolism of the cells. A similar phenomenon was observed in shake flask studies of *E. coli* AFP111 in which *B. sphaericus alaD* was expressed (unpublished results, Lee et al. 2004). Another possibility is an ATP consumption futile cycle may have developed between acetyl CoA synthetase and acetate kinase and phosphotransacetlyase when ACS is overexpressed, thus placing a strain of the energy pool of the cells. Specifically, the production of acetyl CoA from acetate requires the cleavage of two high energy bonds while formation of acetate from acetyl CoA generates only one high energy bond. A significant quantity of material being converted between acetyl CoA and acetate would serve as an energy sink. Such an observation was made when PEP synthase was overexpressed in *E. coli* resulting in higher oxygen and glucose consumption rates (Patnaik et al. 1992). In this case no change in physiology (i.e., production and consumption rates) was observed.

The two strains ALS 929 and KD423 were also compared in chemostats to determine the influence of the overexpression of ACS when the organisms were maintained at a steady state. The strain KD423 had to be studied in an uninduced state for these comparisons. When a fermentation was attempted in which 20 μM IPTG was present, the cells washed out of the

vessel at a dilution rate of only 0.18 h^{-1} despite showing a temporary growth rate of over 0.3 h^{-1} (Table 4). However, since ACS expression without IPTG affected cell metabolism in the batch experiments, it was believed that a physiological difference would be observed in the chemostat. Actually, the only difference observed was an increase of acetate consumption rate for any given glucose consumption rate for KD423 as compared to ALS 929. This observation is consistent with an increase in ACS activity, which would presumably directly affect acetate consumption. Furthermore, although the specific oxygen consumption rates did not differ, the NADH/NAD ratio in KD423 was higher. These observations suggest that KD423 was able to generate more NADH than ALS 929, but that KD423 was not able to covert it to NAD any faster. Since this cofactor is involved in scores of enzymes and regulatory processes, a different intracellular level of NADH would significantly affect metabolism. Since acetate consumption is slightly higher in KD423, the increase in NADH/NAD ratio is consistent with elevated TCA cycle flux. The greatest pyruvate production rate was the observed with the growth rate 0.4 h^{-1} of AKD423. This growth rate is near the maximum growth rate of the strain, and suggests that pyruvate production is growth rate dependent, a conclusion inconsistent with batch fermentation results (Figure 5), but it does illustrate the relationship between glucose uptake and pyruvate generation for this strain.

One would have expected ALS 929 to produce more pyruvate in the nitrogen-limited chemostat than in the glucose-limiting chemostats due to the presence of excess glucose. However, as can be seen from the results, the nitrogen-limited chemostat specific pyruvate production rate was similar to the trend of the specific pyruvate production rates of the glucose-limited chemostats. It may be necessary to repeat the nitrogen-limited conditions with other growth rates. This experiment would provide further information regarding the growth

dependence of pyruvate accumulation, a point that is inconclusive between batch and chemostat fermentations. In addition, it may be possible to produce more pyruvate in the higher growth rates due to a greater accumulation of glucose in the vessel.

Another interesting result was the generation of an unknown compound, which was observed in the batch fermentations as well as the chemostats. The accumulation of the unknown occurred in the batch fermentations once the pyruvate concentration reached above 1 g/L. However, a greater concentration of this unknown formed in the chemostat even though the pyruvate concentrations were typically below 1 g/L. The carbon balance for most of the chemostats, not considering the unknown, was between 80% and 90%. Figure 16 displays the area of the unknown peak in relation to the glucose consumption rate. The specific production rate of the unknown compound (q_U) was greater in ALS 929 than in KD423. The unknown peak area is comparable to that of 2.0 g/L or 3.0 g/L for other compounds such as acetate and succinate. Based on its chromatographic retention time, the unknown was not citrate, malate, fumurate, formate, ethanol, oxalate, glucuronate, isocitrate, a-ketobutyrate, malonate, glyoxylate, sorbitol, acetoin, acetaldehyde, propionate, butanediol, or butyrate. The unknown is believed to be either a carboxylic or hydroxycarboxylic acid of three to four carbons in length with a molecular weight near 150 g/mol. This belief was based upon two observations: 1) the shift in retention time of the unknown with H_2SO_4 versus water as eluent, and 2) the unknown was not produced in the batch fermentations until pyruvate reached about 1.0 g/L. The presence of this amount of unknown could be accounted for the lower percentage of carbon balance. Identification of the unknown by LC-MS was inconclusive. It was not possible to separate the unknown when water was the eluent because of the shift in retention time. With the assumption

Figure 16: Specific production rate of an unknown compound as a function of the specific glucose uptake rate for ALS 929 (●) and KD423 (▲) in glucose-limited chemostat fermentations. Also shown are the specific unknown production rate of ALS 929 under one nitrogen-limited condition (○) and the possible unsteady-state measurement for the KD 423 (△). The rate of production for the unknown compound is not based upon concentration, but rather on the peak area on the HPLC chromatogram.

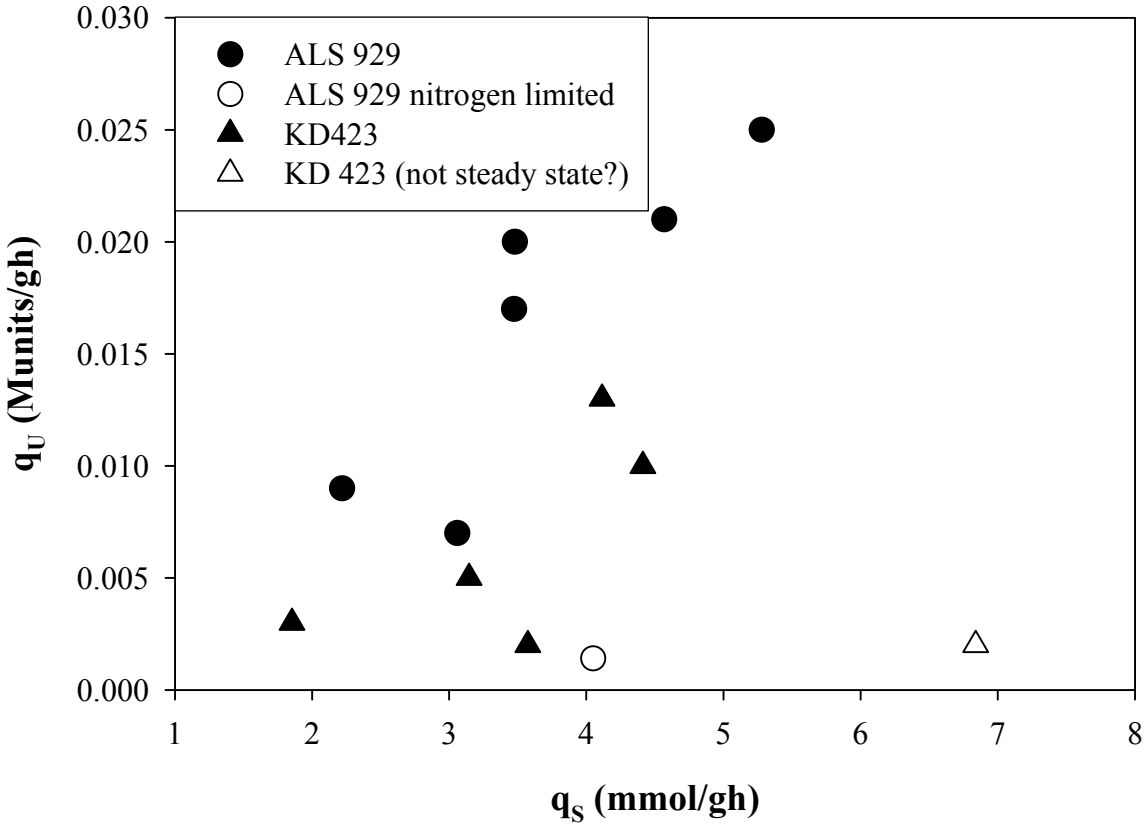
0.030
0.025
0.020
0.015
0.010
0.005
0.000
1
2
3
4
5
6
7
8
ALS 929
ALS 929 nitrogen limited
KD423
KD 423 (not steady state?)
q_U (Munits/gh)
q_S (mmol/gh)

that the unknown was an organic acid, a derivatization process was used to covert it into a methyl ester for measurement on a GC-MS. Unfortunately, this study was also inconclusive.

CHAPTER 6

CONCLUSIONS AND FUTURE DIRECTIONS

E. coli ALS 929 contains several deletions in central metabolic pathways to enable the accumulation of pyruvate, but also requiring acetate for growth. The influence of acetate consumption in this pyruvate accumulating strain of *E. coli* was investigated with the aim of improving pyruvate production. To this end, the enzymes citrate synthase from *B. subtilis* and acetyl CoA synthetase from *E. coli,* which are both involved in acetate utilization were independently overexpressed in this strain. While citrate synthase was not studied completely in this strain due to difficulties encountered in protein expression and enzyme activity, acetyl CoA synthetase was studied in both batch and chemostat fermentations. It was believed that the overexpression of acetyl CoA synthetase would enable to strain to consume acetate at a greater rate, and thus grow at a faster rate and feasibly produce more pyruvate than the parent strain. However, it was observed that while the acetate consumption rate for this strain was higher in the presence of acetyl CoA synthetase, there was no improvement of cell growth or pyruvate production.

While the above results failed to support the hypotheses put forth in this work, they did provide insight to possible research directions for future work. Of primary interest was the actual cause for the difference in rates between glycolysis and the TCA cycle. It was proposed that the independent increase in citrate synthase (CS) or acetyl CoA synthetase (ACS) activities would overcome this discrepancy in rates and increase the acetate consumption of ALS 929. Unfortunately, it was notpossible within the scope of this research to utilize the CS from *B.*

subtilis. While it was important to use a CS enzyme that was not inhibited by NADH the problems posed by the expression of the *B. subtilis citZ* suggested the need for another gene source. One option would be the codon optimization procedure for which the codons negatively preferred by *E. coli* would be converted to those of higher preference. One drawback from such a method was the time and cost restraints. Another equally feasible option would be the search for a comparable CS that is not inhibited by NADH, but from another organism for which the codon usage more closely matches the codon preference of *E. coli*. One possible source would be from another Gram-positive bacteria, archaea or eukaryotes, the CS of which are homo-dimers and are not inhibited by NADH, but instead are isosterically inhibited by ATP (Robinson et al. 1983). Another source would be the dimeric CS-like enzyme (methylcitrate synthase (*prpC*, EC 4.1.3.31), similar to those found in Gram-positive bacteria, archaea and eukaryotes, found in some Gram-negative bacteria including *E. coli* (Patton et al. 1993). This enzyme has comparable preference for acetyl CoA and OAA (Patton et al. 1993) as *B. subtilis* citrate synthase, an is native to *E. coli*.

While it was possible to study the affect of ACS when expressed in ALS 929, the results were not what were originally anticipated. The cells failed to accumulate a greater concentration of pyruvate even though it was clear that the enzyme did increase the acetate consumption and the utilization of acetyl CoA into the TCA cycle. As mentioned above, the pyruvate accumulation was partially improved in an ACS strain by the addition of succinate, which suggested a depletion in one or more metabolites involved in the TCA cycle (i.e. oxaloacetate, OAA). It was possible that the cell upregulated PEP carboxylase (PPC) by the increase of acetyl CoA concentration in the cells. This enzyme would then divert the flow of carbon from pyruvate production to the production of OAA. One possible means of studying this idea would be to

measure the activity of PPC in ALS 929 (pTrc99a-*acs*) grown in media both with and without the addition of succinic acid. Another interesting observation with the organism in which ACS was overexpressed was the cessation of growth of the bacteria past OD 5 when the plasmid was induced. Possible explanations for this observation are found in the above discussion, but another possibility outside of the immediate metabolic control would be the presence of a global regulator that was in some way affected by either the acetyl CoA pool, or the possible depletion of ATP that would be a result of a futile cycle. A complete analysis of the expression of the genes in *E. coli* as a result of the expression of ACS would possibly highlight any genes that may be under such a global regulator.

It is interesting to note that the overexpression of NADH oxidase (NOX) delays the onset of the production of an acetate of *E. coli* MG1655 when grown on glucose. As the growth rate increased for wild type the NADH/NAD ratio increased as well. It wasn't until the ratio reached 0.06 that the organism began to generate acetate. The overexpression of NOX allowed the cells to regenerate NAD from NADH using oxygen, thereby decreasing the ratio of NADH/NAD for a given growth rate and delaying the accumulation of acetate until a higher growth rate (Vemuri et al. 2005). An interesting application of these results would be the overexpression of NOX in ALS 929 to increase the acetate consumption. It is believed that CS is the rate limiting step between glycolysis and the TCA cycle, and that the CS native to *E. coli* is inhibited by the concentration of NADH. If the concentration of NADH were to be lowered by the activity of NOX, then the TCA cycle would be able to match the rate of glycolysis due to the removal of the inhibition of CS. This could be the reason for the delayed onset of acetate accumulation in MG1655-*nox* as a result of the lowered NADH/NAD ratio. However, while the rate of TCA

would be increased, a similar decrease in pyruvate accumulation may be observed for similar reasons as those proposed with the overexpression of ACS.

REFERENCES

1. **Abdel-Hamid, A. M., M. M. Attwood, and J. R. Guest.** 2001. Pyruvate oxidase contributes to the aerobic growth efficiency of *Escherichia coli*. Microbiology. **147:** 1483-1498.
2. **Akiyama, S. K. and G. G. Hammes.** 1980. Elementary steps in the reactions mechanism of the pyruvate dehydrogenase multienzyme complex from *Escherichia coli:* kinetics of acetylation and deacetylation. Biochemistry. **19:** 4208-4213.
3. **Anton, D. L., R. DiCosimo, and V. G. Witterholt.** 1996. Process for the preparation of pyruvic acid using permeabolized transformants of *H. polymorpha* and *P. pastoris* which express glycolate oxidase and catalase. U.S. Patent. **5 538 875.**
4. **Bernofsky, C., M. Swan.** 1973. An improved cycling assay for nicotinamide adenine dinucleotide. Analytical Biochemistry. **53:** 452-458.
5. **Boiteux, A., M. Markus, T. Plesser, and B. Hess.** 1983. Analysis of progress curves: Interaction of pyruvate kinase from *Escherichia coli* with fructose 1,6-bisphosphate and calcium ions. Biochemical Journal. **211:** 631-640.
6. **Borle, A. B. and R. T. Stanko.** Pyruvate reduces anoxic injury and free radical formation in perfused rat hepatocytes. American Journal of Physiology. **270:** G535-G540.
7. **Brown, T. D. K., M. C. Jones-Mortimer, and H. L. Kornberg.** 1977. The enzymic interconversion of acetate and acetyl-coenzyme A in *Escherichia coli*. Journal of General Microbiology. **102:** 327-336.

8. **Bunch, P. K., F. Mat-Jan, N. Lee, and D. P. Clark.** 1997. The *ldhA* gene encoding the fermentative lactate dehydrogenase of *Escherichia coli*. Microbiology. **143:** 187-195.
9. **CaJacob, C. A., G. R. Gavino, and P. A. Frey.** 1985. Pyruvate dehydrogenase complex of *Escherchia coli*: Thiamin pyrophosphate and NADH-dependent hydrolysis of acetyl-CoA. The Journal of Biological Chemistry. **260:** 14610-14615.
10. **Causey, T. B., K. T. Shanmugam, L. P. Yomano, and L. O. Ingram.** 2004. Engineering *Escherichia coli* for efficient conversion of glucose to pyruvate. Proceeds of the National Academy of Sciences. **101:** 2235-2240.
11. **Chang, D-E., S. Shin, J.-S. Rhee, and J.-G. Pan.** 1999. Acetate metabolism in a *pta* mutant of *Escherichia coli* W3110: importance of maintaining acetyl coenzyme A flux for growth and survival. Journal of Bacteriology. **181:** 6656-6663.
12. **Chang, Y.-Y. and J. E. Cronan, Jr.** 1982. Mapping nonselectable genes of *Escherichia coli* by using transposon Tn*10*: location of a gene affecting pyruvate oxidase. Journal of Bacteriology. **151:** 1279-1289.
13. **Chang, Y.-Y., A.-Y. Wang, and J. E. Cronan, Jr.** 1994. Expression of *Escherichia coli* pyruvate oxidase (PoxB) depends on the sigma factor encoded by the *rpoS* (*katF*) gene. Molecular Microbiology. **11:** 1019-1028.
14. **Clark, D. P.** 1989. The fermentative pathways of *Escherichia coli*. FEMS Microbiology Reviews. **63:** 223-234.
15. **Contiero, J. ,C. Beatty, S. Kumari, C. L. DeSanti, W. R. Strohl and A. Wolfe.** 2000. Effects of mutations in acetate metabolism in high-cell-density growth of *Escherichia coli*. Journal of Industrial Microbiology and Biotechnology. **24:** 421-430.
16. **Cooper, B.** 1990. Preparation of pyruvic acid. U. S. Patent. **4 900 668.**

17. **Danson, M. J., A. R. Fersht, and R. N. Perham.** 1978. Rapid intramolecular coupling of active sites in the pyruvate dehydrogenase complex of *Escherichia coli*: Mechanism for rate enhancement in a multimeric structure. Proceedings of the National Academy of Sciences USA. **75:** 5386-5390.

18. **DeBoer**, **L. W., P. A. Bekx, L. Han, and L. Steinke.** 1993. Pyruvate enhances recovery of rat hearts after ischemia and reperfusion by preventing free radical generation. American Journal of Physiology. **265:** H1571-H1576.

19. **Diaz-Ricci, J. C., L. Regan, J. E. Bailey.** 1991. Effect of alteration of the acetic acid synthesis pathway on the fermentation pattern of *Escherichia coli*. Biotechnology and Bioengineering. **38:** 1318-1324.

20. **Diez-Gonzalez, F., J. B. Russell.** 1997. The ability of *Escherichia coli* O157:H7 to decrease its intracellular pH and resist the toxicity of acetic acid. Microbiology. **143:** 1175-1180.

21. **Dürre, P., H. Bahl, and G. Gottschalk.** Membrane processes and product formation in anaerobes. Handbook on Anaerobic Fermentations. Ed. L. E. Erickson and D. Y.-C. Fung. Marcel Dekker, Inc. NY. 1988.

22. **Eisenberg, A., J. E. Seip, J. E. Gavagan, M. S. Payne, D. L. Anton, and R. DiCosimo.** 1997. Pyruvic acid production using methylotrophic yeast transformants as catalyst. Journal of Molecular Catalysis B: Enzymatic. **2:** 223-232.

23. **Eiteman, M. A. and M. J. Chastain.** 1997. Optimization of the ion-exchange analysis of organic acids from fermentation. Analytica Chemica Acta. **338:** 69-75.

24. **Emmerling, M., J. E. Bailey and U. Sauer.** 1999. Glucose catabolism of *Escherichia coli* strains with increased activity and altered regulation of key glycolytic enzymes. Metabolic Engineering. **1:** 117-127.

25. **Farmer, W. and J. C. Liao.** 1997. Reduction of aerobic acetate production by *Escherichia coli*. Applied and Environmental Microbiology. **63:** 3205-3210.

26. **Gerike, U., D. W. Hough, N. J. Russell, M. L. Dyall-Smith, and M. J. Danson.** 1998. Citrate synthase and 2-methylcitrate synthase: structural, functional and evolutionary relationships. Microbiology. **144:** 929-935.

27. **Gokarn, R. R., J. D. Evans, J. R. Walker, S. A. Martin, M. A. Eiteman, and E. Altman.** 2001. The physiological effects and metabolic alterations caused by the expression of *Rhizobium etli* carboxylase in *Escherichia coli.* Applied Microbiology and Biotechnology. **56:** 188-195.

28. **Gottshalk, G.** Bacterial Metabolism 2nd edition. Springer. NY. 1986.

29. **Harary, I., S. R. Korey, and S. Ochoa.** 1953. Biosynthesis of dicarboxylic acids by carbon dioxide fixation. VII. Equilibrium of "malic" enzyme reaction. Journal of Biological Chemistry. **203:** 595-604.

30. **Holms, W. H.** 1986. The central metabolic pathways of *Escherichia coli*: Relationships between flux and control at a branch point, efficiency of conversion to biomass, and excretion of acetate. Current Topics In Cellular Regulation. **28:** 69-105.

31. **Howard, J. W. and W. A. Fraser.** 1932. Pyruvic Acid. Organic Syntheses. **1:** 475-476.

32. **Ivy, J. L., M. Y. Cortez, R. M. Chandler, H. K. Byrne, and R. H. Miller.** 1994. Effects of pyruvate on the metabolism and insulin resistance of obese Zucker rats. Americal Journal of Clinical Nutrition. **59:** 331-337.

33. **Iwakura, M., J. Hattori, Y. Arita, M. Tokushige, and H, Katsuki.** 1979. Studies on regulatory functions of malic enzyme: VI. Purification and molecular properties of NADP-linked malic enzyme from *Escherichia coli* W. Journal of Biochemistry. **85:** 1355-1365.

34. **Izumi, Y., Y. Matsumura, Y. Tani, and H. Yamada.** 1982. Pyruvic acid production from 1,2-propanediol by thiamin-requiring *Acinetobacter* sp. 80-M. Agricultural and Biological Chemistry. **46:** 2673-2679.

35. **Izumi, Y. and J. W. Olney.** 1995. Use of pyruvate to prevent neuronal degeneration associated with ischemia. U.S. Patent. **5 395 822.**

36. **Jin, S. and A. L. Sonenshein.** 1994. Identification of two distinct *Bacillus subtilis* citrate synthase genes. Journal of Bacteriology. **176:** 4669-4679.

37. **Jin, S. and A. L. Sonenshein.** 1996. Characterization of the major citrate synthase of *Bacillus subtilis*. Journal of Bacteriology. **178:** 3658-3660.

38. **Jones, M. E., and F. Lipmann.** 1955. Aceto-CoA-Kinase. Methods in Enzymology. **1:** 585-595.

39. **Kleman, G. L. and W. R. Strohl.** 1994. Acetate metabolism by *Escherichia coli* in high-cell-density fermentation. Applied and Environmental Microbiology. **60:** 3952-3958.

40. **Knappe, J., H. P. Blaschkowski, P. Gröbner, and T. Schmitt.** 1974. Pyruvate formate-lyase of *Escherichia coli*: the acetyl-enzyme intermediate. European Journal of Biochemistry. **50:** 253-263.

41. **Krebs, H. A. and J. M. Lowennstein.** The tricarboxylic acid cycle. Metabolic Pathways 2nd edition. Volume 1. Ed. D. M. Green. Academic Press. NY. 1960

42. **Kumari, S., C. M. Beatty, D. F. Browning, S. J. W. Busby, E. J. Simel, G. Hovel-Miner, and A. J. Wolfe.** 2000. Regulation of acetyl coenzyme A synthetase in *Escherichia coli.* Journal of Bacteriology. **182:** 4173-4179.

43. **Kumari, S., E. J. Simel, and A. L. Wolfe.** 2000. σ^s is the principle sigma factor responsible for transcription of *acs*, which encodes acetyl coenzyme A synthetase in *Escherichia coli*. Journal of Bacteriology. **182:** 551-554.

44. **Kumari, S., R. Tishel, M. Eisenbach, and A. L. Wolfe.** 1995. Cloning, characterization, and functional expression of *acs*, the gene which encodes acetyl coenzyme A synthetase in *Escherichia coli.* Journal of Bacteriology. **177:** 2878-2886.

45. **Lee, M., G. M. Smith, M. A. Eiteman, and E. Altman.** 2004. Aerobic production of alanine by *Escherichia coli aceF ldhA* mutants expressing the *Bacillus sphaericus alaD* gene. Applied Microbiology and Biotechnology. **65**: 56-60.

46. **Leonardo, M. R., Y. Dailly, D. P. Clark.** 1996. Role of NAD in regulating the *adhE* gene of *Escherichia coli*. Journal of Bacteriology. **178:** 6013-6018.

47. **Li, Y., J. Chin, and S.-Y. Lun.** 2001. Biotechnological production of pyruvic acid. Applied Microbiology and Biotechnology. **57:** 451-459.

48. **Luli, G. W.,and W. R. Strohl.** 1990. Comparison of growth, acetate production, and acetate inhibition of *Escherichia coli* strains in batch and fed-batch fermentations. Applied and Environmental Microbiology. **56:** 1004-1011.

49. **Malcovati, M. and G. Valentini.** 1982. AMP- and fructose 1,6-bisphosphate-activated pyruvate kinase from *Escherichia coli*. Methods in Enzymology. **90:** 170-179.

50. **Mather, M. W. and R. B. Gennis.** 1985. Kinetic studies of the lipid-activated pyuravte oxidase flavoprotein of *Escherichia coli*. The Journal of Biological Chemistry. **260:** 16148-16155.

51. **Mat-Jan, F. K. Y. Alam, and D. P. Clark.** 1989. Mutants of *Escherichia coli* deficient in the fermentative lactate dehydrogenase. Journal of Bacteriology. **171:** 342-348.

52. **McAlister, L. E., E. L. Evans, and T. E. Smith.** 1981. Properties of a mutant *Escherichia coli* phosphoenolpyruvate carboxylase deficient in coregulation by intermediary metabolites. Journal of Bacteriology. **146:** 200-208.

53. **Miyata, R. and T. Yonehara.** 1996. Improvement of fermentative production of pyruvate from glucose by *Torulopsis glabrata* IFO 0005. Journal of Fermentation and Bioengineering. **82:** 475-479.

54. **Miyata, R. and T. Yonehara.** 1999. Breeding of high-pyruvate-producing *Torulopsis glabrata* with acquired reduced pyruvate dehydrogenase. Journal of Bioscience and Bioengineering. **88:** 173-177.

55. **Moriguchi, M., K. Shuto, and T. Hashimoto.** 1984. Production of pyruvic acid from saccharified citrus peel extracted by dried cells of *Debaryomyces coudertii.* Journal of Fermentation Technology. **62:** 243-248.

56. **Muirhead, H.** 1990. Isozymes of pyruvate kinase. Biochemical Society Transactions. **18:** 193-196.

57. **Nakazawa, H., H. Enei, S. Okumura, and H. Yamada.** 1972. Synthesis of L-tryptophan from pyruvate, ammonia and indole. Agricultural and Biological Chemistry. **36:** 2523-2528.

58. **Narindrasorasak, S. and W. A. Bidger.** 1977. Phosphoenolpyruvate synthetase of *Escherichia coli*: Molecular weight, subunit composition, and identification of phosphohistidine in phosphoenzyme intermediate. The Journal of Biological Chemistry. **252:** 3121-3127.

59. **Nguyen, N. T., R. Maurus, D. J. Stokell, A. Ayed, H. W. Duckworth, and G. D. Brayer.** 2001. Comparative analysis of folding and substrate binding sites between regulated hexameric type II citrate synthase and unregulated dimeric type I enzymes. Biochemistry. **40:** 13177-13187.

60. **O'Bierne, D. and G. Hamer.** 2000. The utilization of glucose/acetate mixtures by *Escherichia coli* W3110 under aerobic growth conditions. Bioprocess Engineering. **23:** 375-380.

61. **Ogawa, J., C.-L. Soong, M. Ito, and S. Shimizu.** 2001. Enzymatic production of pyruvate from fumarate – an application of microbial cyclic-imide-transforming pathway. Journal of Molecular Catalysis B: Enzymatic. **11:** 355-359.

62. **Park, S.-J., J. McCabe, J. Turna, and R. P. Gunsalus.** 1994. Regulation of the citrate synthase (*gltA*) gene of *Escherichia coli* in response to anaerobiosis and carbon supply: role of the *arcA* gene product. Journal of Bacteriology. **176:** 5086-5092.

63. **Patnaik, R., W. D. Roof, R. F. Young, and J. C. Liao.** 1992. Stimulation of glucose catabolism in *Escherichia coli* by a potential futile cycle. Journal of Bacteriology. **174:** 7527-7532.

64. **Patton, A. J., D. W. Hough, P. Towner, and M. J. Danson.** 1993. Does *Escherichia coli* possess a second citrate synthase gene? European Journal of Biochemistry. **214:** 75-81.

65. **Perham, R. N., L. C. Packman, and S. E. Radford.** 1987. 2-Oxo acid dehydrogenase multi-enzyme complexes: In the beginning and halfway there. Biochemical Society Symposium. **54:** 67-81.

66. **Postma, P. W., J. W. Lengeler, and G. R. Jacobson.** 1993. Phosphoenolpyruvate: carbohydrate phosphotransferase systems of bacteria. Microbiological Reviews. **57:** 543-594.

67. **Reed, L. J., F. H. Pettit, M. H. Eley, L. Hamilton, J. H. Collins, and R. M. Oliver.** 1975. Reconstitution of the *Escherichia coli* pyruvate dehydrogenase complex. Proceeds of the National Academy of Science, USA. **72:** 3068-3072.

68. **Robinson, M. S., M. J. Danson, and P. D. J. Weitzman.** 1983. Citrate synthase from a Gram-positive bacterium. Biochemical Journal. **213:** 53-59.

69. **Sanwal, B. D.** 1970. Regulatory characteristics of the diphosphopyridine nucleotide-specific malic enzyme of *Escherichia coli*. The Journal of Biological Chemistry. **245:** 1212-1216.

70. **Schinschel, C. and H. Simon.** 1993. Preparation of pyruvate from (R)- lactate with *Proteus* species. Journal of Bacteriology. **31:** 191-203.

71. **Shin, S., S. G. Song, D. S. Lee, J. G. Pan, and C. Park.** 1997. Involvement of *iclR* and *rpoS* in the induction of *acs*, the gene for acetyl coenzyme A synthetase of *Escherichia coli* K-12. FEMS Microbiology Letters. **146:** 103-108.

72. **Solomon, M. and P. D. J. Weitzman.** 1983. Occurrence of two distinct citrate synthases in a mutant of *Pseudomonas aeruginosa* and their growth-dependent variations. FEBS Letters. **155:** 157-160.

73. **Srere, P. A., H. Brazil, and L. Gonen.** 1963. The citrate condensing enzyme of pigeon breast muscle and moth flight muscle. Acta Chemica Scandinavica. **17:** S129-S134.

74. **Stafford, K.** Continuous Fermentation. Manual of Industrial Microbiology and Biotechnology. ed. A. L. Demain and N. A. Solomon. American Society of Microbiology. Washington, D.C. 1986.

75. **Stanko, R. T., H. R. Reynolds, R. Hoyson, J. E. Janosky, and R. Wolf.** 1994. Pyruvate supplementation of a low-cholesterol, low-fat diet: effects on plasma lipid concentrations and body composition in hyperlipidemic patients. American Journal of Clinical Nutrition. **59:** 423-427.

76. **Stanko, R. T., R. J. Robertson, R. W. Galbreath, J. J. Reilly, Jr., K. D. Greenawalt, and F. L. Goss.** 1990. Enhanced leg exercise endurance with a high-carbohydrate diet and dihydroxyacetone and pyruvate. Journal of Applied Physiology. **69:** 1651-1656.

77. **Stanko, R. T., D. L. Tietze, and J. E. Arch.** 1992a. Body composition, energy utilization, and nitrogen metabolism with a severely restricted diet supplemented with dihydroxyacetone and pyruvate. American Journal of Clinical Nutrition. **55:** 771-776.

78. **Stanko, R. T., D. L. Tietze, and J. E. Arch.** 1992b. Body composition, energy utilization, and nitrogen metabolism with a 4.25-MJ/d low-energy diet supplemented with pyruvate. American Journal of Clinical Nutrition. **56:** 630-635.

79. **Takao, S. and M. Tanida.** 1982. Pyruvic acid production by *Schizophyllum commune*. Journal of Fermentation Technology. **60:** 277-280.

80. **Tarmy, E. M. and N. O. Kaplan.** 1968. Kinetics of *Escherichia coli* B D-lactate dehydrogenase and evidence for pyruvate-controlled change in conformation. The Journal of Biological Chemistry. **243:** 2587-2596.

81. **Textor, S., V. F. Wendisch, A. A. DeGraaf, U. Müller, M. I. Linder, D. Linder, and W. Buckel.** 1997. Propionate oxidation in *Escherichia coli*: evidence for operation of a methylcitrate cycle in bacteria. Archives of Microbiology. **168:** 428-436.

82. **Tomar, A.** 2002. Production of pyruvate by *Escherichia coli* using metabolic engineering. Masters thesis. Athens, GA. Department of Biological and Agricultural Engineering, University of Georgia.

83. **Tomar, A., M. A. Eiteman, and E. Altman.** 2003. The effect of acetate pathway mutations on the production of pyruvate in *Escherichia coli*. Applied Microbiology and Biotechnology. **62:** 76-82.

84. **Uchio, R., K. Kikuchi, H. Enei, and Y. Hirose.** 1976. Process for producing pyruvic acid by fermentation. U. S. Patent. **3 993 543.**

85. **Underwood, S. A., M. L. Buszko, K. T. Shanmugam, and L. O Ingram.** 2002. Flux through citrate synthase limits growth of ethanogenic *Escherichia coli* KO11 during xylose fermentation. Applied and Environmental Microbiology. **68:** 1071-1081.

86. **Valentini, G., L. Chiarelli, R. Fortin, M. L. Speranza, A. Galizzi, and A. Mattevi.** 2000. The allosteric regulation of pyruvate kinase: A site-directed mutagenesis study. The Journal of Biological Chemistry. **275:** 18145-18152.

87. **van de Walle, M. and J. Shiloach.** 1998. Proposed mechanism of acetate accumulation in two recombinant *Escherichia coli* strains during high density fermentation. Biotechnology and Bioengineering. **57:** 71-78.

88. **Vemuri, G., M. A. Eiteman, E. Altman.** 2005. Pyruvate redirection and redox engineering affects overflow metabolism in *Escherichia coli.* Presentation at the 229th American Chemical Society National Meeting & Exposition at San Diego, CA.

89. **Williams, F. R. and L. P. Hager.** 1966. Crystalline flavin pyruvate oxidase from *Escherichia col*: I. Isolation and properties of the flavoprotein. Archives of Biochemistry. **116:** 168-176.

90. **Yamada, H., H. Kumagai, N. Kashima, and H. Torii.** 1972. Synthesis of L-tyrosine from pyruvate, ammonia and phenol by crystalline tyrosine phenol lyase. Biochemical and Biophysical Research Communications. **46:** 370-374.

91. **Yamaguchi, M., M. Tokuchige, and H. Katsuki.** 1973. Studies on regulatory functions of malic enzyme. II. Purification and molecular properties of nicotinamide adenine dinucleotide-linked malic enzyme from *Escherichia coli*. Journal of Biochemistry. **73:** 169-180.

92. **Yanese, H., N. Mori, M. Masuda, K. Kita, M. Shimao, and N. Kato.** 1992. Pyruvic production by *Enterococcus casseliflavus* A-12 from gluconate in an alkaline medium. Journal of Fermentation and Bioengineering. **73:** 287-291.

93. **Yokota, A., H. Shimizu, Y. Terasawa, N. Takaoka, and F. Tomita.** 1994. Pyruvic acid production by a lipoic acid auxotroph of *Escherichia coli* W1485. Applied Microbiology and Biotechnology. **41:** 638-643.

94. **Yokota, A. and S. Takao.** 1989. Pyruvic acid production by lipoic acid auxotrophs of *Enterobacter aerogenes*. Agricultural and Biological Chemistry. **53:** 705-711.

95. **Yokota, A., Y. Terasawa, N. Takaoka, H. Shimizu, and F. Tomita.** 1994. Pyruvic acid production by an F_1-ATPase-defective mutant of *Escherichia coli* W1485*lip2*. Bioscience, Biotechnology and Biochemistry. **58:** 2164-2167.

96. **Yoshinaga, T.** 1977. Structural specificity of the allosteric inhibitor of phosphoenolpyruvate carboxylase of *Escherichia coli*. Journal of Biochemistry. **81:** 665-671.

97. **Zelic, B., T. Gerharz, M. Bott, D. Vasic-Racki, C. Wandrey, and R. Takors.** 2003. Fed-batch process for pyruvate production by recombinant *Escherichia coli* YYC202 strain. Engineering in Life Sciences. **3:** 299-305.

APPENDICES

APPENDIX A

LIST OF TERMS

μ	Cell growth rate (h^{-1})
q_A	Specific acetate consumption rate (g/g_{cell} h)
q_G	Specific glucose consumption rate (g/g_{cell} h)
q_P	Specific pyruvate production rate (g/g_{cell} h)
D	Dilution rate of chemostat fermentation (h^{-1})
K_m	The dissociation constant of an enzyme for a substrate; a lower K_m value denotes a higher affinity for the substrate
OD	Optical density
Q_A	Volumetric acetate consumption rate (g/L h)
Q_G	Volumetric glucose consumption rate (g/L h)
Q_P	Volumetric pyruvate production rate (g/L h)
$Y_{X/S}$	Biomass yield from glucose ($g_{cell}/g_{glucose}$)

APPENDIX B

ENZYME ASSAYS

B.1: Lactate Dehydrogenase Assay:

The samples were prepared by washing twice with a 20 mM Tris-HCl (pH 8.1) and 20% glycerine solution. The buffered cell suspensions were then disrupted by passing twice through a FRENCH® Press (Spectronic Instrument FRENCH® Pressure Cell and Press Model Y-1517 using the mini cell) at 15,000 psi. After disruption the samples were centrifuged at 20,000 x *g* for 20 minutes at 4° C. The resulting cell free extract was used for analysis of enzyme activity. The activity of lactate dehydrogenase was analyzed by the enzyme assay developed by Bunch et al. (1997). The assay solution contained 21.5 mM MOPS buffer (pH 7.0), 0.192 mM NADH, 30 mM pyruvate for the experimental sample (0 mM pyruvate for control), and brought to a final volume of 900 µL with DI H_2O. The assay was conducted at 340 nm on a Beckman DU50 spectrophotometer using a UV lamp. The sample and control solutions were prepared quartz cuvettes and allowed to reach 37°C for five minutes at which time the instrument was blanked and the read sample option was selected. Immediately and simultaneously 100 µL of cell free extract was added to each cuvette and the kinetic measurement was initiated with readings every 5 s for 60 s total. The cell extract concentration added to the reagent was adjusted so that the change in absorbance was between 0.05 and 0.7 AU in one minute. One unit (U) of lactate dehydrogenase activity was defined as the amount of enzyme required to produce 1.0 µmole of lactate in one minute. The rate change in absorbance was calculated as the difference between the experimental rate and that of the control as seen in equation 1.

$$dA/dt = [rate]_{experimental} - [rate]_{control} \qquad (min^{-1}) \qquad [1]$$

The activity is define as in equation 2 below:

$$Activity = (1000 \times TV \times dA/dt \times D) / (\varepsilon \times V \times CF) \qquad (U/L) \qquad [2]$$

where,

TV = total volume of cuvette (1000 μL)

V = volume of cell free extract used (100 μL)

ε = molar extinction coefficient for NADH (6.22 L/mmol for a path length of 1.0 cm)

D = dilution of cell free extract

CF = concentration factor of cell free extract (For example, if a 100 ml sample is concentrated to 1 ml volume for the French Press, then CF = 100)

The specific activity is the activity calculated using equation 2 above divided by the protein concentration of the cell free extract as illustrated in equation 3

Specific Activity = Activity / Protein conc. (U/mg protein) [3]

The protein concentration is measured in mg/L. The protein concentration was measured using the BCA Protein Assay Kit with bovine serum albumen used as a standard.

B.2: Citrate Synthase Assay:

The samples were prepared by washing twice with a 20 mM Tris-HCl (pH 8.1) and 20% glycerine solution. The buffered cell suspensions were then disrupted by passing twice through a FRENCH® Press (Spectronic Instrument FRENCH® Pressure Cell and Press Model Y-1517 using the mini cell) at 15,000 psi. After disruption the samples were centrifuged at 20,000 x *g* for 20 minutes at 4° C. The resulting cell free extract was used for analysis of enzyme activity. The enzyme assay used to analyze *CitZ* activity was adapted from the protocol developed by Srere et al. (1963). The assay solution contained 20 mM Tris-HCl (pH 8.1), 0.5 mM acetyl CoA, 10 mM OAA for the experimental sample (0 mM OAA for control), 1 g/L DTNB in ethanol, 10 mM KCl, and was brought to a final volume of 900 µL with DI H_2O. The assay was conducted at 412 nm on a Beckman DU50 spectrophotometer using the visible wavelength lamp. The sample and control solutions were prepared quartz cuvettes and allowed to reach 37°C for five minutes at which time the instrument was blanked and the read sample option was selected. Immediately and simultaneously 100 µL of cell free extract was added to each cuvette and the kinetic measurement was initiated with readings every 5 s for 60 s total. The cell extract concentration added to the reagent was adjusted so that the change in absorbance was between 0.05 and 0.7 AU in one minute. One unit (U) of citrate synthase activity was defined as the amount of enzyme required to produce 1.0 µmole of citrate in one minute. The rate change in absorbance was calculated as the difference between the experimental rate and that of the control as seen in equation 4.

$$dA/dt = [rate]_{experimental} - [rate]_{control} \qquad (min^{-1}) \qquad [4]$$

The activity is define as in equation 5 below:

$$Activity = (1000 \times TV \times dA/dt \times D) / (\varepsilon \times V \times CF) \qquad (U/L) \qquad [5]$$

where,

TV = total volume of cuvette (1000 μL)

V = volume of cell free extract used (100 μL)

ε = molar extinction coefficient for reduced DTNB (13.6 L/mmol for a path length of 1.0 cm)

D = dilution of cell free extract

CF = concentration factor of cell free extract (For example, if a 100 ml sample is concentrated to 1 ml volume for the French Press, then CF = 100)

The specific activity is the activity calculated using equation 5 above divided by the protein concentration of the cell free extract as illustrated in equation 6

Specific Activity = Activity / Protein conc. (U/mg protein) [6]

The protein concentration is measured in mg/L. The protein concentration was measured using the BCA Protein Assay Kit with bovine serum albumen used as a standard.

B.3: Acetyl CoA Synthetase Assay:

The samples were prepared by washing twice with a 20 mM Tris-HCl (pH 8.1) and 20% glycerine solution. The buffered cell suspensions were then disrupted by passing twice through a FRENCH® Press (Spectronic Instrument FRENCH® Pressure Cell and Press Model Y-1517 using the mini cell) at 15,000 psi. After disruption the samples were centrifuged at 20,000 x *g* for 20 minutes at 4° C. The resulting cell free extract was used for analysis of enzyme activity. The enzyme assay used to measure the activity of acetyl CoA synthetase was adapted from the protocols developed by Jones and Lipmann (1955) and Brown, Jones-Mortimer and Kornberg (1977). The assay solution contained 50 mM Tris-HCl (pH 8.1), 100 mM hydroxylamine neutralized with equal molar KOH, 5 mM $MgCl_2$, 20 mM sodium acetate, 333 µM CoA lithium salt for the experimental sample (0 mM for the background sample), 5 mM ATP disodium salt, 10 mM glutathione pH 4.5, 50 mM KF and was brought to a final volume of 900 µL with DI H_2O. A standard curve was prepared by reacting lithium potassium acetyl phosphate (LAP) with hydroxylamine in a 50 mM Tris-HCl (pH 8.1) solution concomitantly with the enzyme reaction. The LAP concentrations used were 2.0 µmol/mL, 1.0 µmol/mL, 0.6 µmol/mL, 0.3 µmol/mL, and 0.0 µmol/mL with DI H_2O used to bring the final volume to 1 mL. The test tubes containing the above reaction solution were placed in a 37°C water batch for five minutes. The reaction was initiated by the addition of 100 µL of cell free extract into both the experimental and background tubes, and placed in the 37°C water batch for 20 minutes along with the tubes containing the standards. The reactions were terminated by the addition of 1 ml of 25 g/L $FeCl_3$ in 2.0 M HCl and transferred to microcentrifuge tubes and spun for 5 to 10 minutes at maximum speed to pellet the precipitated protein. The standards and samples were measured at 520 nm using a

Beckman DU50 spectrophotometer using the visible wavelength lamp. The activity of the samples were calculated using equation 7 below

$$\text{Activity} = (1000 \times TV \times m \times Abs \times D) / (t_R \times V \times CF) \quad (U/L) \quad [7]$$

Where,

Abs = absorbance of sample at 520 nm relative to the background

m = the best fitting slope from the standard curve

TV = total volume in cuvette (1000 μL)

V = volume of cell extract used (100 μL)

t_R = time of reaction (20 min)

D = dilution of cell free extract

CF = concentration factor of cell extract (For example, if a 100 ml sample is concentrated to 1 ml volume for the French Press, then CF = 100)

The specific activity is the activity calculated using equation 7 above divided by the protein concentration of the cell free extract as illustrated in equation 8

$$\text{Specific Activity} = \text{Activity} / \text{Protein conc.} \quad (U/mg \text{ protein}) \quad [8]$$

The protein concentration is measured in mg/L. The protein concentration was measured using the BCA Protein Assay Kit with bovine serum albumen used as a standard.

B.4: NADH/NAD Assay:

Upon reaching steady state for each dilution rate samples were taken for analysis of NADH and NAD^+ concentrations as per the assay protocol developed by Bernofsky and Swan (1973) and Leonardo et al. (1996). Two 10 mL samples were withdrawn into and immediately mixed with 10 mL of methanol that had been set in dry ice for one hour. The resulting 20 mL was then added and mixed with another 30 mL of methanol kept in dry ice. The solutions were centrifuged for 5 minutes at 12304 x *g* and –10°C. The cell pellets were resuspended in either 3 mL of 0.2 M HCl or 3 mL of 0.2 M NaOH for analysis of NAD^+ or NADH, respectively. The resuspended cells were then boiled for 10 minutes and centrifuged again for 5 minutes at 12304 x *g* and 4°C. The supernatant was distributed to 1 mL microcentrifuge tubes for analysis. The assay was conducted at 570 nm on a Beckman DU50 spectrophotometer. The assay solution in 1 mL total volume contained 0.1 M Bicine buffer (pH 8.0), 1.66 mM phenazine ethosulfate (PES), 0.42 mM 3-[4,5-dimethylthiazol-2-yl]-2,5-diphenyltetrazolium bromide (MTT), 4 mM EDTA (pH 8.0), 10% ethanol (experimental), 0.05 M NaOH or 0.05 HCl for NAD^+ or NADH, respectively, 100 µL diH_2O (control) and 250 µL cell free extract. The cuvettes are incubated for 1 minute at 30°C at which time the instrument was blanked and the read sample option was selected. Immediately and simultaneously 20 µL of 500 U/ml alcohol dehydrogenase was added and aspirated into each cuvette and the kinetic measurement was initiated with readings every 4 s for 40 s total. The NAD^+ concentration is calculated by using equation 9

$$NAD^+ = 0.058 \times dA/dt \quad \text{(nM)} \quad [9]$$

Where,

dA/dt = the rate of the experimental cuvette less that of the control.

The concentration of NADH is calculated using equation 10

$$NADH = 0.0609 \times dA/dt \quad \text{(nM)} \quad [10]$$

Where,

dA/dt = the rate of the experimental cuvette less that of the control.

APPENDIX C

FERMENTATION RESULTS

C.1 Batch Results for ALS 929

Experiment: ALS 929 fermenation 5/28/04

media: modified Zelic 30 g/L glucose and 5 g/L acetate as (NH4(CH3COO)) [9.32 g/L]

temperature: 37˚ C

pH: 7.0, adjusted with 20% NH4OH

DO controlled above 40% with agitation

agitation: initial 500 rpm

air flow are 1.5 L/min

time (h)	OD (550 nm)	DO (%)	Glc (g/L)	Ace (g/L)	Pyr (g/L)	Lac (g/L)	Volume (L)	comments
0.00	0.16	99.5	28.0	4.6	0.0	0.5	1.54	
3.83	0.27	96.8	27.5	4.5	0.0	0.0	1.52	
7.75	0.34	95.3	28.5	4.6	0.0	0.0	1.50	
11.83	0.68	92.9	27.5	4.4	0.2	0.0	1.49	
12.75	0.84	91.6					1.48	
15.75	2.42	76.0	25.4	3.7	0.8	0.0	1.47	
16.75	3.61	65.7					1.46	
17.25	4.74	56.3	25.3	3.0	1.7	0.0	1.53	added 30 g glc and 9.32 g NH_4CH_3COO in 80 mL total
17.25	4.55	58.9	41.3	7.0	1.5	0.0	1.52	
18.00	5.44	55.9	42.2	6.9	1.9	0.0	1.51	
18.75	6.63	49.5	42.0	6.2	2.4	0.0	1.50	
19.50	7.53	40.8	41.0	5.7	2.9	0.0	1.49	750 rpm
20.25	8.79	60.4	35.1	4.2	3.3	0.0	1.48	
21.00	10.09	51.0	34.2	3.1	4.3	0.0	1.47	
21.75	15.55	39.3	35.6	1.5	6.5	0.0	1.46	1000 rpm
22.50	17.98	80.8	26.0	0.1	8.4	0.0	1.45	

Experiment: ALS 929 fermenation 6/8/04

media: modified Zelic 10 g/L glucose and 5 g/L acetate as (NH4(CH3COO)) [9.32 g/L]

temperature: 37˚ C

pH: 7.0, adjusted with 20% NH4OH

agitation

agitation: initial 500 rpm

air flow rate 1.5 L/min

time (h)	OD (550 nm)	X (g/L)	DO (%)	Glc (g/L)	Ace (g/L)	Pyr (g/L)	Volume L	comments
0.00	0.23	0.06	99.4	10.1	4.9	0.0	1.54	
4.17	0.24	0.07	97.3	10.3	5.0	0.0	1.51	
8.08	0.48	0.13	94.9	9.9	4.9	0.1	1.50	
12.25	1.80	0.49	86.0	8.6	4.2	0.6	1.48	
13.00	2.42	0.67	84.0	8.0	3.9	0.8	1.47	
13.75	3.19	0.88	75.5	7.3	3.6	1.0	1.45	
14.50	4.52	1.24	64.2	6.8	3.3	1.4	1.44	
15.25	6.44	1.77	46.2	4.7	2.2	1.9	1.42	
15.42	6.40	1.76	53.0	23.7	6.2	2.0	1.48	Glc and Ace 70 mL
16.00	7.86	2.16	42.9	23.7	5.9	2.5	1.46	750 rpm
16.75	9.92	2.72	68.0	21.1	4.5	3.2	1.45	
17.50	12.09	3.32	59.1	18.7	3.2	4.2	1.43	
18.25	14.15	3.89	44.9	15.2	1.4	5.9	1.42	
18.83	20.46	5.62	74.9	6.9	0.0	9.4	?	foam out: 100 -200 mL lost
19.83	23.58	6.47	84.9	1.6	0.0	12.4	?	
20.50	22.40	6.15	100.8	0.5	0.0	13.6	?	
21.17	23.76	6.52	101.4	0.4	0.0	14.7	?	

Experiment: ALS 929 fermenation 6/14/04

media: modified Zelic 10 g/L glucose and 5 g/L acetate as (NH4(CH3COO)) [9.63 g/L]

temperature: 37˚ C

pH: 7.0, adjusted with 20% NH4OH

DO controlled above 40% with agitation

agitation: initial 500 rpm

air flow rate 1.5 L/min

time (h)	OD (550 nm)	X (g/L)	DO (%)	Glc (g/L)	Ace (g/L)	Pyr (g/L)	Volume L	comments
0.00	0.1676	0.0460		9.10	4.70	0.00	1.54	pH set 7.2
3.50	0.2357	0.0647		10.06	4.70	0.00	1.53	pH set 7.1
7.67	0.5287	0.1452		10.15	4.79	0.06	1.51	
12.25	1.6210	0.4451		9.07	4.41	0.46	1.50	
12.75	1.9408	0.5329		8.83	4.25	0.55	1.49	
13.50	2.5783	0.7080		8.74	4.12	0.74	1.47	
14.25	3.6251	0.9955		7.14	3.30	0.88	1.46	
15.00	4.9299	1.3538		6.24	2.71	1.22	1.45	
15.75	7.0300	1.9304		4.55	1.73	1.72	1.50	Glc and Ace 70 mL added
16.50	9.4820	2.6038		23.18	5.45	2.27	1.48	750 rpm
17.25	11.9000	3.2677		19.98	3.87	3.02	1.47	
18.00	14.3688	3.9457		18.12	2.50	4.22	1.45	
18.75	18.1532	4.9849		14.04	0.24	6.22	1.44	1000 rpm
19.50	26.7384	7.3424		8.16	0.00	9.26	1.43	
20.25	25.8616	7.1016		3.37	0.00	11.72	1.43	
21.00	25.3331	6.9565		0.21	0.00	13.87	1.42	
21.75	25.1304	6.9008		0.29	0.00	13.88	1.41	foam out 150 mL

Experiment: ALS 929 fermenation 6/22/04

media: modified Zelic 10 g/L glucose and 5 g/L acetate as (NH4(CH3COO)) [9.63 g/L]

temperature: 37˚ C

pH: 7.0, adjusted with 20% NH4OH

DO controlled above 40% with agitation

agitation: initial 500 rpm

air flow rate 1.5 L/min

time (h)	OD (550 nm)	X (g/L)	DO (%)	Glc (g/L)	Ace (g/L)	Pyr (g/L)	Volume L	comments
0.00	0.2596	0.0713	99.5	10.90	4.66	0.00	1.54	pH set 7.05
3.75	0.3120	0.0857	94.8	9.92	4.78	0.00	1.53	pH set 7.00
8.00	0.6528	0.1793	93.0	9.60	4.64	0.10	1.51	
12.00	1.4303	0.3928	84.0	8.22	4.09	0.42	1.50	
12.75	1.9127	0.5252	80.1	8.10	3.99	0.57	1.49	
13.50	2.4493	0.6726	75.2	7.63	3.88	0.74	1.48	
14.25	3.5381	0.9716	68.4	6.72	3.31	0.95	1.47	
15.00	4.6566	1.2787	63.5	5.52	2.66	1.23	1.46	
15.75	6.6767	1.8334	56.7	4.32	1.78	1.71	1.52	750 rpm; Glc and Ace 70 mL total
15.75	6.3632	1.7473	62.9	22.36	6.28	1.76	1.50	
16.50	8.0253	2.2037	59.9	21.41	5.58	2.21	1.48	
17.33	11.4831	3.1533	52.5	19.18	4.24	3.22	1.47	
18.00	14.5126	3.9852	42.3	16.74	2.85	4.23	1.46	
18.75	16.7365	4.5958	28.8	13.00	0.92	5.91	1.45	1000 rpm
19.92	24.0000	6.5904	78.1	3.94	0.00	10.30	1.44	
20.75	21.1320	5.8028	87.7	0.19	0.00	12.30	1.43	
21.50	20.1040	5.5206	92.5	0.34	0.00	12.39	1.42	

Experiment: ALS 929 fermentation 6/30/04 DCW

media: modified Zelic 10 g/L glucose and 5 g/L acetate as (NH4(CH3COO)) [9.63 g/L]

temperature: 37˚ C

pH: 7.0, adjusted with 20% NH4OH

DO controlled above 40% with agitation

agitation: initial 500 rpm

air flow rate 1.5 L/min

time h	OD 550 nm	cell g	volume L	DCW g/L
12.00	3.8143	0.020	0.02	1.00
13.50	7.6169	0.038	0.02	1.88
14.00	8.8226	0.048	0.02	2.39
15.50	13.914	0.080	0.02	3.98
16.50	16.626	0.091	0.02	4.56
17.17	19.609	0.092	0.02	4.60
18.00	20.467	0.095	0.02	4.76

C.2 Batch Results for KD 423

Experiment: KD 423 fermenation 11/04/04

media: modified Zelic 10 g/L glucose and 5 g/L acetate as (NH4(CH3COO)) [9.63 g/L], 2 g/L succinate

temperature: 37˚ C

pH: 7.0, adjusted with 20% NH4OH

DO controlled above 40% with agitation

agitation: initial 500 rpm

air flow rate 1.5 L/min

time (h)	OD (550 nm)	X (g/L)	DO (%)	Glc (g/L)	Suc (g/L)	Ace (g/L)	Pyr (g/L)	Volume L	comments
0.00	0.2402	0.0660		9.35	2.33	4.65	0.00	1.49	
4.50	0.5712	0.1569		9.98	2.55	4.96	0.00	1.49	
8.00	0.3003	0.0825		6.58	1.87	3.83	0.00	1.49	
12.08	1.0329	0.2836		6.39	1.77	3.71	0.00	1.48	
12.75	1.1951	0.3282		6.27	1.74	3.57	0.00	1.47	
13.50	1.5447	0.4242		6.42	1.72	3.52	0.01	1.46	
14.33	1.9915	0.5469			1.61	3.39	0.12	1.45	
15.00	2.5398	0.6974		5.55	1.48	3.12	0.24	1.45	
15.75	3.5336	0.9703		4.64	1.22	2.61	0.39	1.44	
16.75	4.2930	1.1789		4.21	1.09	2.27	0.69	1.44	
17.25	6.3640	1.7476		3.17	0.87	1.73	0.94	1.56	glc, ace and suc 120 mL
17.50	6.3051	1.7314		16.20	2.58	5.18	1.32	1.55	750 rpm
18.25	7.9515	2.1835		15.31	2.20	4.58	1.60	1.54	
19.00	9.0610	2.4882		13.90	1.84	3.58	2.06	1.53	
19.75	12.1423	3.3343		13.00	1.24	2.79	2.62	1.52	
20.50	15.1379	4.1569		11.12	0.99	1.60	3.62	1.51	
21.25	18.2226	5.0039		6.11	0.38	0.00	4.24	1.50	1000 rpm
22.00	19.5452	5.3671		2.75	0	0	5.89	1.50	

Experiment: KD 423 fermenation 11/30/04

media: modified Zelic 10 g/L glucose and 5 g/L acetate as (NH4(CH3COO)) [9.63 g/L]

temperature: 37˚ C

pH: 7.0, adjusted with 20% NH4OH

DO controlled above 40% with agitation

agitation: initial 500 rpm

air flow rate 1.5 L/min

11/30/04 929 acs

time (h)	OD (550 nm)	X (g/L)	DO (%)	Glc (g/L)	Ace (g/L)	Pyr (g/L)	Volume L	spec. act. (U/mg)	comments
0.00	0.2065	0.0567		9.66	4.62	0.00	1.50		
6.00	0.2585	0.0710		9.71	4.94	0.00	1.49		
12.00	1.1390	0.3128		8.59	4.36	0.00	1.49		
12.75	1.6869	0.4632		8.10	3.98	0.00	1.47		
13.50	2.2815	0.6265		7.68	3.89	0.00	1.46		
14.25	3.1695	0.8703		6.64	3.33	0.01	1.45		
15.00	4.5125	1.2391		5.53	2.70	0.02	1.44		
15.75	5.9916	1.6453		4.13	1.85	0.04	1.42		
16.50	7.5741	2.0798		2.24	1.20	0.07	1.40	0.0040	
16.58	7.4627	2.0493		19.67	5.33	0.51	1.51		glc and ace added, 750 rpm
17.50	9.8469	2.7040		17.93	4.33	0.66	1.50		
18.25	13.6719	3.7543		15.09	3.14	0.65	1.49	0.0019	
19.00	16.2252	4.4554		11.96	1.73	0.60	1.48		
19.75	18.8554	5.1777		6.47	0.00	0.55	1.49		1000 rpm
20.75	22.3002	6.1236		1.41	0.00	0.58	1.48		
21.50	20.4967	5.6284		0.18	0.00	0.69	1.50		
22.25	17.6792	4.8547		0.03	0.00	0.71	1.51		375 mL foam lost

Fermentation Summary

OD 550 nm	m h^{-1}	Q_G g/Lh	q_G g/gh	Q_A g/Lh	q_A g/gh	Q_P g/Lh	q_P g/gh	G/A	P/G
5	0.390	1.870	1.420	0.930	0.710	0.023	0.018	2.000	0.013
10	0.350	2.580	0.960	1.270	0.470	0.120	0.043	2.043	0.045

Experiment: KD 423 fermenation 12/16/04

media: modified Zelic 10 g/L glucose and 5 g/L acetate as (NH4(CH3COO)) [9.63 g/L]

temperature: 37˚ C

pH: 7.0, adjusted with 20% NH4OH

DO controlled above 40% with agitation

agitation: initial 500 rpm

air flow rate 1.5 L/min

time (h)	OD (550 nm)	X (g/L)	DO (%)	Glc (g/L)	Ace (g/L)	Pyr (g/L)	Volume L	spec. act. (U/mg)	comments
0.00	0.0910	0.0250		9.98	4.92	0.00	1.49		
6.00	0.1805	0.0496		9.97	4.81	0.00	1.48		
12.33	1.5414	0.4233		8.45	4.17	0.00	1.46		
12.75	1.7828	0.4896		8.21	4.05	0.00	1.45		
13.50	2.6197	0.7194		7.58	3.74	0.00	1.43		
14.25	3.6182	0.9936		5.26	2.66	0.00	1.42		
15.00	4.9425	1.3572		4.12	2.02	0.01	1.41		
15.75	6.7096	1.8425		2.88	1.27	0.05	1.52		glc and ace added, 750 rpm
15.83	6.7705	1.8592		16.65	4.91	0.42	1.50		
16.50	8.0014	2.1972		21.10	5.46	0.68	1.49		
17.25	11.3405	3.1141		18.59	4.34	0.85	1.47	0.005179	
18.00	13.1915	3.6224		16.34	3.05	0.86	1.46		
18.75	16.5042	4.5321		13.16	1.42	0.90	1.44		
19.50	19.0836	5.2404		6.21	0.00	1.01	1.44		1000 rpm
20.25	23.4805	6.4477		2.57	0.00	1.06	1.43		
21.00	21.5774	5.9252		0.32	0.00	0.99	1.43		
21.67	21.8751	6.0069		0.00	0.00	1.00	1.42		135 mL lost by foaming

Experiment: KD 423 fermenation 11/30/04 100 mM IPTG

media: modified Zelic 10 g/L glucose and 5 g/L acetate as (NH4(CH3COO)) [9.63 g/L]

temperature: 37˚ C

pH: 7.0, adjusted with 20% NH4OH

DO controlled above 40% with agitation

agitation: initial 500 rpm

air flow rate 1.5 L/min

time (h)	OD (550 nm)	X (g/L)	DO (%)	Glc (g/L)	Ace (g/L)	Pyr (g/L)	Volume L	spec. act. (U/mg)	comments
0.00	0.1588	0.0436		9.62	4.80	0.00	1.50		
6.00	0.2880	0.0791		9.72	4.78	0.00	1.48		
12.00	1.4805	0.4065		8.78	4.31	0.00	1.48		
12.75	1.8714	0.5139		8.07	4.02	0.00	1.47		13 h induced w/ 100mM IPTG
13.50	2.6245	0.7207					1.46		
14.25	3.4964	0.9601		7.16	3.45	0.03	1.45		
15.00	4.0106	1.1013		6.44	3.17	0.05	1.44		
15.75	4.4532	1.2228		5.92	2.87	0.09	1.43		
16.50	4.9482	1.3588		5.36	2.63	0.13	1.40	0.0727	
16.58	4.5699	1.2549		24.87	7.44	0.49	1.51		glc and ace added
17.50	4.9004	1.3456		25.85	7.78	0.50	1.50		
18.25	5.0440	1.3851		25.57	7.66	0.52	1.48	0.0699	
19.00	4.8250	1.3249		25.63	7.56	0.54	1.47		
19.75	4.7550	1.3057		24.91	7.37	0.53	1.46		
20.75	4.7165	1.2952		25.03	7.49	0.56	1.45		
21.50	4.5220	1.2417		24.57	7.22	0.52	1.43		

Fermentation Summary

m h^{-1}	Q_G g/Lh	q_G g/gh	Q_A g/Lh	q_A g/gh	Q_P g/Lh	q_P g/gh	G/A	P/G
0.427	0.671	0.977	0.388	0.565	0.015	0.022	1.730	0.023

Experiment: KD 423 fermenation 12/09/04 20 mM IPTG

media: modified Zelic 10 g/L glucose and 5 g/L acetate as (NH4(CH3COO)) [9.63 g/L]

temperature: 37˚ C

pH: 7.0, adjusted with 20% NH4OH

DO controlled above 40% with agitation

agitation: initial 500 rpm

air flow rate 1.5 L/min

time (h)	OD (550 nm)	X (g/L)	DO (%)	Glc (g/L)	Ace (g/L)	Pyr (g/L)	Volume L	spec. act. (U/mg)	comments
0.00	0.0688	0.0189		9.06	4.46	0.00	1.49		
6.00	0.2247	0.0617		8.94	4.53	0.00	1.49		
12.17	1.1701	0.3213		8.37	4.23	0.00	1.49		
12.75	1.5793	0.4337		8.55	4.27	0.00	1.48		
13.50	2.1469	0.5895		8.09	4.10	0.01	1.46		induced 30 mL 1M IPTG
14.25	2.8858	0.7924		7.04	3.55	0.03	1.45		
15.00	3.6391	0.9993		6.50	3.24	0.06	1.44		
15.75	4.2260	1.1605		5.81	2.94	0.07	1.44		
16.50	4.7074	1.2927		5.15	2.56	0.10	1.42	0.0550	
16.58	4.5608	1.2524		23.28	7.05	0.48	1.53		added glc and ace
17.25	4.8655	1.3361		25.89	7.70	0.49	1.51		
18.00	4.9552	1.3607		25.03	7.49	0.54	1.49	0.0602	
18.75	5.0046	1.3743		23.78	7.08	0.50	1.48		
19.50	5.0303	1.3813		23.40	6.98	0.51	1.47		
20.25	5.0144	1.3770		25.03	7.35	0.55	1.46		

Fermentation Summary

OD 550 nm	m h-1	Q_G g/Lh	q_G g/gh	Q_A g/Lh	q_A g/gh	Q_P g/Lh	q_P g/gh	G/A	P/G
2.5	0.36	0.95	1.38	0.47	0.68	0.02	0.035	2.03	0.025

Experiment: KD 423 fermenation 12/16/04 20 mM IPTG

media: modified Zelic 10 g/L glucose and 5 g/L acetate as (NH4(CH3COO)) [9.63 g/L]

temperature: 37˚ C

pH: 7.0, adjusted with 20% NH4OH

DO controlled above 40% with agitation

agitation: initial 500 rpm

air flow rate 1.5 L/min

time (h)	OD (550 nm)	X (g/L)	DO (%)	Glc (g/L)	Ace (g/L)	Pyr (g/L)	Volume L	spec. act. (U/mg)	comments
0.00	0.0639	0.0175		9.78	4.82	0.00	1.49		
6.00	0.1610	0.0442		9.62	4.70	0.00	1.49		
12.33	1.0868	0.2984		8.74	4.40	0.00	1.48		
12.75	1.2555	0.3448		8.31	4.18	0.00	1.46		
13.50	1.5981	0.4388		7.79	3.83	0.00	1.45		30 mL IPTG
14.25	2.3460	0.6442		8.02	3.93	0.02	1.44		
15.00	3.0000	0.8238		7.24	3.58	0.03	1.43		
15.75	3.5925	0.9865		6.59	3.19	0.05	1.42		
16.50	4.0813	1.1207		6.34	3.14	0.11	1.52	0.071499	glc and ace added
16.58	3.8880	1.0676		25.45	7.85	0.37	1.50		
17.25	4.2403	1.1644		25.54	7.86	0.44	1.49		
18.00	4.3319	1.1895		26.11	7.83	0.53	1.47	0.0696	
18.75	4.4730	1.2283		25.25	7.59	0.53	1.45		
19.50	4.3987	1.2079		24.02	7.23	0.54	1.44		
20.25	4.3299	1.1890		24.26	7.28	0.54	1.43		
21.00	4.2075	1.1554		24.05	7.35	0.56	1.41		

Fermentation Summary

OD	m	Q_G	q_G	Q_A	q_A	Q_P	q_P	G/A	P/G
550 nm	h^{-1}	g/Lh	g/gh	g/Lh	g/gh	g/Lh	g/gh		
2.5	0.336	0.515	0.756	0.279	0.409	0.023	0.033	1.850	0.044

C.3 Continuous Results for ALS 929

Calculations for Glc-limited chemostat ALS 929 10/14/04				
Aimed D (h^{-1})		0.15	0.25	0.34
Aimed Acetate (g/L)		5	5	5
Flowrate (L/h)		0.21	0.39	0.48
Final Volume (L)		1.44	1.44	1.44
Actual D (h^{-1})	flowrate/final volume	0.146	0.271	0.333
Sample volume(L)		0.02	0.02	0.02
Boat 1 Wt. before (g)		0.9854	0.9852	0.9871
Boat 1 Wt. after (g)		1.0218	1.0284	1.039
Cell Wt. 1 (g)	cell wt. =boat wt. after - boat wt.	0.0364	0.0432	0.0519
Boat 2 Wt. before (g)	before	0.9855	~~0.9859~~	0.987
Boat 2 Wt. after (g)		1.0204	~~1.0089~~	1.0374
Cell Wt. 2 (g)		0.0349	~~0.023~~	0.0504
Ave. Cell Wt. (g)		0.03565	0.0432	0.05115
DCW (g/L)	DCW=cell wt. / sample volume	1.783	2.160	2.558
OD (550 nm)		5.7917	6.6685	7.6555
Glucose in Feed (g/L)		4.8815	4.994	4.796
Glucose in Effluent (g/L)		0	0	0
Acetate in Feed (g/L)		4.75	4.862	4.708
Acetate in Effluent (g/L)		0.55	0.979	0.517
$Y_{X\|S}$ (g/g)	$Y_{X\|S}$ = DCW/(S_{in}-S_{out})	0.365	0.433	0.533
Q_A (g/Lh)	Q_A=(Ace_{out}-Ace_{in})*D	0.613	1.052	1.397
q_A (g/gh)	q_A =Q_A/X	0.344	0.487	0.546
q_A (mmol/gh)	q_A = qA*1000/59.04	5.820	8.246	9.252
Qs (g/Lh)	Qs=(Glc_{in}-Glc_{out})*D	0.712	1.353	1.599
qs (g/gh)	qs =Qs/X	0.399	0.626	0.625
qs (mmol/gh)	qs = qs*1000/180	2.219	3.479	3.473
qs/qa (g/g)		1.162	1.286	1.144
qs/qa (mol/mol)		0.381	0.422	0.375
Pyruvate in Feed (g/L)		0.000	0.000	0.000
Pyruvate in Effluent (g/L)		0.084	0.134	0.000
Q_P (g/Lh)	Q_P=(Pyr_{out}-Pyr_{in})*D	0.012	0.036	0.000
q_P (g/gh)	q_P =Q_P/X	0.007	0.017	0.000
Unknown in Feed (MU/L)		0.000	0.000	0.000
Unknown in Effluent (MU/L)		0.116	0.157	0.132
Q_{UN} (MU/Lh)	Q_{UN}=(Un_{out}-Un_{in})*D	0.017	0.042	0.044
q_{UN} (MU/gh)	q_{UN} =Q_{UN}/X	0.009	0.020	0.017
Qgas (L/min)		1.5	1.5	1.5
oxygen initially		20.99	20.99	20.99
oxygen at steady state		19.76	19.02	18.44
Density of O_2 at 0°C (g/L)		1.429	1.429	1.429
OUR (g oxygen/min)	OUR=($O_{2,ini}$-$O_{2,steady}$)*Qgas*ρ/100	0.026	0.042	0.055
OUR (mmol oxygen/h)	FW = 32	49.434	79.176	102.486
qo (mmol O2/g DCW h)	Specific OUR=OUR/(V*DCW)	19.259	25.455	27.828
CO_2 initially		0	0	0
CO_2 at steady state		0.62	0.99	1.29
Density of CO_2 at 0°C (g/L)		1.977	1.977	1.977
CER (g carbon dioxide/min)	CER=($CO_{2,steady}$-$CO_{2,in}$)*Qgas*ρ/100	0.018	0.029	0.038
CER (mmol carbon dioxide/h)	FW = 44	25.07	40.03	52.17
q_{CO2} (mmol CO_2/g DCW h)	Specific CER=CER/(V*DCW)	9.77	12.87	14.16
RQ	RQ=CER/OUR	0.51	0.51	0.51
C-produced: CO_2 (mmol C/h)	CER	25.07	40.03	52.17
C-produced: Biomass (mmol C/h)		10.61	23.88	34.80
C-produced: pyruvate (mmol C/h)	(Pyr_{out}-Pyr_{in})*3*1000*D/88.06	0.42	1.24	0.00
total C-produced (mmol C/h)		36.10	65.15	86.96
C-consumed: Acetate (mmol C/h)	(Ace_{out}-Ace_{in})*2*1000*D/59.04	20.75	35.62	47.32
C-consumed: Glucose (mmol C/h)	(Glc_{out}-Glc_{in})*6*1000*D/180	23.73	45.08	53.29
total C-consumed: Glu(mmol C/h)		44.48	80.71	100.61
Carbon Balance (%)	C-produced/C-consumed	0.81	0.81	0.86
NADH (nM)		0.19	~~-0.76~~	0.14
NAD (nM)		3.59	~~5.36~~	4.01
NADH/NAD		0.05	~~-0.14~~	0.03

Calculations for Glc-limited chemostat ALS 929 04/23/05 without IPTG		C-limited	C-limited	C-limited	N-limited
Aimed D (h^{-1})		0.18	0.33	0.4	0.26
Aimed Acetate (g/L)		5	5	5	5
Flowrate (L/h)		0.2617	0.489	0.5629	0.403
Final Volume (L)		1.54	1.54	1.54	1.54
Actual D (h^{-1})	flowrate/final volume	0.170	0.318	0.366	0.262
Sample volume(L)		0.02	0.02	0.02	0.02
Boat 1 Wt. before (g)		0.9847	0.9846	0.9863	0.9856
Boat 1 Wt. after (g)		1.0145	1.0235	1.0252	1.0189
Cell Wt. 1 (g)	cell wt. =boat wt. after - boat wt.	0.0298	0.0389	0.0389	0.0333
Boat 2 Wt. before (g)	before	0.9858	0.9839	0.9836	0.986
Boat 2 Wt. after (g)		1.015	1.0197	1.0234	1.0217
Cell Wt. 2 (g)		0.0292	0.0358	0.0398	0.0357
Ave. Cell Wt. (g)		0.0295	0.0389	0.0389	0.0345
DCW (g/L)	DCW=cell wt. / sample volume	1.475	1.945	1.945	1.725
OD (550 nm)		4.6192	7.5058	6.5934	5.6758
Glucose in Feed (g/L)		4.78	5.036	5.056	4.806
Glucose in Effluent (g/L)		0	0	0	0
Acetate in Feed (g/L)		4.748	4.93	4.924	4.662
Acetate in Effluent (g/L)		0.296	0.47	0.658	0.98
$Y_{X\|S}$ (g/g)	$Y_{X\|S}$ = DCW/(S_{in}-S_{out})	0.309	0.386	0.385	0.359
Q_A (g/Lh)	Q_A=(Ace_{out}-Ace_{in})*D	0.757	1.416	1.559	0.964
q_A (g/gh)	q_A =Q_A/X	0.513	0.728	0.802	0.559
q_A (mmol/gh)	q_A = q_A*1000/59.04	8.688	12.333	13.579	9.461
Qs (g/Lh)	Qs=(Glc_{in}-Glc_{out})*D	0.812	1.599	1.848	1.258
qs (g/gh)	qs =Qs/X	0.551	0.822	0.950	0.729
qs (mmol/gh)	qs = q_s*1000/180	3.059	4.568	5.279	4.050
qs/qa (g/g)		1.074	1.129	1.185	1.305
qs/qa (mol/mol)		0.352	0.370	0.389	0.428
Pyruvate in Feed (g/L)		0.000	0.000	0.000	0.000
Pyruvate in Effluent (g/L)		0.632	0.246	0.236	0.642
Q_P (g/Lh)	Q_P=(Pyr_{out}-Pyr_{in})*D	0.107	0.078	0.086	0.168
q_P (g/gh)	q_P =Q_P/X	0.073	0.040	0.044	0.097
unknown in (MU/L)		0.000	0.000	0.000	0.000
unknown out (MU)/L		0.062	0.128	0.133	0.091
Q_{UN} (MU/Lh)	Q_{UN}=(Un_{out}-Un_{in})*D	0.011	0.041	0.049	0.024
q_{UN} (MU/gh)	q_{UN} =Q_{UN}/X	0.007	0.021	0.025	0.014
Qgas (L/min)		1.5	1.5	1.5	1.5
oxygen initially		21.02	21.02	21.02	21.02
oxygen at steady state		20.02	19.28	19.28	19.85
Density of O_2 at 0°C (g/L)		1.429	1.429	1.429	1.429
OUR (g oxygen/min)	OUR=($O_{2,ini}$-$O_{2,steady}$)*Qgas*ρ/100	0.021	0.037	0.037	0.025
OUR (mmol oxygen/h)	FW = 32	40.191	69.932	69.932	47.023
qo (mmol O2/g DCW h)	Specific OUR=OUR/(V*DCW)	17.693	23.347	23.347	17.701
CO_2 initially		0.04	0.04	0.04	0.04
CO_2 at steady state		0.78	1.46	1.56	1.06
Density of CO_2 at 0°C (g/L)		1.977	1.977	1.977	1.977
CER (g carbon dioxide/min)	CER=($CO_{2,steady}$-$CO_{2,in}$)*Qgas*ρ/100	0.022	0.042	0.045	0.030
CER (mmol carbon dioxide/h)	FW = 44	29.92	57.42	61.47	41.25
q_{CO2} (mmol CO_2/g DCW h)	Specific CER=CER/(V*DCW)	13.17	19.17	20.52	15.53
RQ	RQ=CER/OUR	0.74	0.82	0.88	0.88
C-produced: CO_2 (mmol C/h)	CER	29.92	57.42	61.47	41.25
C-produced: Biomass (mmol C/h)		10.23	25.21	29.02	18.42
C-produced: pyruvate (mmol C/h)	(Pyr_{out}-Pyr_{in})*3*1000*D/88.06	3.66	2.66	2.94	5.72
total C-produced (mmol C/h)		43.81	85.29	93.42	65.40
C-consumed: Acetate (mmol C/h)	(Ace_{out}-Ace_{in})*2*1000*D/59.04	25.63	47.97	52.82	32.64
C-consumed: Glucose (mmol C/h)	(Glc_{out}-Glc_{in})*6*1000*D/180	27.08	53.30	61.60	41.92
total C-consumed: Glu(mmol C/h)		52.70	101.28	114.42	74.56
Carbon Balance (%)	C-produced/C-consumed	0.83	0.84	0.82	0.88
NADH (nM)		0.20	0.20		
NAD (nM)		5.17	7.62		
NADH/NAD		0.04	0.03		
enzyme activity (U/L)		1.20	0.45	2.77	2.65
protein concentration (mg/L)		306.23	357.32	370.86	324.25
specific enzyme activity (U/mg)	spec. act. = enzyme act. / [protein]	0.0039	0.0013	0.0075	0.0082

C.4 Continuous Results for KD 423

Calculations for Glc-limited chemostat KD 423 03/02/05 without IPTG					
Aimed D (h^{-1})		0.14	~~0.18~~	0.26	0.34
Aimed Acetate (g/L)		10	~~10~~	10	10
Flowrate (L/h)		0.205	~~0.295~~	0.37	0.48
Final Volume (L)		1.44	~~1.44~~	1.44	1.44
Actual D (h^{-1})	flowrate/final volume	0.142	~~0.205~~	0.257	0.333
Sample volume(L)		0.02	~~0.02~~	0.02	0.02
Boat 1 Wt. before (g)		0.999	~~0.985~~	0.9843	0.9834
Boat 1 Wt. after (g)		1.0397	~~1.0185~~	1.0274	1.03
Cell Wt. 1 (g)	cell wt. =boat wt. after - boat wt.	0.0407	~~0.0335~~	0.0431	0.0466
Boat 2 Wt. before (g)	before	0.981	~~0.9828~~	0.9804	0.9831
Boat 2 Wt. after (g)		1.0243	~~1.0182~~	1.0233	1.0258
Cell Wt. 2 (g)		0.0433	~~0.0354~~	0.0429	0.0427
Ave. Cell Wt. (g)		0.042	~~0.0335~~	0.0431	0.04465
DCW (g/L)	DCW=cell wt. / sample volume	2.100	~~1.675~~	2.155	2.233
OD (550 nm)		5.3948	~~4.2123~~	5.8409	6.3836
Glucose in Feed (g/L)		4.92	~~4.7~~	4.75	4.96
Glucose in Effluent (g/L)		0	~~0~~	0	0
Acetate in Feed (g/L)		9.77	~~9.82~~	9.51	9.61
Acetate in Effluent (g/L)		3.69	~~3.85~~	5.35	4.79
$Y_{X\|S}$ (g/g)	$Y_{X\|S}$ = DCW/(S_{in}-S_{out})	0.427	~~0.356~~	0.454	0.450
Q_A (g/Lh)	Q_A=(Ace_{out}-Ace_{in})*D	0.866	~~1.223~~	1.069	1.607
q_A (g/gh)	q_A =Q_A/X	0.412	~~0.730~~	0.496	0.720
q_A (mmol/gh)	q_A = q_A*1000/59.04	6.981	~~12.367~~	8.401	12.190
Qs (g/Lh)	Qs=(Glc_{in}-Glc_{out})*D	0.700	~~0.963~~	1.220	1.653
qs (g/gh)	qs =Qs/X	0.334	~~0.575~~	0.566	0.741
qs (mmol/gh)	qs = q_s*1000/180	1.853	~~3.194~~	3.146	4.114
qs/qa (g/g)		0.809	~~0.787~~	1.142	1.029
qs/qa (mol/mol)		0.265	~~0.258~~	0.375	0.338
Pyruvate in Feed (g/L)		0.000	~~0.000~~	0.000	0.000
Pyruvate in Effluent (g/L)		0.270	~~0.420~~	1.030	0.440
Q_P (g/Lh)	Q_P=(Pyr_{out}-Pyr_{in})*D	0.038	~~0.086~~	0.265	0.147
q_P (g/gh)	q_P =Q_P/X	0.018	~~0.051~~	0.123	0.066
unknown in (MU/L)		0.000	~~0.000~~	0.000	0.000
unknown out (MU)/L		0.048	~~0.039~~	0.042	0.085
Q_{UN} (MU/Lh)	Q_{UN}=(Un_{out}-Un_{in})*D	0.007	~~0.008~~	0.011	0.028
q_{UN} (MU/gh)	q_{UN} =Q_{UN}/X	0.003	~~0.005~~	0.005	0.013
Qgas (L/min)		1.5	~~1.5~~	1.5	1.5
oxygen initially		20.99	~~21.00~~	21.00	21.00
oxygen at steady state		20.12	~~20.17~~	19.86	19.15
Density of O_2 at 0°C (g/L)		1.429	~~1.429~~	1.429	1.429
OUR (g oxygen/min)	OUR=($O_{2,ini}$-$O_{2,steady}$)*Qgas*ρ/100	0.019	~~0.018~~	0.024	0.040
OUR (mmol oxygen/h)	FW = 32	34.966	~~33.358~~	45.817	74.353
qo (mmol O2/g DCW h)	Specific OUR=OUR/(V*DCW)	11.563	~~13.830~~	14.765	23.128
CO_2 initially		0	~~0~~	0	0
CO_2 at steady state		0.88	~~0.89~~	1.02	1.32
Density of CO_2 at 0°C (g/L)		1.977	~~1.977~~	1.977	1.977
CER (g carbon dioxide/min)	CER=($CO_{2,steady}$-$CO_{2,in}$)*Qgas*ρ/100	0.026	~~0.026~~	0.030	0.039
CER (mmol carbon dioxide/h)	FW = 44	35.59	~~35.99~~	41.25	53.38
q_{CO2} (mmol CO_2/g DCW h)	Specific CER=CER/(V*DCW)	11.77	~~14.92~~	13.29	16.60
RQ	RQ=CER/OUR	1.02	~~1.08~~	0.90	0.72
C-produced: CO_2 (mmol C/h)	CER	35.59	~~35.99~~	41.25	53.38
C-produced: Biomass (mmol C/h)		12.20	~~14.01~~	22.60	30.37
C-produced: pyruvate (mmol C/h)	(Pyr_{out}-Pyr_{in})*3*1000*D/88.06	1.31	~~2.93~~	9.02	5.00
total C-produced (mmol C/h)		49.10	~~52.93~~	72.86	88.75
C-consumed: Acetate (mmol C/h)	(Ace_{out}-Ace_{in})*2*1000*D/59.04	29.32	~~41.43~~	36.21	54.43
C-consumed: Glucose (mmol C/h)	(Glc_{out}-Glc_{in})*6*1000*D/180	23.35	~~32.09~~	40.68	55.11
total C-consumed: Glu(mmol C/h)		52.67	~~73.53~~	76.89	109.54
Carbon Balance (%)	C-produced/C-consumed	0.93	~~0.72~~	0.95	0.81
NADH (nM)		0.12	~~0.50~~	0.32	0.31
NAD (nM)		3.81	~~1.23~~	3.95	4.94
NADH/NAD		0.03	~~0.40~~	0.08	0.06
enzyme activity (U/L)		10.34	~~2.56~~	6.43	5.68
protein concentration (mg/L)		453.68	~~237.61~~	376.30	406.32
specific enzyme activity (U/mg)	spec. act. = enzyme act. / [protein]	0.0228	~~0.0108~~	0.0171	0.0140

Calculations for Glc-limited chemostat KD 423 03/24/05 without IPTG			
Aimed D (h^{-1})		0.3	0.4
Aimed Acetate (g/L)		10	10
Flowrate (L/h)		0.43	0.57
Final Volume (L)		1.48	1.48
Actual D (h^{-1})	flowrate/final volume	0.29	0.39
Sample volume(L)		0.02	0.02
Boat 1 Wt. before (g)		0.999	1.0028
Boat 1 Wt. after (g)		1.0344	1.0326
Cell Wt. 1 (g)	cell wt. =boat wt. after - boat wt.	0.0354	0.0298
Boat 2 Wt. before (g)	before	0.9995	1.0035
Boat 2 Wt. after (g)		1.0317	1.0338
Cell Wt. 2 (g)		0.0322	0.0303
Ave. Cell Wt. (g)		0.0354	0.03005
DCW (g/L)	DCW=cell wt. / sample volume	1.770	1.503
OD (550 nm)		6.3871	5.893
Glucose in Feed (g/L)		4.838	4.802
Glucose in Effluent (g/L)		0	0
Acetate in Feed (g/L)		9.356	9.388
Acetate in Effluent (g/L)		4.266	6.1
$Y_{X\|S}$ (g/g)	$Y_{X\|S} = DCW/(S_{in}-S_{out})$	0.366	0.313
Q_A (g/Lh)	$Q_A=(Ace_{out}-Ace_{in})*D$	1.479	1.266
q_A (g/gh)	$q_A =Q_A/X$	0.836	0.843
q_A (mmol/gh)	$q_A = q_A*1000/59.04$	14.152	14.275
Qs (g/Lh)	$Qs=(Glc_{in}-Glc_{out})*D$	1.406	1.849
qs (g/gh)	qs =Qs/X	0.794	1.231
qs (mmol/gh)	$qs = q_s*1000/180$	4.412	6.838
qs/qa (g/g)		0.950	1.460
qs/qa (mol/mol)		0.312	0.479
Pyruvate in Feed (g/L)		0.000	0.000
Pyruvate in Effluent (g/L)		0.432	1.140
Q_P (g/Lh)	$Q_P=(Pyr_{out}-Pyr_{in})*D$	0.126	0.439
q_P (g/gh)	$q_P =Q_P/X$	0.071	0.292
unknown in (MU/L)		0.000	0.000
unknown out (MU)/L		0.060	0.008
Q_{UN} (MU/Lh)	$Q_{UN}=(Un_{out}-Un_{in})*D$	0.018	0.003
q_{UN} (MU/gh)	$q_{UN} =Q_{UN}/X$	0.010	0.002
Qgas (L/min)		1.5	1.5
oxygen initially		20.99	20.99
oxygen at steady state		19.11	19.83
Density of O_2 at 0^oC (g/L)		1.429	1.429
OUR (g oxygen/min)	$OUR=(O_{2,ini}-O_{2,steady})*Qgas*\rho/100$	0.040	0.025
OUR (mmol oxygen/h)	FW = 32	75.558	46.621
qo (mmol O2/g DCW h)	Specific OUR=OUR/(V*DCW)	28.843	20.966
CO_2 initially		0	0
CO_2 at steady state		1.46	1.16
Density of CO_2 at 0^oC (g/L)		1.977	1.977
CER (g carbon dioxide/min)	$CER=(CO_{2,steady}-CO_{2,in})*Qgas*\rho/100$	0.043	0.034
CER (mmol carbon dioxide/h)	FW = 44	59.04	46.91
q_{CO2} (mmol CO_2/g DCW h)	Specific CER=CER/(V*DCW)	22.54	21.09
RQ	RQ=CER/OUR	0.78	1.01
C-produced: CO_2 (mmol C/h)	CER	59.04	46.91
C-produced: Biomass (mmol C/h)		20.99	23.62
C-produced: pyruvate (mmol C/h)	$(Pyr_{out}-Pyr_{in})*3*1000*D/88.06$	4.28	14.96
total C-produced (mmol C/h)		84.31	85.49
C-consumed: Acetate (mmol C/h)	$(Ace_{out}-Ace_{in})*2*1000*D/59.04$	50.10	42.90
C-consumed: Glucose (mmol C/h)	$(Glc_{out}-Glc_{in})*6*1000*D/180$	46.85	61.65
total C-consumed: Glu(mmol C/h)		96.95	104.54
Carbon Balance (%)	C-produced/C-consumed	0.87	0.82
NADH (nM)		0.34	0.33
NAD (nM)		5.31	4.00
NADH/NAD		0.06	0.08
enzyme activity (U/L)		5.39	7.17
protein concentration (mg/L)		411.70	382.17
specific enzyme activity (U/mg)	spec. act. = enzyme act. / [protein]	0.0131	0.0188

Calculations for Glc-limited chemostat KD 423 04/04/05 without IPTG		
Aimed D (h^{-1})		0.18
Aimed Acetate (g/L)		10
Flowrate (L/h)		0.26
Final Volume (L)		1.48
Actual D (h^{-1})	flowrate/final volume	0.18
Sample volume(L)		0.02
Boat 1 Wt. before (g)		0.9891
Boat 1 Wt. after (g)		1.0148
Cell Wt. 1 (g)	cell wt. =boat wt. after - boat wt.	0.0257
Boat 2 Wt. before (g)	before	0.9863
Boat 2 Wt. after (g)		1.0134
Cell Wt. 2 (g)		0.0271
Ave. Cell Wt. (g)		0.0264
DCW (g/L)	DCW=cell wt. / sample volume	1.320
OD (550 nm)		5.3531
Glucose in Feed (g/L)		4.834
Glucose in Effluent (g/L)		0.000
Acetate in Feed (g/L)		9.418
Acetate in Effluent (g/L)		3.942
$Y_{X\|S}$ (g/g)	$Y_{X\|S} = DCW/(S_{in}-S_{out})$	0.273
Q_A (g/Lh)	$Q_A=(Ace_{out}-Ace_{in})*D$	0.962
q_A (g/gh)	$q_A =Q_A/X$	0.729
q_A (mmol/gh)	$q_A = q_A*1000/59.04$	12.344
Qs (g/Lh)	$Qs=(Glc_{in}-Glc_{out})*D$	0.849
qs (g/gh)	qs =Qs/X	0.643
qs (mmol/gh)	$qs = q_s*1000/180$	3.574
qs/qa (g/g)		0.883
qs/qa (mol/mol)		0.290
Pyruvate in Feed (g/L)		0.000
Pyruvate in Effluent (g/L)		0.130
Q_P (g/Lh)	$Q_P=(Pyr_{out}-Pyr_{in})*D$	0.023
q_P (g/gh)	$q_P =Q_P/X$	0.017
unknown in (MU/L)		0.000
unknown out (MU)/L		0.016
Q_{UN} (MU/Lh)	$Q_{UN}=(Un_{out}-Un_{in})*D$	0.003
q_{UN} (MU/gh)	$q_{UN} =Q_{UN}/X$	0.002
Qgas (L/min)		1.5
oxygen initially		20.92
oxygen at steady state		19.93
Density of O_2 at 0^oC (g/L)		1.429
OUR (g oxygen/min)	$OUR=(O_{2,ini}-O_{2,steady})*Qgas*\rho/100$	0.021
OUR (mmol oxygen/h)	FW = 32	39.789
qo (mmol O2/g DCW h)	Specific OUR=OUR/(V*DCW)	20.367
CO_2 initially		0.04
CO_2 at steady state		0.87
Density of CO_2 at 0^oC (g/L)		1.977
CER (g carbon dioxide/min)	$CER=(CO_{2,steady}-CO_{2,in})*Qgas*\rho/100$	0.025
CER (mmol carbon dioxide/h)	FW = 44	33.56
q_{CO2} (mmol CO_2/g DCW h)	Specific CER=CER/(V*DCW)	17.18
RQ	RQ=CER/OUR	0.84
C-produced: CO_2 (mmol C/h)	CER	33.56
C-produced: Biomass (mmol C/h)		9.46
C-produced: pyruvate (mmol C/h)	$(Pyr_{out}-Pyr_{in})*3*1000*D/88.06$	0.78
total C-produced (mmol C/h)		43.81
C-consumed: Acetate (mmol C/h)	$(Ace_{out}-Ace_{in})*2*1000*D/59.04$	32.59
C-consumed: Glucose (mmol C/h)	$(Glc_{out}-Glc_{in})*6*1000*D/180$	28.31
total C-consumed: Glu(mmol C/h)		60.90
Carbon Balance (%)	C-produced/C-consumed	0.72
NADH (nM)		0.35
NAD (nM)		3.70
NADH/NAD		0.09
enzyme activity (U/L)		10.45
protein concentration (mg/L)		299.03
specific enzyme activity (U/mg)	spec. act. = enzyme act. / [protein]	0.0350